

STATUS OF THESIS

Title of thesis

OPTIMIZATION OF *n*-HEXANE REFORMING AND  
KINETICS OF CATALYST REGENERATION

I, REEM AHMED MOHAMMED ISMAIL

hereby allow my thesis to be placed at the Information Resource Center (IRC) of Universiti Teknologi PETRONAS (UTP) with the following conditions:

1. The thesis becomes the property of UTP.
2. The IRC of UTP may make copies of the thesis for academic purposes only.
3. This thesis is classified as

Confidential

Non-confidential

If this thesis is confidential, please state the reason:

---

---

---

The contents of the thesis will remain confidential for \_\_\_\_\_ years.

Remarks on disclosure:

---

---

---

Endorsed by

\_\_\_\_\_  
Signature of Author

Permanent: Sudan / Jabal Awliya  
Address: Tel. NO: +249912853483

Date: \_\_\_\_\_

\_\_\_\_\_  
Signature of Supervisor

Dr. Chandra Mohan Sinnathambi

Date: \_\_\_\_\_

UNIVERSITI TEKNOLOGI PETRONAS

APPROPTIMIZATION OF *n*-HEXANE REFORMING AND KINETICS OF  
CATALYST REGENERATION

By

REEM AHMEDMOHAMMED ISMAIL

The undersigned certify that they have read, and recommend to the Postgraduate Studies Programme for acceptance this thesis for the fulfillment of the requirements for the degree stated.

Signature: \_\_\_\_\_

Main Supervisor: Dr. Chandra Mohan Sinnathambi

Signature: \_\_\_\_\_

Co-Supervisor: Prof. Dr. Duvvuri Subbarao

Signature: \_\_\_\_\_

Head of Department: Assoc. Prof. Dr. Shuhaimi Mahadzir

Date: \_\_\_\_\_

UNIVERSITI TEKNOLOGI PETRONAS

OPTIMIZATION OF *n*-HEXANE REFORMING AND KINETICS OF CATALYST  
REGENERATION

By

REEM AHMED MOHAMMED ISMAIL

A Thesis

Submitted to the Postgraduate Studies Programme  
as a Requirement for the Degree of

MASTERS OF SCIENCE

CHEMICAL ENGINEERING DEPARTMENT

UNIVERSITI TEKNOLOGI PETRONAS

BANDAR SRI ISKANDAR

PERAK

March 2011

## DECLARATION OF THESIS

Title of thesis

OPTIMIZATION OF *n*-HEXANE REFORMING AND  
KINETICS OF CATALYST REGENERATION

I, REEM AHMED MOHAMMED ISMAIL

hereby declare that the thesis is based on my original work except for quotations and citations which have been duly acknowledged. I also declare that it has not been previously or concurrently submitted for any other degree at UTP or other institutions.

Witnessed by

\_\_\_\_\_  
Signature of Author

Permanent: Sudan / Jabal Awliya

Address: Tel. NO: +249912853483

Date: \_\_\_\_\_

\_\_\_\_\_  
Signature of Supervisor

Dr. Chandra Mohan Sinnathambi

Date: \_\_\_\_\_

## ACKNOWLEDGEMENT

First and above all, I praise Allah, the almighty for providing me with this opportunity and granting me the capability to proceed with this work successfully.

Very special thanks to my supervisor, Dr. Chandra Mohan who has been the ideal supervisor. His sage advice, insightful criticisms, and patient encouragement aided the writing of this thesis in innumerable ways. I attribute the level of my Masters degree to his encouragement and effort for the success of this thesis.

Special thanks to my co. supervisor, Prof. D.Subbarao for his help, especially in the reaction section. I benefited from his advice, particularly so when exploring new ideas.

I also would like to express sincere thanks to the department of chemical and electrical engineering technicians for their assistance in fixing my MTR equipment.

My warmly thank and appreciate to my parents and my husband for their material and spiritual support during the whole period of study.

Finally, I would like to thank all the catalyst group researchers and lecturers for their assistance in experiments, knowledge and patience, and all the other fellow students for the good memories and friendship for during the whole period of study.

## ABSTRACT

Catalytic naphtha reforming is practiced extensively in the petroleum-refining industry to convert low research octane number (straight chain paraffin) naphtha feed into high RON component (aromatics and branch isomers) with minimum average molecular weight changes needed for the modern auto-industry. A valuable by-product, hydrogen, from the process is added bonus needed for hydro processing operations in the refinery. Depending on the operating conditions, hydrogen may be consumed in unwanted hydrocracking reactions which directly contribute to deactivate the catalyst. The present study looks into the optimization of process variable (pressure, temperature and contact time) to maximize isomerization and aromatization (increasing RON value) reaction while minimizing the hydrocracking (catalyst deactivation and reducing RON) reactions in *n*-hexane reforming using commercially available Pt/Al<sub>2</sub>O<sub>3</sub> catalyst. From the results it is found that high temperature (723 K) with low hydrogen partial pressure (300 KPa) and low contact time (1.78 to 2.4 minutes) favor the production of isomers and aromatics over coke precursors and cracked product species. Addition of CCl<sub>4</sub> to the *n*-hexane reforming process which increases the catalyst acidity, promotes the formation of cracked products. Selective poisoning using dimethyl-disulfide on the other hand is found to decrease monofunctional metal-catalyzed reactions and increased the activity for the isomerization reactions..

To understand and enhance *n*-hexane reforming the kinetics and catalyst regeneration are also investigated using TGA and TPO analysis. From TPO analysis it was found that applying slow heating rate was the most efficient and convenient way to control the regeneration process. The TGA results indicate that there exist three types of coke categorize as soft, hard and laid coke which can be distinguished by a temperature profile. It was found that the hard coke followed by soft coke makes up the major constituent of the coked catalyst which can be removed successfully by proper regeneration process.

## ABSTRAK

Reformasi pemangkinan nafta laras digunakan diperkilang penapisan minyak mentah untuk mengubah komponen-komponen oktana yang rendah (rantai parafin selari) melalui penyusunan naphtha kepada kandungan RON komponen yang lebih tinggi (cabang isomer dan aromatik) dengan minima rata-rata berat molekul berubah untuk keperluan kenderaan industri automatik. Produk sampingan yang berharga iaitu hidrogen proses adalah bonus kepada operasi hidro pemrosesan didalam kilang penapisan minyak mentah. Penyelidikan ini memfokuskan kepada pengoptimuman bagi proses reformasi n-heksana bertujuan untuk memaksimumkan tindakbalas antara proses-proses pengisomeran dan pengaromasian disamping meminimumkan tindakbalas perekahan dan penyahaktifan pemangkin. Ini melibatkan beberapa pembolehubah-pembolehubah (tekanan, suhu dan masa sentuhan) dengan menggunakan pemangkin komersil-Pt/Al<sub>2</sub>O<sub>3</sub>. Selain itu, pemerhatian terhadap reformasi kinetik dan penjanaan semula pemangkin turut dilaksanakan. Dari hasil kajian, didapati bahawa keadaan suhu yang tinggi (723 K) dengan tekanan hydrogen separa rendah (300 KPa), dan masa sentuhan yang rendah menyokong penghasilan isomer dan aromatik dengan mengurangkan taraf kenaikan penyahaktifan dan meningkatkan kepekatan bahan pemula-coke. Keracunan selektif menggunakan dimetil-disulfida didapati mengurangkan tindakbalas monofungsi pemangkin-logam dan telah meningkatkan aktiviti tindakbalas-tindakbalas pengisomeran.

TGA dan TPO telah digunakan untuk mempelajari tentang kinetik bagi proses penjanaan semula pemangkin yang telah digunakan. Daripada analisa TPO, ianya dapat diperhatikan bahawa penggunaan kadar pemanasan yang perlahan merupakan kaedah yang paling efisien dan bersesuaian untuk mengawal proses penjanaan semula. Keputusan-keputusan TGA menunjukkan tiga jenis coke yang dikategorikan sebagai coke-coke lembut, keras dan letak telah wujud yang dikenalpasti melalui profil suhu. Ianya turut didapati bahawa coke-keras diikuti dengan coke-lembut membentuk pemangkin coke berkonsistensi utama yang boleh disingkirkan melalui proses penjanaan semula yang bersesuaian.

In compliance with the terms of the Copyright Act 1987 and the IP Policy of the university, the copyright of this thesis has been reassigned by the author to the legal entity of the university,

Institute of Technology PETRONAS Sdn Bhd.

Due acknowledgement shall always be made of the use of any material contained in, or derived from, this thesis.

© REEM AHMED MOHAMMED ISMAIL, 2010

Institute of Technology PETRONAS Sdn Bhd

All rights reserved.

## TABLE OF CONTENTS

STATUS OF THESIS .....	I
TITLE PAGE .....	III
DECLARATION OF THESIS .....	IV
ACKNOWLEDGEMENT .....	V
ABSTRACT .....	VI
ABSTRAK .....	VII
TABLE OF CONTENTS .....	IX
LIST OF TABLES .....	XII
LIST OF FIGURES .....	XIII
LIST OF NOMENCLATURE.....	XVI
CHAPTER 1.....	1
INTRODUCTION.....	1
1.1 HISTORY OF REFORMING PROCESS.....	1
1.1.1 Reforming catalyst functions .....	2
1.2 PROBLEM STATEMENT.....	5
1.3 OBJECTIVES AND SCOPE OF THE STUDY .....	5
CHAPTER 2.....	7
LITERATURE REVIEW .....	7
2.1 CATALYTIC NAPHTHA REFORMING PROCESS .....	7
2.2 PROPERTIES OF REFORMING REACTIONS .....	8
2.3 REFORMING MECHANISM.....	9
2.4 N-HEXANE REFORMING CHEMISTRY .....	10
2.4.1 n-Hexane cracking.....	10
2.4.2 n-Hexane Isomerization .....	11
2.4.3 Dehydrocyclization / Dehydrogenation Reactions.....	11
2.5 REFORMING CONDITIONS.....	12
2.6 REFORMING CATALYSTS.....	15

2.7 EFFECTS OF SULFUR ON REFORMING CATALYSTS.....	17
2.8 CATALYSTS ACIDITY .....	19
2.9 CATALYSTS DEACTIVATION.....	23
2.9.1 Mechanisms of Deactivation of Heterogeneous Catalysts.....	23
2.9.2 Coke deposits on the catalyst surface.....	24
2.9.3 Mechanism of coke formation.....	26
2.9.4 Coke characterization and regeneration .....	28
2.9.5 Prevention of coke formation.....	31
CHAPTER 3.....	33
EXPERIMENTAL WORK.....	33
3.1 RESEARCH MATERIALS .....	33
3.1.1 Catalyst Properties.....	33
3.1.2 Gases and Chemicals.....	33
3.2 GENERAL DESCRIPTION OF REACTOR RIG.....	34
3.2.1 Micro-Tubular Reactor.....	35
3.3 EXPERIMENTS METHOD.....	36
3.4 GAS CHROMATOGRAPH.....	37
3.4.1 Mechanisms of sample analysis by GC.....	38
3.4.2 GC-Operating Conditions .....	39
3.5 CALCULATIONS .....	40
3.5.1 Conversion .....	40
3.5.2 Products selectivity .....	40
3.6 CATALYST CHARACTERIZATION.....	41
3.6.1 Field emission scanning electron microscope (FESEM) .....	41
3.6.2 Thermo-analytical techniques .....	42
3.6.3 Fourier Transform infrared spectroscopy (FTIR) .....	47
CHAPTER 4.....	49
RESULTS AND ANALYSIS.....	49
4.1 CHAPTER OVERVIEW .....	49
4.2 REFORMING PROCESS VARIABLES AND MODIFICATION OF THE CATALYST SUPPORT	
.....	50
4.2.1 Process variables and product classification for n-hexane reforming.....	50
4.2.2 Effect of contact time against pressure and temperature on n-hexane	
conversion .....	51
4.2.3 Effect of contact time against process variables on reformate species .....	54
4.3 DESIGN EXPERT SOFTWARE (VERSION 6.0.6) USING A TAGUCHI ORTHOGONAL	
ARRAY DESIGN .....	60

4.3.1 Optimization of percentage conversion of n-hexane reforming using Taguchi OAD method .....	61
4.3.2 Optimization of aromatics reformat % yield using Taguchi OAD method .....	64
4.3.3 Optimization of isomers reformat % yield using Taguchi OAD method.	65
4.3.4 Minimizing of cracked reformat % yield using Taguchi OAD method...	67
4.3.5 Minimizing coke precursors reformat % yield using Taguchi OAD method .....	69
4.4 KINETICS STUDY OF N-HEXANE REFORMING .....	70
4.4.1 Reversible reactions .....	71
4.4.2 Irreversible reactions .....	74
4.5 EFFECTS OF ADDING CCl <sub>4</sub> AS AN ACID BOOSTER FOR N-HEXANE REFORMING REACTIONS .....	76
4.5.1 Effect of adding CCl <sub>4</sub> on n-hexane conversion .....	76
4.5.2 Effects of addition of CCl <sub>4</sub> on selectivity of reformat species .....	78
4.6 EFFECTS OF DIMETHYL DISULFIDE (DMDS) ON N-HEXANE REFORMING .....	80
4.6.1 Effects of DMDS on the yield selectivity of reformat product species....	80
4.7 KINETICS AND REGENERATION OF INDUSTRIAL SPENT REFORMING CATALYST ...	82
4.7.1 Thermal gravimetric analysis (TGA) .....	84
4.7.2 Fourier Transform infrared spectroscopy (FTIR) .....	88
4.7.3 Temperature Programmed Oxidation (TPO).....	90
4.7.4 Temperature Programmed Reduction (TPR) .....	99
4.7.5 Temperature Programmed desorption (TPD).....	101
4.7.6 Field Emission Scanning Electron Microscopy (FESEM).....	102
CHAPTER 5 .....	104
CONCLUSION AND RECOMMENDATION .....	104
5.1 CONCLUSION .....	104
5.2 WORK CONTRIBUTIONS .....	106
5.3 RECOMMENDATIONS AND FUTURE WORK.....	106
APPENDIX A .....	118
APPENDIX B .....	122
APPENDIX C .....	123
APPENDIX D .....	124

## LIST OF TABLES

Table 2-1: Describe type, mechanism, and definition of the catalysts deactivation ...	23
Table 2-2: Coke percentages of various reforming hydrocarbons at same reforming conditions (773 K, 101 KPa, WHSV=2, H <sub>2</sub> /HC = 4, run length=5 h), [31].	28
Table 2-3: Elimination of the catalyst deactivation by catalyst and process modification. Taken from [42].	31
Table 3-1: Textural properties of Pt/Al <sub>2</sub> O <sub>3</sub> fresh commercial catalyst	33
Table 3-2: Description of GC operating conditions	39
Table 4-1: Grouping of Products from Reforming Reactions	50
Table 4-2: The average conversion at contact time 2.4 to 7 min, pressures 300, 500 and 700 KPa and temperatures 723,673 and 623 K.	52
Table 4-3: Reforming conditions and levels used in this experiment	60
Table 4-4: L9 Array for Design of Experiment by Taguchi Method	61
Table 4-5: The ANOVA table of <i>n</i> -hexane conversion	62
Table 4-6: Reaction rate constants: $k_1$ , $k_2$ and $K_c$ at varied temperatures for <i>n</i> -hexane reforming	73
Table 4-7: Rate constants ( $k$ ) at 700 KPa at varied temperatures for <i>n</i> -hexane irreversible reforming reaction	75
Table 4-8: The effect of CCl <sub>4</sub> doping on yield selectivity of reformat species during <i>n</i> -hexane reforming over industrial Pt/Al <sub>2</sub> O <sub>3</sub> catalyst	78
Table 4-9: The effect of DMDS doping on yield selectivity of reformat species during <i>n</i> -hexane reforming over industrial Pt/Al <sub>2</sub> O <sub>3</sub> catalyst	81
Table 4-10: Coke and volatile species desorption from TGA at different heating rates.	85
Table 4-11: Activation energies and pre-exponential factors for the 3 coke species taken from TGA run at ramp rate of 10 K min <sup>-1</sup>	88

## LIST OF FIGURES

Figure 1-1: Simplified reaction network for <i>n</i> -hexane reforming reactions [9].....	2
Figure 2-1: Schematic isomerization mechanism on a Pt/Al <sub>2</sub> O <sub>3</sub> catalyst. Adapted from [26].....	9
Figure 2-2: Chlorination zone in the regeneration tower .....	20
Figure 2-3: Fouling, crystallite encapsulation and pore plugging of a supported metal catalyst due to Coke accumulation on the catalyst adapted from [35]. .....	27
Figure 3-1 A schematic diagram of the basic parts of a micro-tubular reactor.....	34
Figure 3-2: High-pressure micro tubular reactor schematic diagram .....	35
Figure 3-3 A schematic diagram of the <i>n</i> -hexane desired and undesired products.....	37
Figure 3-4 A schematic diagram of gas chromatography sampling valve diagram....	38
Figure 3-5: Flow chart of thermo-gravimetric analysis [92].....	45
Figure 4-1: <i>n</i> -hexane % conversion over the Pt/Al <sub>2</sub> O <sub>3</sub> catalyst at 723 K [A], 673 K [B] and 623 K [C] using H <sub>2</sub> pressures of 300, 500 and 700 KPa.....	53
Figure 4-2:Yield % to reformat products as a function of contact time over the Pt/Al <sub>2</sub> O <sub>3</sub> catalyst, at 723 K and pressures at A-300, B-500 & C-700 KPa.....	56
Figure 4-3:Effect of reaction temperature on H <sub>2</sub> partial pressure of 300 KPa, as function of contact time on <i>n</i> -hexane reforming over a Pt/Al <sub>2</sub> O <sub>3</sub> catalyst. [Reaction temperature A=623; B=673 and C = 723 K]. .....	59
Figure 4-4: Percentage contribution of individual factors on variation in <i>n</i> -hexane conversion. ....	62
Figure 4-5: Effect of reaction temperature (A: A), contact time (C: C) and hydrogen pressure (B: B) on hexane conversion. ....	63
Figure 4-6: Percentage contribution of individual factors for aromatics yield. ....	64
Figure 4-7: Effect of H <sub>2</sub> pressure (B: B) and contact time (C: C) level for aromatic yields. ....	65
Figure 4-8: Percentage contribution of individual factors on isomers yield. ....	66
Figure 4-9: Effect of reaction temperature (A: A), contact time (C: C), and H <sub>2</sub> partial pressure (B:B) level on isomers yield. ....	66
Figure 4-10: The percentage contribution of individual factors on ‘cracked’ yield. ...	68

Figure 4-11: The effect of contact time (C:C) and reaction temperature (A:A) level on ‘cracked’ yield. ....	68
Figure 4-12: The percentage contribution of individual factors on variation in coke precursor’s yield.....	69
Figure 4-13: The effect of contact time (C: C) and reaction temperature (A: A) level on coke precursor’s yield.....	69
Figure 4-14: A plotting of $-\ln(1-X_A/X_{Ae})$ versus $t$ (min) for $n$ -hexane kinetics at 300 KPa and varied temperatures over a Pt/Al <sub>2</sub> O <sub>3</sub> catalyst.....	73
Figure 4-15: A plot of $\ln(k)$ versus $1/T$ .....	73
Figure 4-16: A plot of $-\ln(1-X_A)$ versus $t$ (min) for irreversible $n$ -hexane kinetics at 700 KPa at varied temperatures over a Pt/Al <sub>2</sub> O <sub>3</sub> catalyst.....	75
Figure 4-17: A plot of $\ln(k)$ versus $1/T$ (K) for $n$ -hexane irreversible reforming reactions.....	75
Figure 4-18: $n$ -hexane conversion % over the Pt/Al <sub>2</sub> O <sub>3</sub> catalyst, at 723 K and H <sub>2</sub> pressure at 300 KPa for 1 %, 3 %, 5 % CCl <sub>4</sub> and pure hexane (W-CCl <sub>4</sub> ). ....	77
Figure 4-19: The original TGA curve; shows the catalyst weight [mg] versus the time [min] and temperature [°C] at heating rate 10 K min <sup>-1</sup> .....	85
Figure 4-20: FTIR spectrum for spent Pt/Al <sub>2</sub> O <sub>3</sub> catalyst prior and after pre-treatment with N <sub>2</sub> gas.....	89
Figure 4-21: TPO results on commercial spent reforming catalyst at different heating rates, [a=heating rate 20 K min <sup>-1</sup> ; b=15 K min <sup>-1</sup> ; c=10 K min <sup>-1</sup> ]......	91
Figure 4-22: TPO results from a commercial spent reforming catalyst at different temperatures [I= 873 K II = 973 K III = 1073 K]......	92
Figure 4-23: TPO result for industrial spent Pt/Al <sub>2</sub> O <sub>3</sub> reforming catalyst, at < 5% O <sub>2</sub> in N <sub>2</sub> , with a flow rate of 20 ml min <sup>-1</sup> and a heating rate of 10 K min <sup>-1</sup> .....	93
Figure 4-24: TPO results on weight % loss of soft coke (Sc %) during the 1 <sup>st</sup> stage with different heating rates and temperature under a nitrogen atmosphere (A = 10 K min <sup>-1</sup> ; B = 15 K min <sup>-1</sup> ; C = 20 K min <sup>-1</sup> ). .....	94
Figure 4-25: TPO results on weight % loss of Hard Coke (Hc %) at 2nd stage with different heating rates and temperatures under 5.0 v/v % O <sub>2</sub> in N <sub>2</sub> . (A = 10 K min <sup>-1</sup> ; B = 15 K min <sup>-1</sup> ; C = 20 K min <sup>-1</sup> ). .....	95
Figure 4-26: The sum of % weight loss of total coke from 1st and 2nd stage at different heating rates and temperatures (A = 10 K min <sup>-1</sup> ; B = 15 K min <sup>-1</sup> ; C = 20 K min <sup>-1</sup> ). .....	96
Figure 4-27: Effect of dwell time and varied regeneration temperature on industrial spent Pt/Al <sub>2</sub> O <sub>3</sub> spent catalyst [Dwell time for A= 120 min, B= 60 min & C= 30 min]. (Sc=soft coke, Hc= hard coke and Total=hard coke + soft coke). .....	98

Figure 4-28: A plotting of $1/T$ versus $\ln [-\ln (1-x)/T^2]$ for the coked $\text{Pt}/\text{Al}_2\text{O}_3$ catalyst. .....	99
Figure 4-29: TPR traces for the consumption of $\text{H}_2$ in a monometallic $\text{Pt}/\text{Al}_2\text{O}_3$ catalyst, Peak I and Peak II for catalysts before and after calcinations, respectively. ....	100
Figure 4-30: TPD trace for the fresh $\text{Pt}/\text{Al}_2\text{O}_3$ catalyst.....	101
Figure 4-31: FESEM for fresh and spent catalyst by the in-lens (right image) and SE2 (left image). ....	102

## LIST OF NOMENCLATURE

$X\%$	The conversion of reactant A.
$N_{Ao}^{\circ}$	The molar flow of reactant A at the reactor inlet ( $\text{mol s}^{-1}$ ).
$N_A^{\circ}$	The molar flow of reactant A at the reactor outlet ( $\text{mol s}^{-1}$ ).
$M_{Ao}^{\circ}$	The mass flow rate of reactant A at the inlet of the reactor ( $\text{g s}^{-1}$ ).
$M_A^{\circ}$	The mass flow rate of reactant A at the exit of the reactor ( $\text{g s}^{-1}$ ).
$A_A$	The GC area of reactant A.
$A_{Tot}$	Outlet hydrocarbon components total area.
$\frac{A_A}{A_{TOT}}$	GC area fraction of A.
$S_i\%$	The products selectivity.
$A_i$	The area of the chromatographic peak of product i.
$f_i$	The response factor for each product.
$n_i$	The number of carbon atoms of product i.
$M_i$	The molecular weight of i ( $\text{g mol}^{-1}$ ).
$k_1$	Forward reaction rate constant ( $\text{min}^{-1}$ ).

$k_2$	Back reaction rate constant ( $\text{min}^{-1}$ ).
$K_c$	Equilibrium constant.
$E$	Activation energy ( $\text{kJ mol}^{-1}$ ).
HC %	‘Soft’ coke present on the catalyst.
Sc %	‘Hard’ coke on the catalyst.
Total %	The total weight loss from the sample.
$C_c$	Coke concentration (mg)
$C_c^o$	Initial coke concentration (mg)
h	Heating rate ( $^{\circ}\text{C min}^{-1}$ )
$k_r$	Rate constant
$k_o$	Pre-exponential factor
$PO_2$	Partial pressure of $O_2$
R	$8.314 \text{ Jmol}^{-1} \text{ K}^{-1}$
T	Temperature (K)
$X_C$	Coke conversion (%)



## Chapter 1

### Introduction

#### 1.1 History of Reforming Process

The first reformer unit was designed in the 1950s using monometallic platinum on chlorinated alumina support [1]. Catalytic naphtha reforming is a key process in petroleum refining and it is used for rearranging hydrocarbon molecules providing high value-added reformat for the gasoline pool.

Gasoline is a mixture of hydrocarbons ( $C_4$ – $C_{12}$ ) that boils below 473 K (200 °C). The process is frequently applied to low-quality gasoline stocks to improve their combustion characteristic, without significantly changing carbon numbers in the molecule and boiling point range [2]. Reforming of  $C_6$ – $C_{10}$  hydrocarbons (olefin free) containing roughly 10-20 wt % aromatics, 20-50 wt % naphthenes and 40-70 wt % paraffins, which produce high octane gasoline with less tendency to knocking in an automobile engine [3]. Until 1974, tetraethyl lead was added to the gasoline pool as an octane booster [4]. Considering the environmental situation, the use of lead in gasoline was banned in 1990.

The first catalytic reforming process, which used molybdenum oxide-on alumina catalysts, was jointly developed in 1939 by Standard Oil of New Jersey (EXXON), Standard of Indiana (Amoco) and M.W. Kellogg Company. In 1949, UOP introduced the first industrial process (Platforming <sup>TM</sup>) using a platinum-on-alumina catalyst which was a dual-function catalyst having both acidic sites and metallic sites. This soon became the catalyst of choice [5] and [6].

A new catalyst composed of platinum supported on an acidic oxide was introduced after World War II [6]. It was noticed that when the catalytic process is operated at high pressures (30-35 kg  $cm^{-2}$ ), the catalysts have a good

selectivity toward aromatics and an acceptable stability with operation cycles of about 10 months. Nearly 20 years later, bimetallic catalysts appeared. In the 1970s, the new catalysts were introduced which had one or more additional metallic components such as rhenium, iridium and tin. These bimetallic catalysts and multimetallic catalysts have exhibited greatly improved stability (cycle length) and selectivity.

### 1.1.1 Reforming catalyst functions

Both metal and catalyst support play key roles in the catalysis. The role of platinum is to catalyze dehydrogenation-hydrogenation reactions, because, Pt has high activity for cleaving C-H bonds while it has low activity for C-C bond rupture [7]. The role of the catalyst support is to provide the acid sites, which are responsible for isomerization reactions. These acid sites are generated by addition of chlorine to an alumina support. Chlorided alumina acts as an acid and catalyzes a carbon skeletal rearrangement through carbonium ion mechanisms [8]. The improvement of the catalyst acidity, which has limited information in the open literature, is reported here in this thesis. This acidity affects the chemistry of *n*-hexane reactions.

Figure 1-1 describes a simplified diagram of *n*-hexane reforming reactions. The reactions involved are exhibited by both the metal and acid functions. The vertical axis describes the reactions occurring on the metal site, while the horizontal one is for the reactions on the acid sites.

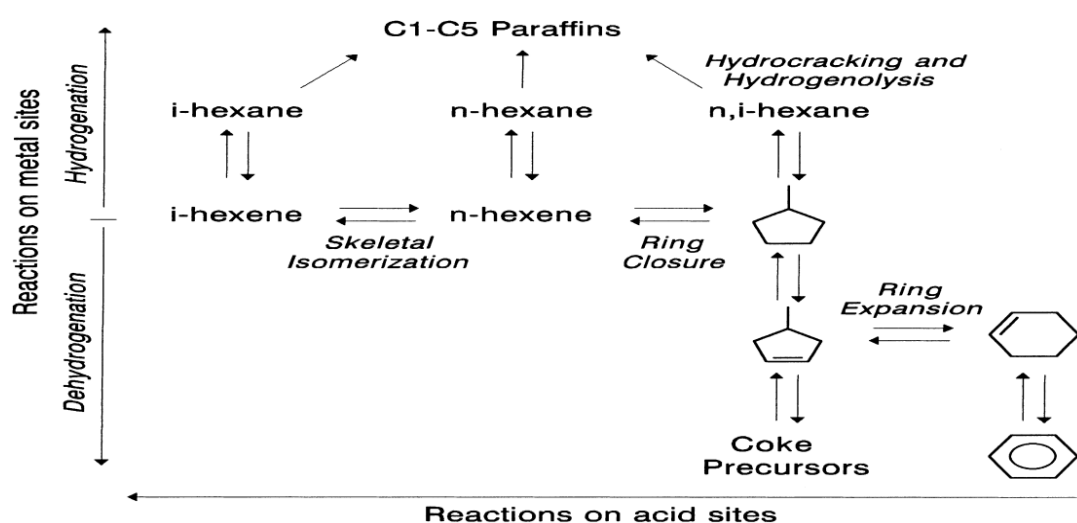


Figure 1-1: Simplified reaction network for *n*-hexane reforming reactions [9].

A summary of reaction mechanism network includes.

- The dehydrogenation of *n*-hexane on metal sites to *n*-hexene.
- The isomerization and the dehydrocyclization of *n*-C<sub>6</sub> to *i*-C<sub>6</sub> and methyl cyclopentane (MCP), through bi-functional mechanisms involving metal and acid-catalyzed steps respectively.
- The hydrogenolysis and hydro-cracking of *n*-C<sub>6</sub> and *i*-C<sub>6</sub> to methane, ethane, propane and pentane.
- The aromatization of MCP to Benzene through the ring expansion reaction of methyl-cyclo-pentene (MCPe).
- Dehydrogenation of MCPe to methyl-cyclo-pentadiene (MCPde) on metal sites producing coke precursors.

Normally, catalytic naphtha reforming might be operated to produce hydrogen, which is a valuable reforming byproduct used for hydro-treating and hydro-cracking processes [10]. The desirable reversible reactions involved in hydrogen production are favored by low hydrogen partial pressures and a high reaction temperature. Catalytic reforming units operate best when the process variables are adjusted to produce the maximum yield of the desired products within the limits of an acceptable catalyst cycle life [8].

The *n*-hexane reforming reactions whose products are directly present in reformat was discussed above. Another major class of the reactions, whose products do not appear in gasoline are the coke formation reactions, Coke formation reactions have significant impact on the rates of the main reactions.

Coking reactions occurs during transformation of non saturated hydrocarbons over an acidic reforming catalyst. These non adsorbed products consist of a large number of non-volatile, low boiling-point, hydrogen depleted components. This coke is the main cause of the catalyst deactivation due to the poisoning of the active sites [11]. It is generally accepted, that coke consists of highly unsaturated polycyclic compounds derived from olefinic precursors. Once olefinic intermediates are formed, it can either go to a desired product or dehydrogenate further and polymerize to coke precursors [12, 13].

This coke is singly the most important factor which affects the life span of the catalyst. Coke deposition can lower the activity of the catalyst by one or more of the following effects:

- Coke adsorbs strongly on the active sites (metal, acid centers).
- Physically envelopes the active center (metal crystallite).
- Plugs the physical texture or shape of the catalyst through growth of the carbonaceous materials.
- Encapsulation of the metal particles and the blocking of the catalysts pores, [14].

With regards to the operating conditions, as demonstrated by Liu et al. [3], stated that, increasing the reaction temperature, thermodynamically shifts the equilibrium of the main reaction in the desired direction. Studies by Fung et al [15].and Taskar [4], showed that side reactions and accelerated coking rate will lower the product yield. Coke formed at a low reaction temperature is more easily removed from the catalyst than that formed at high reaction temperature according to works by Wang et al. [11]. Coke is more aromatic and stable at high reaction temperature than at low reaction temperature. Lower pressure  $H_2$  partial favors higher aromatics yield. Unfortunately, it also causes more rapid coke formation on the catalyst. Increasing hydrogen partial pressure increases catalyst life span (decreasing the coking rate) but, it causes a rise in cracking products yield.

The coke deposits become larger and more aromatic with an increasing time on stream. The amount of coke deposited on the active metal sites often reaches a constant value within the first few minutes of reaction. However, coke accumulating on the support, continues during the reaction and this coke becomes more dehydrogenated than that originally deposited on the metal as explained by Hill [7].

Coke on the metal is called insensitive coke or reactive coke (soft), which is formed at the vicinity of the active sites of the metal [15]. The 'soft' 'coke' can be readily removed by hydrogen or nitrogen gases. In coke-sensitive or un-reactive (hard coke) reactions, coke is deposited on active sites of the catalyst [16]. The presence of this un-reactive 'hard coke' leads to decline in catalytic activity and can be removed by burning in diluted  $O_2$  gas. Beltramini et al. [17], found that by using temperature

programmed oxidation (TPO) techniques, the nature of carbonaceous species deposited on the catalyst is made up of two species represented by 2 different peaks. The high temperature peak corresponds to the coke deposited on the support (non reactive coke), while the lower temperature peak corresponds to coke associated with the metal sites (reactive coke).

## 1.2 Problem Statement

In this thesis, finding solutions to limit the deactivation rate by optimizing the operating conditions is one of the main criteria. Monitoring of these parameters during reforming is necessary in order to produce high octane aromatics and isomers as well as to reduce the coke precursors which are the main source for coke formation. Moreover, regeneration processes have been applied to restore the catalyst activity.

A great portion of the chlorine is lost during regeneration process of the coked catalyst, in industrial reformers units. As a result after each regeneration process it is necessary to add or replenish chlorine to revert it to the initial level. Deactivation process by coking can be caused by stripping off the chlorine during reforming reactions.

The kinetics of de-coking by TGA and TPO can be used to study the mechanism of coke deposition, its nature and morphology which is critical for catalytic activity. Characterizations of the fresh and spent commercial Pt/Al<sub>2</sub>O<sub>3</sub> catalysts have been conducted by TPR, FESEM, TPD, and FTIR to have a better understanding of the onset of deactivation mechanism.

Reforming conditions which involve hydrogen partial pressure, reaction temperature and contact time which influence products distribution and selectivity can be tackled by using Taguchi analysis to fine tune product preference. Others like addition of carbon tetrachloride and dimethyl disulfide (DMDS) to feedstock are important because they can influence the catalyst activity and acidity which directly affects the selectivity of products.

### 1.3 Objectives and scope of the study

The aim of the study is focused on the following general goals.

- Effect of process variables on reforming conditions in particular temperature, H<sub>2</sub> partial pressure and contact time, on *n*-hexane reforming and reformate product species yields over a commercial Pt/Al<sub>2</sub>O<sub>3</sub> reforming catalyst.
- Optimization of the reformate products via process variables using Taguchi orthogonal array design.
- Effects of adding carbon tetra chloride as an acid booster for *n*-hexane reforming reactions and reformate product species.
- Effects of di-methyl disulfide (DMDS) on *n*-hexane reforming and reformate product species
- Kinetics and regeneration of commercial Pt/Al<sub>2</sub>O<sub>3</sub> reforming spent catalyst using thermo-gravimetric analysis (TGA) and temperature programs oxidation (TPO) and classification of coke deposits.

Under normal reforming conditions, *n*-hexane is less readily dehydrocyclized as compared to *n*-heptane. The conversion rates of *n*-octane and *n*-nonane are at least twice that of *n*-heptane [4]. But in this study, *n*-hexane has been selected as a model of the reaction, because the heavier normal paraffins such as *n*-heptane, *n*-octane, and *n*-nonane are expensive to obtain at high enough purity for analytical work, and the analysis of their reaction products is quite complex, accordingly, the kinetics of *n*-hexane reforming would seem to be the simplest choice. In spite of this, it has a poor selectivity to aromatics compared with C7-C9 paraffins, while at the same time reacting to form isohexanes with a high octane number.

The scope of the project will be carried out with an industrial naphtha reforming catalyst obtained from a local naphtha refiner. *n*-hexane will be used as a feedstock to evaluate the industrial Pt/Al<sub>2</sub>O<sub>3</sub> catalyst in a high pressure micro-reactor. The temperature used for the study will be between 623 K to 723 K (350-450 °C), pressure 300 to 700 KPa (3-7 bar), contact time 1.02 to 7.11 min.

## Chapter 2

### Literature Review

#### **2.1 Catalytic Naphtha Reforming Process**

Catalytic naphtha reforming is practiced extensively in the petroleum-refining industry to produce high-octane gasoline compounds, from low octane hydrocarbons. This is achieved mainly by conversion of straight chain paraffins in naphtha to iso-paraffins and aromatics, (benzene, toluene and xylene (BTX)) for petrochemical feedstocks over a reforming catalyst. Isomerization of straight-chain hydrocarbons to branched hydrocarbons is an important process for the production of a high-performance, clean-burning gasoline fuel in the petroleum refining industry [18].

Research octane number (RON) or octane number is generally used by refiners to evaluate and measure the performance and quality of gasoline fuel [19]. The reformate octane number can be determined by using the engine test method but, this method is not well investigated in pilot plant screening studies of reforming catalysts. The reason being it is time consuming, very expensive and not suitable for an industrial scenario as time is of the essence when it comes to optimizing the operating conditions at short notice. An alternative test to predict the RON is desirable especially if it is faster, less expensive and requires smaller samples [20]. The common practice by refiners to analyze RON is by utilizing a GC method known as PIONA analysis.

Fresh straight heart cut light naphtha comes with an octane number rating of 40 to 75 and is mostly made up of C4–C8 hydrocarbon [8, 21, 22]. Since the motor industries need gasoline with an octane rating of 85+, the naphtha has to be upgraded. One of the major upgrading reaction techniques is catalytic reforming. In catalytic reforming, the following reactions take place:

dehydrogenation of cycloalkanes to aromatics, isomerization of n-alkanes to branched alkanes, dehydrocyclization of alkanes to aromatics, and hydro-cracking or hydrogenolysis of alkanes and cycloalkanes to low molecular weight alkanes [23, 24]. A general rule to improve the octane number is by increasing the yield of multi-branched isoparaffins and reducing the content of aromatic hydrocarbons in the reformat pool (increase of isoparaffins/aromatics ration).

## 2.2 Properties of reforming reactions

The general properties of reforming reactions can be summarized as the bullets given below

- Generally, all the catalytic naphtha reforming reactions produce an increase in octane number.
- Reversible reactions usually reach thermodynamics equilibrium very rapidly while irreversible reactions like paraffin cracking are kinetically controlled.
- A high process temperature and a low pressure favor the thermodynamic equilibrium and increase the reaction rate for both the reversible and irreversible reactions. In the case of a reversible reaction like dehydrogenation of naphthenes or cyclohexanes and dehydrocyclization of paraffins there is a strong influence, but for isomerization reactions this influence is much less. For an irreversible reaction like hydro-cracking, high temperature and low pressure would seem most desirable, but the same conditions favor deactivation of the catalyst [4]. For these reasons the process operating conditions are critical.
- The two main reactions i.e. dehydrogenation and dehydrocyclization of paraffins are endothermic and generally dominate the heat balance, resulting in a decrease in temperature along the catalyst bed.
- The overall catalytic reforming process is a net hydrogen producer because of the dehydrogenation reactions involved [10].

### 2.3 Reforming mechanism

As the main reactions during the naphtha reforming process are paraffin dehydrocyclization and naphthenes dehydrogenation, the dominant products are aromatics and hydrogen. This reaction can proceed either by a monofunctional or a bifunctional mechanism. The latter mechanism has been reported to be controlled by the acid catalyzed and/or the metal catalyzed step. With the fresh catalyst, dehydrocyclization on the metal function is important, but after a few hours on stream the acid function becomes the controlling factor for this reaction [10, 24-26].

Isomerization can occur either involving only the metal function of the catalyst by the “bond shift” mechanism, or can take place by a bifunctional mechanism, whereby the *n*-alkane is first dehydrogenated by the metal function to form the alkene, which is then isomerizes by the acid function to an *i*-alkene and eventually the *i*-alkene is hydrogenated to the *i*-alkane on the metal function [27]. A schematic representation of the isomerization mechanism on the Pt/Al<sub>2</sub>O<sub>3</sub> catalyst is shown in Figure 2-1.

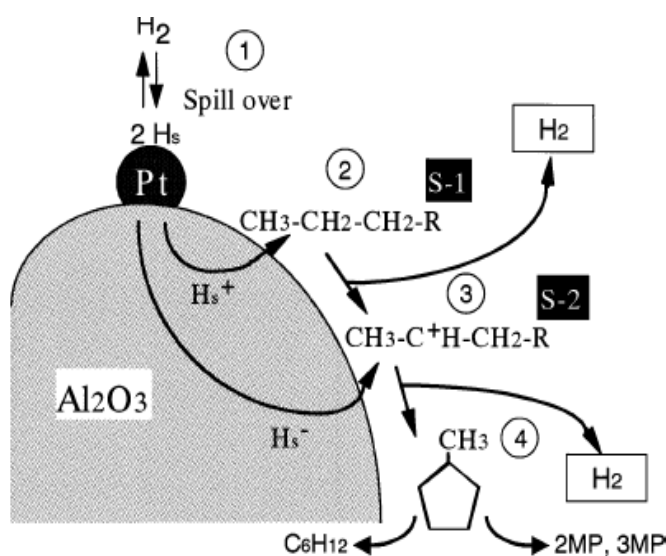
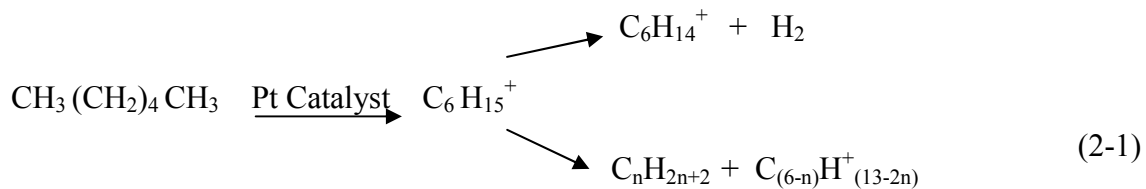


Figure 2-1: Schematic isomerization mechanism on a Pt/Al<sub>2</sub>O<sub>3</sub> catalyst. Adapted from reference [25].

The figure above illustrates the mechanism of the isomerization reaction by the spillover hydrogen that can react with paraffin(S-1) and then produce a carbonium ion (S-2), followed by cyclization to methyl cyclopentane.

## 2.4 *n*-Hexane reforming chemistry

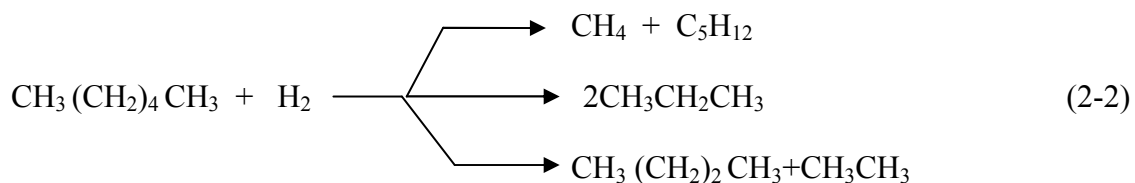
*n*-hexane is protonated by Bronstead acid sites to form a carbonium ion. A shorter paraffin chain or hydrogen and a carbonium ion are produced when the carbonium ion is cracked or dehydrogenated.



The adsorbed carbonium ion can either be desorbed as an olefin or may start the bimolecular cracking mechanism. Carbonium ions can also rearrange to get skeletal isomers. Coke is formed from the alkenes produced in the cracking reactions and proceeds through a sequence of reaction steps, i.e. protonation, alkylation, isomerization and hydride-transfer, deprotonation and ring closure, finally leading to the formation of large polyaromatic molecules [28].

### 2.4.1 *n*-Hexane cracking

The breaking of a high molecules weight C-C bond into low molecules weight compounds in reforming reactions is called cracking. An example of a cracking reaction can be referred to below.

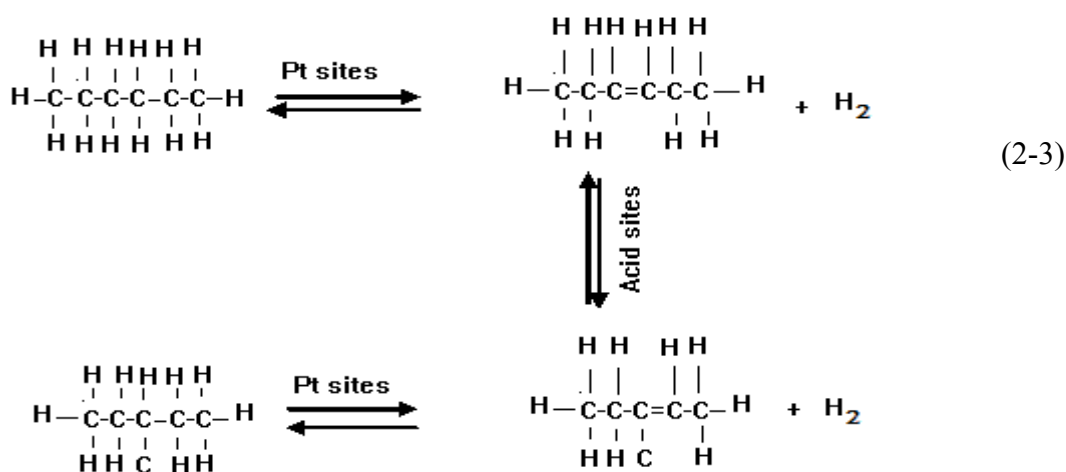


This reaction causes a significant gasoline yield loss. However, in the process, this reaction also helps improve the octane by removing the low octane number paraffins from the reformate pool by producing lighter hydrocarbons, which are outside the gasoline boiling range. This reaction is totally irreversible, exothermic and consumes hydrogen [4].

### 2.4.2 *n*-Hexane Isomerization

Isomerization of paraffin is the rearrangement of the molecule with essentially no change in yield but with a marked increase in the octane value. This is because branched paraffins in general have significantly higher octane values than their straight chain counterpart with similar molecular weight. Isomerization is a moderately fast reaction on the reforming catalyst, but not as rapid as dehydrogenation of naphthenes, but more rapid than the other reforming reactions. In the reforming process, isomerization of paraffins reaches near thermodynamic equilibrium, but since this is a very dynamic equilibrium; the paraffins continue to react in various other reactions to generate by-products. Paraffin isomerization requires the platinum function for dehydrogenation to olefin and hydrogenation of the olefin and the acid function for carbon skeletal rearrangement [4].

The isomerization reaction mechanism for *n*-hexane can be described as:

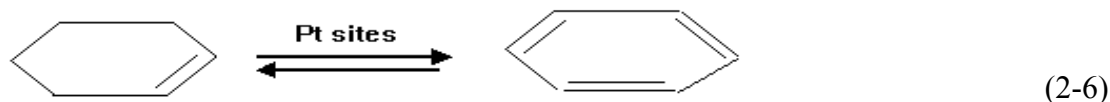
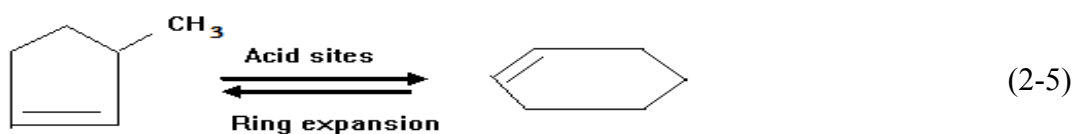
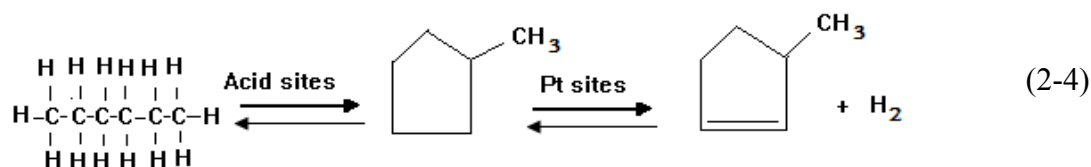


### 2.4.3 *Dehydrocyclization / Dehydrogenation Reactions*

Isomerization reactions alone are not enough to produce reformates with a high octane number. Dehydrocyclization of paraffins is the most difficult reaction to promote, but it is the most desirable reaction in reforming to give aromatics. The paraffin ring closure reactions usually occur in the acid site followed by ring expansion and finally dehydrogenation on the metal sites to produce aromatics. Dehydrogenation reactions are faster than all other reactions [4, 10]. The overall catalytic reforming reaction is

endothermic. The dehydrocyclization reactions of paraffin is endothermic typically with values of 600-1200 kJ per kilogram of feed, whereas the isomerization reactions are essentially thermal –neutral [29].

A typical dehydrocyclization and dehydrogenation are:



The dehydrocyclization of paraffins to give aromatics (benzene) (equation (2-4) to (2-6)), is an endothermic reaction promoted by high temperature and low hydrogen partial pressure. For cyclization reactions to proceed, the paraffins with a minimum of six carbons are needed. The greater the increase in the paraffin straight-chain homolog, the more readily the dehydrocyclization reaction proceeds.

## 2.5 Reforming conditions

Catalytic reforming units operate at a medium or slightly low pressure regime for optimum production of aromatics, which increases with the decrease of pressure. Some catalytic reformers operate at a low pressure of 689 kPa, while others operate at >3447 KPa. Reforming at low operating pressure involves a combination of an increase in aromatic yield and catalytic deactivation [8, 29, 30].

To elucidate the effects of hydrogen removal in the catalytic reforming of *n*-hexane (used as a model paraffin), it was found that when no hydrogen was added to the *n*-hexane feed, a gradual decrease in the conversion with time on stream was

observed [25]. This decrease may be most probably due to the deactivation of the catalyst. This undesired phenomenon was solved by adding hydrogen into the *n*-hexane feed stream. The usual practice is to add an excess of hydrogen 2–8 moles per mole of feed prior to reforming reactions [31]. Reformers designed during the 1980s however, operate in the range of 2-5 H<sub>2</sub>/hydrocarbons molar ratio and at 344.7 to 1034.2 kPa [8].

Coke formation in a reforming reaction is believed to proceed via a reversible reaction and it can be regenerated with hydrogen. This result was confirmed by Liu et al. [32]. Moreover, in their studies they showed that hydrogen plays an important role in the de-coking of reforming catalysts. The de-coking properties of hydrogen can be explained by the reaction properties given below.

- Hydrogen inhibits the dehydrogenation reactions by lowering the concentration of the coke precursors, and so less coke forms.
- Hydrogen hinders the transformation of coke from a reversible to an irreversible form by an “ensemble effect”
- Hydrogen plays a positive role in the removal of coke deposited from the catalyst by reacting with the coke precursor and as a result, retarding the formation of significant amounts of polycyclic aromatics which deactivate the catalyst.
- Lower hydrogen partial pressure favors dehydrogenation of naphthenes and dehydrocyclization of paraffins [8].

Although the reforming reactions involve the loss of hydrogen, the dehydrogenation of alkanes to unsaturated products or to aromatics can occur without hydrogen, but the active life of the catalyst is very short under these conditions. Hydrogen can form metal-hydrogen combined sites which accordingly would be the active centers for hydrocarbon reactions. The importance of the geometric configuration of diene and triene implies that an abundant supply or a real pool of surface hydrogen may be necessary to promote the trans-cis isomerization and thus reduce coke formation on the catalyst surface [31]. This would explain why an increase in the hydrogen concentration, increases the residual activity of the catalyst.

The new catalysts including the bimetallic and trimetallic catalysts have more resistance to deactivation, so low pressure operation has become routine with the application of these new catalysts. Therefore, a minimum hydrogen partial pressure must be maintained to avoid excessive coke formation. Using a large hydrogen pool could prevent the reorganization of carbonaceous species into toxic coke and avoid the deep dehydrogenating of the carbonaceous species on the metal supported catalyst [33]. At higher hydrogen partial pressure, a correspondingly higher fraction of the metallic function is freed of coke. This is because the coke on the metallic function is richer in hydrogen than that on the acid function as found by Parera et al. [6]. They found that the H/C ratio is greater when a greater proportion of the coke is on the metal, and it decreases when the coke is eliminated from the metal. The choice of hydrogen pressure for a reformer is a matter of balancing product yields against deactivation rates [3, 24].

The effect of reaction temperature in reforming processes was investigated by Bartholomew [35], and he found that a higher reactor temperature increased the octane rating (aromatics formation) but reduced run time while increasing the cracked products yield. Temperature may also be raised in case of declining catalyst activity or to compensate for lower quality feedstock. It was found that, if the catalytic reaction is conducted at a high temperature, thermal degradation may occur in the form of active phase crystallite growth, the support or carrier pore structure might collapse, and solid-state reactions of the active phase with the carrier or promoters may occur [34].

It was mentioned by Aristidis et al. [37] and Moulijn et al. [35, 36] that, coke formation is expected to increase with increasing reaction temperature. At high temperatures, poly-aromatic or even graphitic compounds are formed which deactivate the catalysts. These unwanted polymerization and unsaturated organic molecules can be present in the feed or formed as product. The effect of the reaction temperature on the deactivation by coke was mainly reported by Agbajelola et al. [25] and Patrick et al. [24, 37]. With very reactive compounds such as olefins or alkyl-aromatics at a low temperature there is generally no coke formation from paraffins or saturated naphthenes as they cannot be transformed into more reactive compounds

(essentially olefins). However, over strong acid catalysts, paraffins and naphthenes can be cracked and coke can be produced even at a low temperature.

The higher temperatures on the other hand increase the desorption rate of coke precursors. At high temperatures, the retention of coke is mainly due to trapping in the blocked pores, whereas at low temperatures, coke retention is due to a stronger adsorption that lowers the volatility of the formed molecules. The results by Parera et al. [6] showed that, the operation temperature does not influence the nature and position of the coke whereas, increasing the pressure and time on stream produces a decrease in the H/C ratio of coke. The catalyst activity, selectivity and stability are influenced by temperature, time and partial pressure of hydrogen [38].

## **2.6 Reforming catalysts**

Alumina supported Pt catalysts are very important for many industrial processes including oxidation, reforming, hydrogenation processes and others. The naphtha reforming catalysts contain both metal and acid functions. An adequate balance between both functions (metal and acid) is important to achieve a high selectivity of aromatic hydrocarbons and a low coke deposition rate [39].

Platinum is a key ingredient in most dehydrogenation catalysts due to its high activity for C-H bond rupture coupled with its poor ability to cleave C-C bonds. Improvements in selectivity and in particular with respect to the catalyst stability towards deactivation due to coking may be achieved by catalyst modification with the addition of a promoter [40]. Although a number of patents have emerged over time using different recipes and metals, Pt still remains the major active component for all modern naphtha reforming catalysts. The addition of a second metal like Re, Ge, Sn, Pd, Ag or Pb, can be used to modify the catalytic properties of mono-metallic Pt catalysts, but this modification is based on electronic and/or geometrical considerations [5].

Iridium–platinum catalysts have been used for naphtha reforming, and one of the roles of the platinum may be to combine with the iridium in alloy like bimetallic clusters to suppress an undesired structure-sensitive reaction, via, paraffin hydrogenolysis [41]. Platinum is more active than any other known metal (except

iridium) in a number of reactions that increase the octane number of paraffins without substantially changing their molecular weights. These reactions include dehydrogenation, such as conversion of methylcyclohexane to toluene, dehydrocyclization of paraffins to aromatics, e.g. the conversion of *n*-heptane to toluene, and the skeletal isomerization which is also a desired reaction, but this reaction is mainly acid catalyzed, and Pt atoms have only a low activity for this type of reaction [10].

Some of the new catalysts formulations have a higher resistance to coke deactivation and a higher selectivity to aromatics and isoparaffins. They also enabled the process to be performed at a lower pressure [2, 18, 42, 43]. With regards to Pt and Re catalysts, Pt is a better dehydrogenation metal than Re and it can be explained by the fact that benzene formation is higher on Pt/Al<sub>2</sub>O<sub>3</sub> than on Re/Al<sub>2</sub>O<sub>3</sub> [9]. On the contrary, Pt-Re catalysts promote hydrogenolysis reactions and it retards coking activity during hydrocarbon reforming reactions [44-47]. Although Pt-Re/Al<sub>2</sub>O<sub>3</sub> and Pt-Ir/Al<sub>2</sub>O<sub>3</sub> bimetallic catalysts had a high hydrogenolytic activity producing methane and other light alkanes, this drawback (hyper hydrogenolysis) can be eliminated by pre-sulfiding the catalysts. Unfortunately, these treatments make the activation process difficult [48].

On the other hand, Pt-Ge/Al<sub>2</sub>O<sub>3</sub> and Pt-Sn/Al<sub>2</sub>O<sub>3</sub> catalysts have the advantage of not needing pre-sulfidation. This enables their use in processes with continuous catalyst regeneration. The Pt-Sn/Al<sub>2</sub>O<sub>3</sub> catalyst is one of the most important catalysts for reforming and dehydrogenation of hydrocarbon feedstock [14]. Geomar et al. [49] reported that, the addition of Sn to supported Pt catalysts has a significant effect on catalytic behavior. Sn strongly interacts with the alumina support and if present as Sn (II) it weakens and reduces the number of acid sites on alumina and also eliminates basic sites. Luciene et al. [39], explained that the electron transfer from tin to platinum makes the Pt-C bond weaker, thus increasing the resistance against coke formation. It was pointed out by Luciene et al. [39], that Pt-Sn systems have a better selectivity to aromatic hydrocarbons compared to Pt and Pt-Re due to the inhibition of hydro-cracking and coke deposition on the surface of the catalysts.

Study by Matussek et al. [50] on “Reactions of *n*-hexane on Pt-Sn/Al<sub>2</sub>O<sub>3</sub> and removal of retained hydrocarbons by hydrogenation”, they found that there are three

types of carbonaceous deposit on Pt/Al<sub>2</sub>O<sub>3</sub>. These are; one on metal particles, another on the metal– support perimeter and the third one entirely on the support. Tin removes some of the carbonaceous deposits on the catalyst surfaces, which blocks the passage to the catalyst active site. Addition of Sn to Pt inhibits the carbon deposition on metallic surfaces [51]. The modification of Pt/Al<sub>2</sub>O<sub>3</sub> catalyst studies conducted by Ordonez et al. [52], using vanadium caused a slight decline in the catalysts activity but, proved to be more resistant to deactivation.

The latest improvements in the naphtha reforming technology have been aimed at increasing the length of the operation cycle time and for this purpose new trimetallic catalysts have reached the market. These bifunctional trimetallic catalysts are gradually replacing the previous industrial bimetallic catalysts because of their higher stability, selectivity and adaptability to different feedstock and resistance to poisons [2]. Epron et al. [53], found that the addition of tin on a bimetallic Pt–Ir catalyst can replace the sulfiding step that is necessary to decrease the hydrogenolysis activity of this type of catalyst. A

Additions of small amounts of Ge in trimetallic Pt-Re-Ge/Al<sub>2</sub>O<sub>3</sub> catalysts produce some improvements in the liquid yield and the catalyst stability [18]. The modification of the Pt–Re/Al<sub>2</sub>O<sub>3</sub> by decationized NaY and NaZSM-5 zeolites were found to increase the isomerization activity [54].

Finally the tri-metallic catalysts are more resistant to deactivation by coke deposition and have better selectivity to isomers and aromatics (high octane products) than mono and bi-metallic catalysts.

## **2.7 Effects of sulfur on reforming catalysts**

The effect of sulfur on coking rate of reforming catalyst is still a matter of debate. The reforming catalysts activity may be completely lost, because of sulfur poisoning. In order to avoid sulfur poisoning, it is recommended that the reforming feed should not contain more than 1 ppm of S. On the other hand, sulfur is not totally unwanted, because a low concentration of sulfur in the feed or during the start-up of units can suppress excessive hydrogenolysis at the beginning of the run and improve the catalyst stability [19, 55]. Sulfur affects both the nature and location of the coke

deposit. It has been proposed that coke is more dehydrogenated and located mainly on the support on sulfided catalysts. Sulfur greatly reduces the hydrogenolytic activity of the catalyst, increasing the amount of dehydrogenated compounds that desorbs from the metal function of catalysts [8, 56].

Reports from [34, 57] suggested that the pre-sulfided reforming catalyst has a great impact on reducing the hard coke, which is mainly responsible for the catalytic deactivation. These demonstrations were reported by Carvalho et al. [28] and Parera et al. [6, 27] that the pre-sulphidation of the skewed catalyst is widely applied to control the hyper- activity towards hydrogenolysis reactions. For the bimetallic Pt-Re catalysts in their partially sulfided form, the experimental results by Parera et al. [6], indicates that the skewed metal catalyst produces more gases and aromatics than the balanced metal catalyst. Sulfur increases the dehydrogenated activity due to the Pt-Re-S interaction and at the same time decreases the metal ensemble size resulting in a higher amount of coke and fewer cracking activities [55, 56, 58].

James et al. [45], suggested that the electron acceptor properties of sulfur decrease the electron density on the Pt metal. The electronic properties of metal are changed when sulfur is incorporated into the catalyst. This results in a weak Pt-H bond formation as electrons are transferred from platinum to sulfur. Sulfur not only drastically changes the coke profile on Pt-Re but also the amount of coke, its nature and its distribution on the Pt-Re /Al<sub>2</sub>O<sub>3</sub> catalyst [33].

It was reported by Querini and Fung [58] that, the coke deposition rate on the catalyst depends on the concentration of sulfur and chlorine in the system. However, the influence of chlorine is smaller than that of sulfur when the coke precursor formation is concerned. The investigation made by Jovanovic et al. [59] suggested that, the role of Re for hindering the polymerization reactions is improved when sulfur incorporates into the rhenium atoms.

The Pt/ Al<sub>2</sub>O<sub>3</sub> and Pt-Re/ Al<sub>2</sub>O<sub>3</sub> reforming catalysts activity was significantly decreased by adsorbed sulfur, which deactivated the catalysts by dilution of surface active sites [60]. It was reported by Lin et al. [47] that, the addition of Pd to the supported Pt catalyst evidently improves the sulfur resistance of the catalyst. The explanation was that, the electrons are transferred from Pt to Pd by bimetallic

interactions. The decrease of electron density on Pt inhibits H<sub>2</sub>S adsorption and thereby enhances catalyst sulfur resistance.

## **2.8 Catalysts acidity**

The regeneration process practiced by a local refiner is divided into 3 main areas which include; a burning zone, a chlorination zone and a drying /cooling zone.

In the burning zone, the spent catalyst from the bottom of the reactor first enters the regeneration tower where coke is burnt off the catalyst in the presence of heat and air. The amount of oxygen used is vital and is maintained at 0.6 - 0.8 mol %. Greater than this level can lead to a high temperature runaway which could destroy the catalyst morphology. Low oxygen levels, on the other hand leads to incomplete catalyst regeneration.

After coke burning, the catalyst gets chlorinated in the chlorination zone. A chlorinated compound containing adequate chlorine is injected into this zone in the presence of air. The main function of chlorine addition is to re-disperse platinum on the catalyst surface [8]. Most of the naphtha reforming processes have chlorine compounds added in the hydrocarbon feed [30]. The actual amount of chlorine added is dependent on the humidity of the recycled gas & feed and the reactor temperature. Chlorination is also important, as a certain amount of chlorine is needed on the catalyst to boost catalyst activity. It is also important to ensure that all coke is completely burned in the burning zone so that no coke is present in this oxygen rich environment.

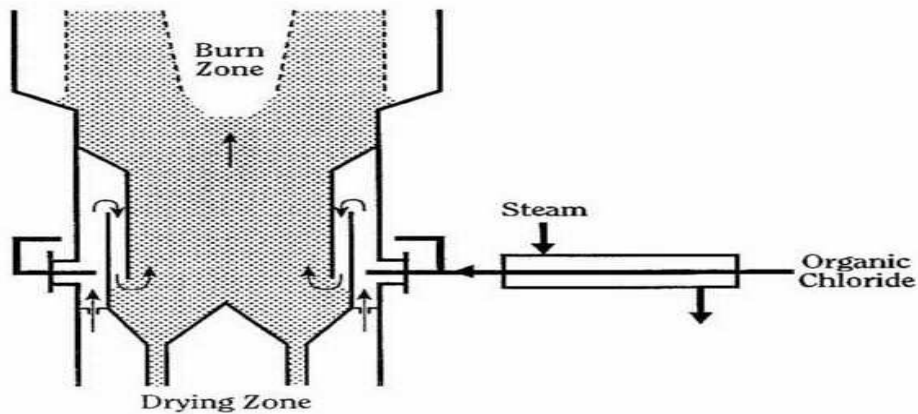


Figure 2-2: Chlorination zone in the regeneration tower

In the drying zone, the water accumulated on the catalyst from the burning zone and chlorination zone is removed in this stage. Too much water will cause the chloride to be stripped off from the catalyst in the reactor. Thus the catalyst is first dried using hot air and then cooled using cold air before leaving the regenerator and entering into the reactor.

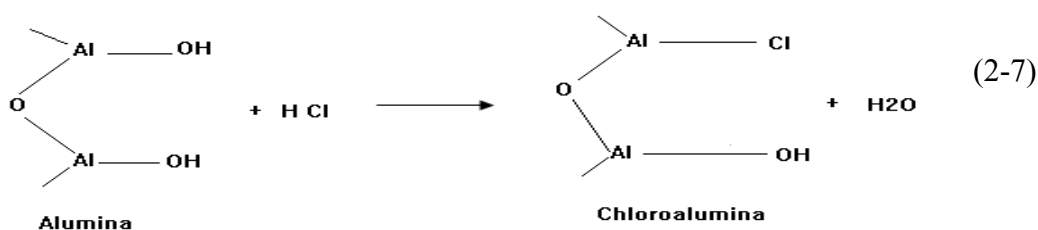
Catalytic naphtha reforming catalysts are bi-functional in nature; the metal function is provided by platinum and the acid function is provided by the high specific surface area alumina whose intrinsic acidity is enhanced by chlorine. Maintaining the balance between metal and acid function is a critical issue for optimizing the performance of the catalyst. A desirable amount of 0.8-0.9% chlorine concentration is generally used in several commercial reforming catalysts and the operation of a reforming process is strictly maintained to keep chlorine between these limits [30].

Mazzieri et al. [19] and George et al. [8, 18], reported that, both strong and weak acid are undesirable for reforming reactions, as it will increase catalyst deactivation. Milder acid strengths are beneficial for the isomerization rate due to the reduction of consecutive cracking and polymerization reactions.

Moisture in the naphtha feed and chlorine concentration in the catalyst are the two main keys which control the acidity of the catalyst under actual reforming conditions [30, 31]. Water enhances the Bronstead acid sites on the alumina support but, when the level of water exceeds 20 ppm, it becomes undesirable as it strips off the chlorine from the catalyst, thereby lowering the catalyst acidity. In such cases, stripping of

chloride from the catalyst in wet conditions and a high temperature results in the formation of HCl which may cause the acute corrosion in downstream equipment if not controlled. On the other hand, working under dry conditions is also not good for the catalyst and products. In the later (dry) condition, it will destroy the acid sites as there is no regeneration of acid sites to compensate for those deactivated by coke deposits.

Water is necessary to ensure a homogeneous distribution of chloride on the catalyst. Water-chloride balance can be restored according to the following reaction as given by George et al. [8].



In reforming catalysts, the catalyst chlorination is usually performed by injection of chloro-carbon or chloro-compounds with sulfur into the feed [21, 29, 30, 61]. Some reforming units use a mixture of HCl and water according to a preset industrial level, while others injected the carbon tetrachloride (CCl<sub>4</sub>) in ppm proportion to enhance the acidity of the catalyst. Studies by George et al. [8] on the effects of chloride agents such as, CCl<sub>4</sub> and/or HCl on the selectivity for the hydrogenolysis and the isomerization reactions over a Pt/alumina catalyst, suggested that, there is only a minor decrease of the hydrogenolysis reactions for the catalyst chlorided with HCl gas. Chlorinating with CCl<sub>4</sub> is more effective in influencing the Pt sites responsible for hydrogenolysis [21]. They found that injection of about 2–3 % of CCl<sub>4</sub> at high temperature 673 K (400 °C), the CCl<sub>4</sub> is converted to coke which is deposited on the catalyst surface.

The study made by Geomar et al. [49] reported that, the presence of chlorine produces a more uniform deposition of Pt over the alumina. Chlorine addition has a positive effect by improving the dispersion of the metallic phase over the support. Unfortunately, in a bimetallic catalyst, chlorine destroys the interaction between the

metals. Study done by Pieck et al. [62], on the influence of chlorine over the Pt-Re interaction and their catalytic properties, they found that, chlorine inhibits Pt-Re interaction and produces a decrease in the coke deposition over the metallic function. Chlorine has two opposite effects; first, it influences the spillover of hydrogen from the metal to the support, and via hydrogenation reactions where the coke precursors can easily be eliminated; secondly, the polymerisation of coke precursors is enhanced by the addition of chlorine [62].

During the regeneration process (burning the coke) of the Pt/Al<sub>2</sub>O<sub>3</sub>-Cl catalyst system under oxidizing atmospheres, the formation of water at high reaction temperature cause the platinum crystallites to grow (sintering process). In order to re-establish the platinum dispersion and to restore the acidity of the support, the catalyst undergoes an oxychlorination treatment followed by reduction. Borgna et al. [63], reported that, the addition of chlorinated compounds to the oxidizing mixture during the regeneration process inhibits the platinum particle growth (reduces sintering). Fung [64] also found that the re-dispersion of agglomerated metal catalysts involves a direct reaction between the catalyst and reactive gaseous components such as Cl<sub>2</sub>, HCl, O<sub>2</sub> and H<sub>2</sub>O, and it is directly dependent on the oxygen and chlorine partial pressures. Oxychlorination treatment applications are most common in catalytic reforming units (CRU) using continuous catalytic regeneration (CCR) cycles rather than adding the chlorine to reforming feed. These treatments can restore almost completely the original acidity of the catalysts [12].

Chlorine was analyzed by dissolving the catalyst with sulfuric acid by distillation followed by titration of the distillate according to the method of Volhard-Charpenter, [5, 18, 30, 65].

Catalyst acidity of the reforming catalyst can be done by using temperature program desorption of pyridine (TPD) [27, 65]. Here pyridine is adsorbed on acid sites due to its basic character at low temperature. Desorption pyridine content at low temperatures is related to the presence of weak acid sites while desorption at high temperatures is related to the presence of strong acid sites. The total area under the TPD trace is representative of the total acidity of the catalyst.

## 2.9 Catalysts deactivation

### 2.9.1 Mechanisms of Deactivation of Heterogeneous Catalysts

Table 2-1: Describe type, mechanism, and definition of the catalysts deactivation

Number	Mechanism	Type	Definition/description
1	Poisoning	chemical	Strong chemisorptions of species on catalytic sites which block sites for catalytic reactions(sulfur compounds)
2	Fouling	mechanical	Physical deposition of species from fluid phase into catalyst surface or catalyst pores (carbon or coke)
3	Thermal degradation	thermal	Thermal loss of catalytic surface area, support area and active phase support reactions
4	Vapor formation	chemical	Reaction of gas (oxygen) with catalyst phase to produce volatile materials (oxides compounds)
5	Vapor-solid and solid-solid reactions	chemical	Reaction of vapor, support or promoters with catalytic phase to produce inactive phase
6	Attrition/ crushing	mechanical	Loss of catalytic materials due to abrasion loss of internal surface area by mechanical induced crushing of the catalyst particles

Deactivation of a reforming catalyst is an important topic not only for the future development of a more stable catalyst, but also for the operational control for a commercial reformer and its catalyst regeneration processes. There are many reasons why catalyst deactivation takes place. Some of these reasons include fouling by carbon or coke, which are produced by condensation of unsaturated hydrocarbon (olefinic compounds). Others may come about from poisoning materials present in the feedstock which can chemisorb on the catalyst active site and totally deactivate the catalyst. Additionally, the catalyst thermal degradation or sintering process (metal growth) may occur if the catalytic reactions are conducted at high temperatures. Furthermore, collapse of the support pore structure and solid–state reactions between the active phase and promoter or support may also happen at high temperatures. The catalysts used in power plant flue gas can be deactivated by dust and plugged with fly ash. Based on the following assumption given above, the mechanisms of solid catalyst deactivation can be grouped into six intrinsic mechanisms of catalyst decay as mentioned in Table 2-1. adapted from references [34, 41].

### ***2.9.2 Coke deposits on the catalyst surface***

During hydrocarbon reactions catalyzed by solid acidic catalysts, the catalyst always suffers from strong deactivation due to formation and retention of heavy byproducts, so-called coke, which deactivates both metal and acid sites of the catalysts. Coke components can be classified into coke precursors and hard coke, [62, 66]. The coke precursors or reactive coke are the coke components that can be removed from the coked catalyst sample simply through volatilization in inert nitrogen, while the hard coke or un-reactive remains on the catalyst even at high temperature (873 K) and can be removed by burning in diluted oxygen gas.

Studies conducted on the deactivation of naphtha reforming catalysts by coke deposition cover a broad spectrum of problems: starting from the role of coking in catalyst degradation to the effects of numerous process parameters on the rate of carbon deposition, its mechanism such as the nature and morphology of coke, the quantity and distribution of coke between metal clusters and the support, and the degree of condensation of coke and its nature which depend on the catalyst, feed and

operation parameters in the reforming process [67]. It has been shown by Jovanovic et al. Wang & Manos and Govind et al. [31, 59, 66] that, trying to model the kinetics of the coking process based only on the amount of coke deposited on the catalyst while ignoring the location and molecular structure of coke, may be erroneous and misleading.

The investigation made by Borgna et al. [9] on the simultaneous deactivation by coke and sulfur of monometallic Pt/Al<sub>2</sub>O<sub>3</sub> and bimetallic Pt–Re (Ge, Sn)/Al<sub>2</sub>O<sub>3</sub> catalysts by using *n*-hexane reforming as a bi-functional test reaction and thiophene as a poisoning molecule, demonstrated that, at the beginning of the reaction test, acid-controlled isomerization reactions such as the selectivity of *i*-C<sub>6</sub> isomers are only marginally affected by coking over all the catalysts. The explanation provided by them was that in the short-term catalytic tests, coke precursors are essentially formed on the metallic function. The coke precursors (unsaturated compounds) are mainly aromatic and/or olefinic hydrocarbons, which are either contained in the starting materials or are formed as intermediate products in the process [68].

In the study of the effects of Sn on Pt catalyst by Hill [7], it was mentioned that, during the reaction between hydrocarbons and the Pt–Sn catalyst, Sn weakened the chemisorptions bond (Pt–C), thereby enhancing the migration of the carbonaceous species away from the Pt sites and support. Sn suppressed catalyst deactivation even while having a higher coking rate than the other catalyst without Sn. This is because the transportation of coke from the active sites becomes easier when tin joins the catalyst. This theory is supported by temperature programmed oxidation, which showed that tin-promoted catalysts had higher peak temperatures meaning that the coke is on the support rather than on the platinum atoms.

It was shown by Macleod et al. [69] that, the weakening Pt–C bond strength on adsorption of alkane reactants makes the catalyst less susceptible to deactivation by carbonaceous species onto the metal surface and it also alters the products selectivity. Another study by Hill [7] explained that, Pt single crystals are very effective hydrogenation-dehydrogenation catalysts, even when the catalyst is extensively covered by carbonaceous deposits.

Coke can basically be classified as two types of carbonaceous deposits: one of a low polymerization degree (H/C atomic ratio about 1) deposited on the metal which can be referred to as 'soft coke', and the other of a higher degree of polymerization (H/C ratio about 0.5) deposited on the support referred to as 'hard coke' [67, 70, 71]. It was shown by Zhongmin et al. [72] that the carbonaceous materials formed on different zeolites are different in nature based on H/C ratio. The coking reaction on an HZSM-5 zeolite takes place not only on the outer surface, but also inside the pores and channels with the species of  $-(CH_2)$  or cyclo-paraffins and some mono-cyclic aromatics as coke precursors.

The deactivation studies by Jovanovic et al. [59] on coke deposited on bi-metallic catalysts and mono-metallic catalysts proved that, during the reforming reaction, coke accumulates in the catalysts pores and it shifts the mean pore diameter towards the lower values in the case of a mono-metallic catalyst. The demonstration according to [70] was that, in mono-metallic catalyst the coke occupies the pore wall thereby moving the mean pore diameter towards the lower values. But in the bi-metallic catalyst, the coke fills the pores entirely and the mean pore diameter moves towards the higher values.

### **2.9.3 Mechanism of coke formation**

Deactivation of supported metals by carbon or coke may occur chemically due to chemisorptions or carbide formation, or physically due to adsorption in multilayers. In both cases, it was shown by Calvin & Bartholomew [34] that, carbon blocks access of reactants to metal surface sites, accordingly the metal crystallites are totally deactivated and encapsulated by carbon (see Figure 2-2). These carbonaceous species causes plugging of the catalyst micro- and mesopores. Sometimes the access of reactants is denied to the many crystallites inside these pores to the extent that they stress and fracture the support material, eventually, destruction of catalyst pellets by carbon filaments, and plugging of the reactor void occurs.

The mechanism of coke formation will depend on the catalyst pore structure, acidic properties, the nature of reactants and reaction conditions [37, 70]. The

dependence of coke on the reactants (hydrocarbon feed) is reported in Table 2-2: by Hsu et al. [29].

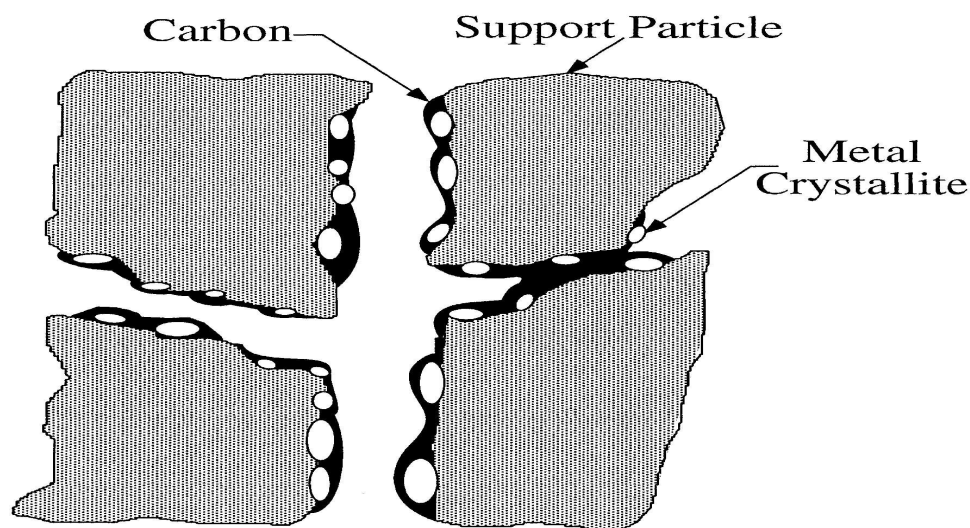


Figure 2-3: Fouling, crystallite encapsulation and pore plugging of a supported metal catalyst due to Coke accumulation on the catalyst adapted from reference [34].

Two mechanisms of coke formation proposed by George et al. [8] are given below.

- (i) The first mechanism suggests that successive dehydrogenation reactions lead to the formation of carbon atoms. These atoms may combine by polymerizations reactions to form more graphitic and more toxic coke deposits.
- (ii) The routes of coke deposition are based on polymerization reactions with the formation of different types of carbonaceous deposits on the catalyst surface.

At the beginning of the operation cycle, coke is rapidly deposited on the metal. Some bare metal islands remain uncovered in a pseudo stationary state, after that it remains constant when coke continues to be accumulated on the acidic support [8, 44, 73]. George et al. [8], showed that with the increase in the metallic dispersion, the coke coverage on the metallic phase decreases at a steady state. Increasing the platinum content, with the same metallic dispersion, increases the amount of coke on the whole catalyst.

Table 2-2: Coke percentages of various reforming hydrocarbons at same reforming conditions (773 K, 101 KPa, WHSV=2, H<sub>2</sub>/HC = 4, run length=5 h), [31].

Feed hydrocarbon	Coke yield (Wt %)	Feed hydrocarbon	Coke yield (Wt %)
<i>n</i> -hexane	3.5	benzene	0.3
<i>n</i> -nonane	4.4	Ethyl benzene	2.3
Cyclohexanes	0.1	Indan	25
1,2-dimethylcyclohexane	2.1	Methylcyclopentane	13
Methylcyclopentane	37	Cyclo pentadiene	67

#### 2.9.4 Coke characterization and regeneration

Characterization of coke depends on three factors which are the most important; the nature (H/C ratio), amount and distribution of coke (coke location). Although coke has different natures, the oxidation of coke usually applies to reactivation of the catalyst. The coke combustion is typically carried out in diluted air, but in some cases partial coke removal is achieved with hydrogen or inert gases [74]. Studies done by Guisnet et al.[76] and Patrick et al.[37, 75] on the nature of coke in zeolite were conducted using methods of dissolving the catalyst with a solution of hydrofluoric acid because it does not modify or alter the coke particles. Wang [76], studied the coke molecules and their nature and distribution which are generally formed and trapped in catalyst micropores using GC/MS coupling or MS, UV-VIS and IR recovered by using dichloromethane (soluble coke).

Other studies by other researchers used Fourier Transform IR Spectroscopy to analyze the structures of adsorbed molecules on a catalyst surface (soluble coke), and

it has applicability in investigating the structure of carbon deposits on supported metal catalysts [48]. The insoluble coke which is composed of highly polyaromatic compounds are analyzed by temperature program oxidation (TPO) [17, 40, 48, 51, 73] or by thermo gravimetric analysis (TGA) [11, 28, 77, 78]. For the study on the characteristics of coke in the MTG Process FTIR technique was used by Pedro et al. [79] to characterize the soluble coke at different reaction temperatures. The FTIR analysis was applied by Li et al. [80] to study the soluble composition of the coke deposits on a spent industrial reforming Pt–Sn/-Al<sub>2</sub>O<sub>3</sub> catalyst, detection of polycyclic aromatic compounds such as chrysene was noted. Similar technique was applied by Karge et al. [81] to study the effect of coke deposition on zeolite catalysts during hydrocarbon reactions.

Two types of coke were described by Pedro et al. [79] over H-ZSM5 Zeolite which include light coke (high H/C ratio), which is soluble in pyridine, and heavy coke (low H/C ratio), insoluble in pyridine. It was observed that temperature noticeably affects not only the content of coke but also its nature. It was found that the H/C ratio decreased with increase in reaction temperature. This means the soluble light coke decreases and the insoluble heavy coke increases when reaction temperature is increased simultaneously.

The investigation of de-coking conducted by Parera and Macleod et al. [69, 73], explained that the coke burning at low temperatures corresponds to highly hydrogenated coke, which deposits on the metal function. Whereas the coke that burns at high temperatures corresponds to amorphous polymerized coke, deposits on the acid sites of the support. The de-coking process follows the same sequence to that of the deactivation by coke formation. The elimination of coke by TPO occurs first on the metallic function where the metallic activity is recovered. Then, towards the end of the regenerating process, coke is eliminated from the acidic function resulting in the recovery of the catalytic activities for reactions of dehydrocyclization and isomerization [73].

In the study of the regeneration and rejuvenation of naphtha reforming trimetallic catalysts, it is well demonstrated by Vanina et al. [12] that, the fully regenerated trimetallic catalysts have a higher activity than the fresh ones, indicating that the

metal promoters become segregated during the coke burning-off. Therefore the concentration of free Pt sites and the dehydrogenation activity are increased.

Periodic reactivation of the catalyst is necessary to save cost and time. This periodical regeneration can be done by burning the coke off at controlled conditions. Optimizing the operating conditions, such as, temperature, heating rate and time of regeneration were cited in literature. JGlio et al. [82], reported that low heating rates are usually maintained for good regeneration processes. It was found that, the catalyst activity decreased by 30% when the catalyst was regenerated at a high heating rate.

Combustion temperatures, which is probably the most critical parameter in a regeneration process because of its impact on the stability of the metallic phase and the support [82]. In addition to de-structuring of the metallic phase (agglomeration, crystallization or volatilization), sintering of the support and reaction of the catalytic phases themselves or with the support (thus forming inactive species) may occur.

Ordonez et al. [52], in their study using vanadium-modified Pt/Al<sub>2</sub>O<sub>3</sub> catalysts, noticed that the lower combustion temperature of coke deposits on the Pt catalysts would indicate that their H/C or H/Cl ratios being higher. For a regeneration temperature, which is normally above 773 K (500 °C), extra care must be taken to properly control temperature runaway resulting from coke ignition. Time for regeneration, another important criterion, must also be accounted for as it is directly dependent on the regeneration temperature. A short regeneration cycle only allows a partial recovery of the catalytic activity [82].

In general, the oxidation reactions for all types of coke are highly exothermic, as indicated by the formation enthalpies of the oxidation products. Exothermicity of the catalyst reactivation by coke oxidation is one of the key concerns in the design of a regenerator. If the rates of the reactions are not closely controlled, the generated heat may cause damage to the catalyst and the regeneration unit. If a safe operation is to be devised, the reaction rates occurring in the regeneration unit must be known. A kinetic model that describes the rates of regeneration reactions is therefore needed for the design of a catalyst regeneration unit [74].

### 2.9.5 Prevention of coke formation

Catalyst deactivation is a common problem in the petrochemical industry. This phenomenon has negative consequences on the activity and selectivity of the catalyst. Deactivation in the reforming process is caused by coke formation and deposition. The coke is derived from the degradation of reactants or products subject to successive condensations with elimination of hydrogen [83].

Table 2-3: Elimination of the catalyst deactivation by catalyst and process modification. Taken from [41].

Process modification	Catalyst modification
Change reaction conditions: Temperature, Flow rate, Pressure, space velocity, Feed composition ....etc.	Change materials: Different promoters, supports and active phases
Reactor modification: Different reactor geometry, multiple reactor stages, different reactor type	Optimize catalyst: Density, porosity, distribution of active phase in catalyst pellet
Remove poisons: Guards beds, purifications, overdesign of catalyst bed	Modify Preparation method: Impregnation vs. precipitation, drying and activation temperature, heating rate and reducing agent.
Change operating strategy: Increasing temperature with time, swing reactors, continuous regeneration	Modify forming method: Monolith vs. pellet vs. extrudates, spray drying and binders.

General methods of elimination of the catalyst deactivation are mentioned in Table 2-3. In coke or carbon formation, one important fundamental principle must be underlined i.e. carbon or coke results from a balance between the reactions that produce atomic carbon or coke precursors and the reactions of these species with  $H_2$ ,  $H_2O$ , or  $O_2$  to remove them from the catalyst surface. If the conditions favor formation over gasification, these species accumulate on the surface and react further to less active forms of carbon or coke, which either coat the surface with an inactive film or plug the pores, causing loss of catalyst effectiveness, pore plugging or even destruction of the support matrix.

The formation and growth of carbon or coke species on metal surfaces are minimized by choosing reaction conditions that minimize the formation of atomic carbon or coke precursors and by introducing gasifying agents. Regarding the catalyst modification, coke can be minimized by using a catalyst with a small crystal size. This result was proven by Patrick et al. [37]. They found that, when a large crystal size HBEA zeolite was used, the deactivation by coke formation was enhanced resulting in rapid deactivation due to the large crystal size of the zeolite and the low diffusion of coke-makers (aromatic and olefins) through the crystallite of these BEA zeolite forms. From their studies, they concluded that small crystallite zeolites are more appropriate to deter coke formation and catalytic deactivations since large crystallite zeolites retain coke-makers better than their smaller counterparts, resulting in enhanced coke formation and rapid catalyst deactivation.

## Chapter 3

### Experimental Work

#### 3.1 Research Materials

##### 3.1.1 Catalyst Properties

The table below describes the textural properties of commercial Pt/Al<sub>2</sub>O<sub>3</sub>:

Table 3-1: Textural properties of Pt/Al<sub>2</sub>O<sub>3</sub> fresh commercial catalyst

Catalyst particles size	0.39-0.40 mm
Surface area of Pt/Al <sub>2</sub> O <sub>3</sub>	150 m <sup>2</sup> /g
Pore volume	0.6 cm <sup>3</sup> /g
Bulk density	0.67 g/cc
Average pore diameter	164 Å

##### 3.1.2 Gases and Chemicals

The following chemicals were used in the study

- Hydrogen gas with a purity of 99.9% from MOX, used for reduction.
- Pure nitrogen gas with a purity of 99.90% from MOX, used for releasing the hydrogen and other sample impurities after reduction.
- 5% H<sub>2</sub> in pure N<sub>2</sub> reducing gas obtained from MOX.
- RGA (standard gas) for GC calibration from Agilent company
- *n*-hexane of analytical grade (Merck, ACS, 99.8% purity) used as a reforming feedstock.

- Carbon tetra-chloride (CCl<sub>4</sub>) with a purity of 99.9% obtained from Merck, used for acid chlorination.
- Dimethyl-disulfide with a high purity of 99.9% obtained from Merck is used as a sulfiding agent.
- Fresh and spent commercial reforming Pt/Al<sub>2</sub>O<sub>3</sub> catalyst with 0.29 wt % Pt content.

### 3.2 General Description of Reactor Rig

A schematic diagram of the reactor set up is shown in figure 3-1. The reactor consists of a control panel (1); which consists of a temperature display and controller, main switch, safety switch and valve switches. Also, the reactor contains the liquid reactant tank (2), high pressure pump (3), and stainless steel SS316 catalyst basket, which is 30mm long and has a cylindrical chamber with several channels at the bottom to allow the reaction products to pass through it (4). The catalyst basket can be removed and tightened by using a custom-made Allen key rod. The crushed catalyst sample (5) was loaded inside the cylindrical basket. This reactor system is equipped with a split-type electric tubular furnace (custom-made) with controllable temperature from ambient to 450 °C and accuracy of  $\pm 0.5$  °C (6&7). Two cylinder gases have been used, a nitrogen cylinder (8) and a hydrogen cylinder (9) connected with a gas flow meter (10), in order to maintain the flow rate. The product effluent is heated up using an external heater (11), before being sent to GC (12).

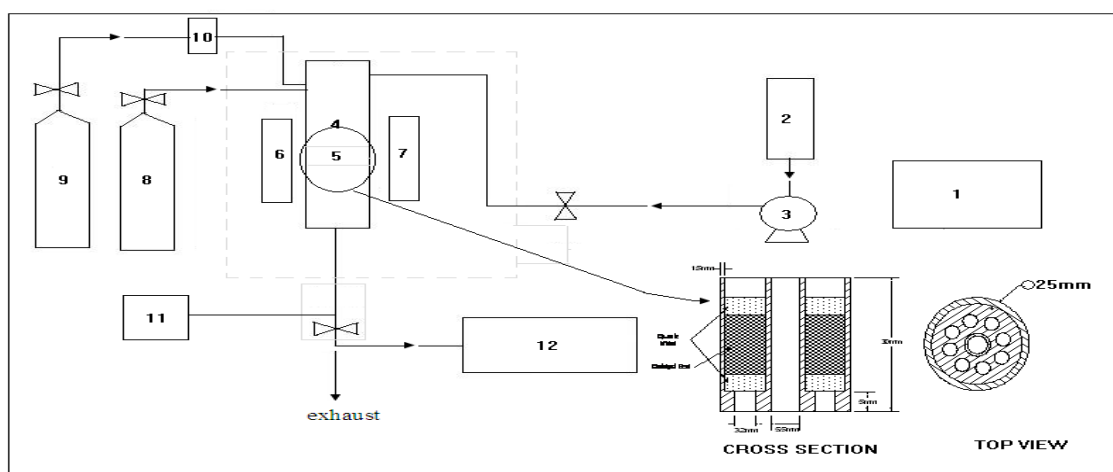


Figure 3-1 A schematic diagram of the basic parts of a micro-tubular reactor

### 3.2.1 Micro-Tubular Reactor

This reactor rig was supplied by Biofoam engineering Sdn. Bhd., Shah Alam. It consists of top and bottom support flaps tied with cylindrical steel. The reactor tubular body was fabricated from stainless steel SS 316. The body of the micro-tubular reactor has the dimensions of 25mm I.D., 60mm O.D. and 500 mm length. Permitting a total reactor volume of  $2.45 \times 10^{-4} \text{ m}^3$ .

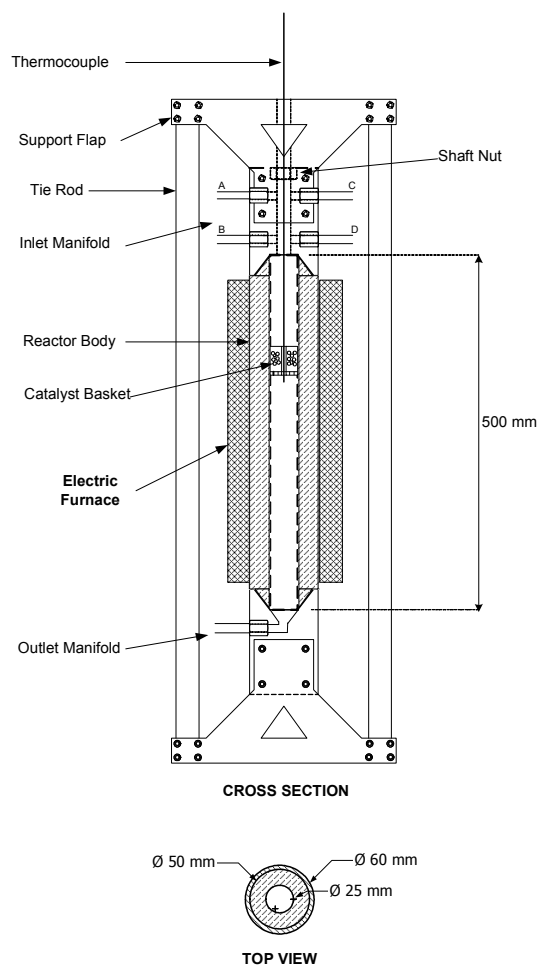


Figure 3-2: High-pressure micro tubular reactor schematic diagram

The micro-reactor is equipped with four different inlet manifolds (labeled A, B, C and D) located on the top side. Label (A) for the n-hexane flow into the reactor, and (B) for the  $\text{H}_2$  gas. A height-adjustable K-type thermocouple probe was tightened on the top side of the reactor with its bottom end reaching the catalyst basket inside the reactor body. The allowable pressure for this reactor system is up to 50 bars.

It is floor mounted in a 1/8 inch thick carbon steel cabinet with both front and back openings for easy access to the reactor system. On top of the cabinet, a single hole was provided for fitting the adjustable (height) thermocouple into the reactor body. It has three different gas ports (for reactants and reduction gas) accessible into the reactor and one port connected directly to the gas exhaust system (carrying reaction effluent). Please refer to figure 3-2.

### 3.3 Experiments Method

A commercially obtained fresh Pt/Al<sub>2</sub>O<sub>3</sub> catalyst in the form of 1.6mm extrudates was supplied by a local refiner. It was then crushed and sieved to 0.39-0.4 mm in order to avoid the internal mass diffusion limitations. This catalyst form was used in all further catalyst evaluations unless stated otherwise.

The MTR reactor was loaded with 5g of catalyst placed in the center of the reactor supported by alumina balls (inert packing). Reducing nitrogen gas blended with 5%H<sub>2</sub> in N<sub>2</sub> with a flow rate of 20 cm<sup>3</sup> /min was allowed to flow into the reactor chamber through ¼ inch stainless steel tubing. Here, the catalyst was then reduced at 573 K (300 °C) reduction temperature with a constant flow of the reducing gas to ensure the completion of the catalyst reduction. Then, the reduction gas was replaced with pure N<sub>2</sub> inert gas to clean the line and remove the water and any impurities present from the reduced catalyst sample. Then liquid *n*-hexane using a high pressure pump together with pure H<sub>2</sub> gas using a high pressure gas valve were pumped into the reactor system at a preset pressure and flow rate. In the reactor, the *n*-hexane was vaporized with a tubular electric furnace surrounding the reactor body. The hydrogen gas and the *n*-hexane vapor react together over the reduced Pt/Al<sub>2</sub>O<sub>3</sub> catalyst to produce high octane products.

This reactor system was pressurized using the original pressure from the reactant (pure hydrogen) gas which is adjusted between 3 to 7 bars (300-700 kPa) at ambient temperature. The reactor was then heated from ambient to temperatures between 623 to 723 K (350 to 450 °C) for further studies on the influence of temperature and pressure on reforming. Carbon tetrachloride between 1 to 5 vol/vol percent were mixed with *n*-hexane feed to study the effects of increasing the catalyst acidity on the

product yield. Selective poisoning of sulfur was also performed by doping dimethyl disulphide with the feed at various concentrations between 10 to 200 ppm. The outlet of the reactor effluent was trace piped to the gas chromatography unit (Hewlett Packard GC 6890 series) equipped with flame ionization (FID) and a thermal conductivity detector (TCD) to quantify conversion and products selectivity.

### 3.4 Gas Chromatograph

GC is a widely used technique for identification and quantification in the hydrocarbon industry. It is an extremely sensitive and versatile unit which when coupled with an automated system allows for an easy, accurate and reliable method for hydrocarbon analysis. A GC equipped with an FID is a powerful separation method for identifying and quantifying hydrocarbons in naphtha.

The products from the reactor effluent are divided into desired (isomerization and dehydrocyclization) and undesired (cracking and dehydrogenation) products according to the reactions describe below:

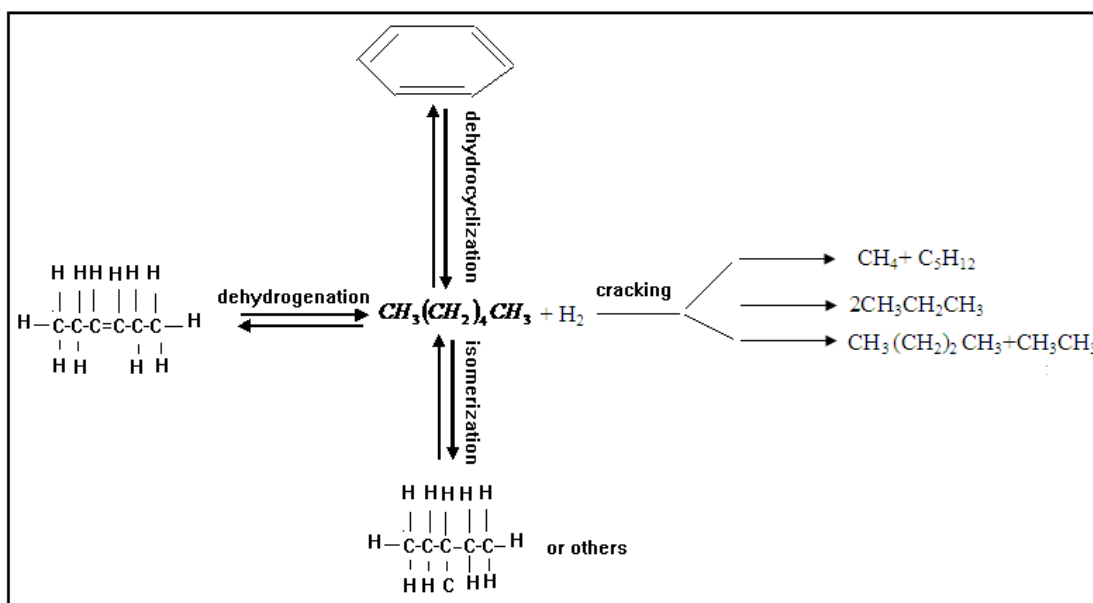


Figure 3-3 A schematic diagram of the *n*-hexane desired and undesired products

Gaseous effluent products from the reforming reaction were analyzed via an online gas chromatograph (Hewlett Packard (HP) GC 6890 series) equipped HP-Plot U capillary column (15 meters ) and HP-Mole-sieve (30 meters) which separate C1-

C7 hydrocarbons, CO<sub>2</sub>, CO, H<sub>2</sub>O, H<sub>2</sub> and the like; and is attached in a series and ends at the TCD while the GC-AL/KCL column system separates light hydrocarbons ends at the FID end. All the columns mentioned above are capillary type. The mobile phase used for both columns was He. For the GC-AL/KCL column the flow rate used was 5 ml min<sup>-1</sup>. The ignition mixture for the FID system consists of air flowing at 400 ml min<sup>-1</sup> and H<sub>2</sub> at 30 ml/min together with a He make up of 25 ml min<sup>-1</sup> with the pressure at the gas tank for H<sub>2</sub> set at 300 kPa (3 bars) and air at 158.6 kPa.

A 3 way valve system was installed between the reactor effluent line and the GC sampling valve. A ¼ inch high pressure stainless steel tubing was used to connect the reactor outlet to the GC inlet. This tubing was trace heated and controlled at 60 °C using the custom –made heating tape equipped with a Watlow temperature controller to ensure that the effluent products are always in vapor phase.

### 3.4.1 Mechanisms of sample analysis by GC

The sample effluent from the reactor transfers by mobile phase to the GC column and it is interacted with the stationary phase, where the component separation takes place. The gas sampling system consisted of three pneumatic valves which are valve 1, valve 2, and valve 3. Figure 3-4 shows the flow diagram for the sequence of valves system. Gas analysis was started when these valves were opened at 0.00 min run time to allow the gas sample to be injected into the respective columns.

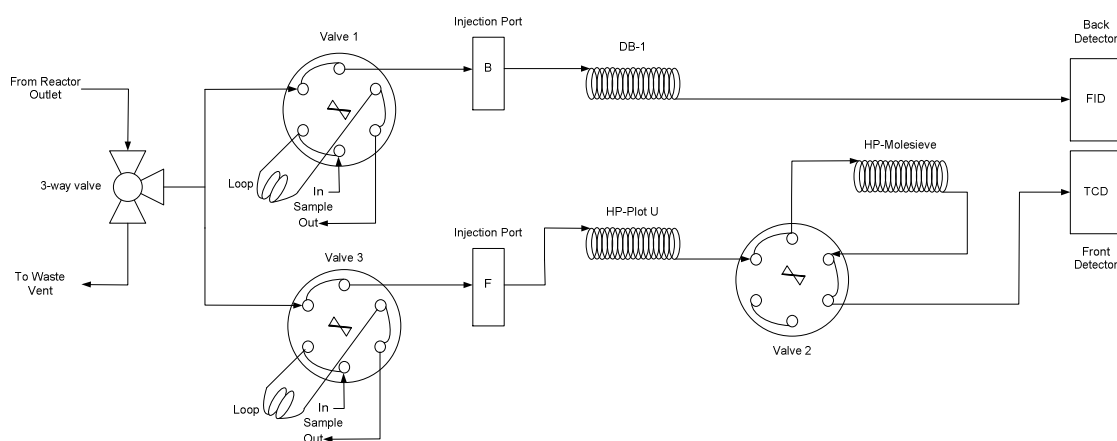


Figure 3-4 A schematic diagram of gas chromatography sampling valve diagram

To analyze the gaseous products from the MTR reactor through the back detector (FID), Valve 1 was turned on at 0.01 min to allow the gas sample to enter the line. Then the sample was passed directly to the back line towards GC-AL/KCL, eventually the individual analytes are sent to the FID detector, where the constituents of the sample are detected, eventually the results are recorded by sending a signal to the computer. Before starting the experiments the GC was calibrated with standard mixtures of hydrocarbons, please refer to (Appendix C).

### 3.4.2 GC-Operating Conditions

In gas chromatography analysis, a temperature program is generally used to ensure adequate separation of the compounds in a short time.

The temperature programs used for the analysis are given in Table 3-2:

Table 3-2: Description of GC operating conditions

Type	Condition
Injector temperature	200 °C
Detector temperature	200 °C
Oven temperature 1	50 °C
Oven temperature 2	190 °C
Ramp rate 1	5 °C min <sup>-1</sup>
Column pressure	0.49 bar
Spilt ratio	30

### 3.5 Calculations

#### 3.5.1 Conversion

Dietz W.A.'s [84], method was used to calculate the conversion and is given in equation 3-1. The calculation is based on the mass fractions of the reactant which are equal to the area fraction under the chromatographic peak.

$$X = \frac{HC^i - HC^o}{HC^i} \quad (3-1)$$

Where  $HC^i$  is the concentration of the fed hydrocarbon at the reactor inlet and  $HC^o$  is the concentration of the non-reacted hydrocarbon at the reactor outlet. the conversion of reactant A ( $X_A$ ) was calculated using equation (3-2).

$$X_A = \frac{\left( \frac{N_{A_0}^o - N_A^o}{N_{A_0}^o} \right)}{\left( \frac{M_{A_0}^o - M_A^o}{M_{A_0}^o} \right)} = 1 - \left( \frac{M_A^o / M_{A_0}^o}{M_A^o / M_{A_0}^o} \right) = 1 - \left( \frac{A_A / A_{TOT}}{A_A / A_{TOT}} \right) \quad (3-2)$$

Where  $X_A$  is the conversion of reactant A,  $N_{A_0}^o$  is the molar flow of reactant A at the inlet of the reactor,  $N_A^o$  is the molar flow of reactant A at the exit of the reactor,  $M_{A_0}^o$  is the mass flow rate of reactant A at the inlet of the reactor, which is equal to the total mass flow,  $M_A^o$  is the mass flow rate of reactant A at the exit of the reactor,  $A_A$  is the GC area of reactant A.  $A_{TOT}$  is the total GC area of the hydrocarbon reaction components and  $(A_A / A_{TOT})$  is the GC area fraction of A.

#### 3.5.2 Products selectivity

Mazzieri *et.al* [18], method was used here to calculate the reforming products selectivity, and is defined as the equation 3-3:

$$S_i = \frac{yield(i)}{X} = \frac{A_i f_i n_i}{M_i \left( \sum A_i f_i n_i / M_i \right) X} 100 \quad (3-3)$$

Where  $A_i$  is the area of the chromatographic peak of product i,  $f_i$  is its response factor,  $n_i$  is the number of carbon atoms of i and  $M_i$  is its molecular weight.

### **3.6 Catalyst Characterization**

Characterization of a heterogeneous catalyst refers to the measurement of its physical and chemical properties (pore size, surface area, particle size, catalyst composition and strength). There are many important reasons for measuring the characteristics of a solid catalyst, such as understanding the catalyst structure and its function, elucidating cause of deactivation, designing methods for regeneration and ensuring quality control in catalyst manufacturing [85].

#### **3.6.1 *Field emission scanning electron microscope (FESEM)***

FESEM is a type of electron microscope that images the sample surface by scanning it with a high-energy electron beam (10 KV). The produced electron beam interacts with the atoms that make up the sample producing signals that contain information about the sample's surface topography composition. It has a large depth of field yielding, a characteristic of three-dimensional appearance useful for understanding the surface structure of a sample.

Ultra High Resolution FESEM with excellent imaging properties has various applications such as material science, life science and semiconductor technology. It produces clearer, less electro-statically distorted images with spatial resolution which is better than the conventional SEM. The advantages of the FESEM technique are that it; has a high efficiency 'In-lens SE detector' and good resolution down to 0.1 kV, requires minimal adjustments when changing operating voltage low magnetic fields at the specimen level, enables examination of non-conducting specimens without time consuming preparation reducing penetration of low kinetic energy electron probes closer to the immediate material surface, and has smaller-area contamination spots and can be examined at high quality with low voltage images with negligible electrical charging of samples. The field emission SEM (FESEM) increases the useful magnification range for observation and imaging up to 500,000X. Moreover, low-voltage FE-SEM reduces damage of delicate samples, reduces sample charging for nonconducting materials and, enhances surface sensitivity [86].

For the present study, the Zeiss Supra 55VP field emission scanning electron microscope (FESEM) compatible with Energy Dispersive X-ray (EDX) Spectroscopy

was used to study the catalyst surface morphology (commercial fresh and spent) including the size of the supported crystallites using ‘SMART SEM’ and ‘INCA’ as software for FESEM and EDX respectively.

### **3.6.2 Thermo-analytical techniques**

Thermo-analytical techniques can be considered as transient response techniques; they describe the characteristic property of a solid sample which is related to the temperature in a process of programmed heating. The energy exchanges between the sample and its surroundings provide a means to detect and follow its physical or chemical transformations via a temperature function measured response. The thermogram reflects the nature of the system under study and the experimental conditions. It can be used as a tool for both quantitative and qualitative analysis for determining the effects of different factors on the sample reactivity [87].

The method of temperature programmed techniques consists of heating the sample at a linear rate in a flowing stream of gas. The sample may be monitored during the heating using thermogravimetry, or by monitoring the exit gas stream using mass spectrometry. Mass spectrometry (MS) can detect very small concentrations, but it is not good for the compounds having the same mass, they cannot be separated, and independently it cannot be determined which species is present [7].

For the present study, the programmed thermo-analytical study was conducted by an SNG instrument- TPDR0 1100 series using TPDR0 software. This equipment is constructed in such a way that it can be modified to accommodate the following techniques which include Temperature-programmed reduction/desorption and oxidation. The unit is connected to TCD detector. A brief discussion of these various techniques, their theory and application is given below.

#### **3.6.2.1 Temperature-programmed reduction (TPR) Principle**

The popular well known thermal analysis technique was proposed in 1975 by Delannay [88]. An oxidic catalyst precursor is submitted to a programmed temperature rise, while a reducing gas mixture is flowed over it (usually, hydrogen

diluted in some inert gas). The reduction rate is continuously measured by monitoring the composition of the reducing gas at the outlet of the reactor.

The TPR analytical technique can be used to study the metal reduction state (metal surface activation) which has many applications as demonstrated by Kanervo [87]. These include; studying the reactivity of the metal, the reduction properties of materials, investigating the kinetics and reduction mechanism, it is also used as an indicator of alloy formation in bimetallic catalysts, the interactions between metal oxide and support, the temperature range of consumption; the total consumption of the reducing agent is also monitored by TPR.

TPR method:

The TPR analysis was carried out using the TPDRO-1100-MS instrument by SNG. The sample was pre-treated in N<sub>2</sub> gas at 110 °C for 1hr to remove water prior to analysis. It was then cooled to room temperature under N<sub>2</sub> atmosphere before being heated from room temperature to 800 °C with a heating rate of 10 K min<sup>-1</sup> in a reducing gas stream made up of 5.1 v/v% H<sub>2</sub> in N<sub>2</sub> gas at a flow rate of 20 cm<sup>3</sup> min<sup>-1</sup>.

Two types of reforming Pt/Al<sub>2</sub>O<sub>3</sub> catalyst samples (calcining and non-calcining samples) were analyzed by the TPR technique. The calcination was carried out *in-situ* (TGA) prior to reduction in the presence of air at 673 K for 3 h. The hydrogen consumption was monitored by a thermal conductivity detector (TCD).

### 3.6.2.2 *Temperature-programmed desorption (TPD)*

Temperature-Programmed Desorption (TPD) was developed in 1963 by Delannay [88] and was first extended to the study of supported metal catalysts by Amenomiya and Cvetanovic [89]. It was mentioned by [87] that TPD was effectively an extension to powder solids of the flash desorption technique developed by Redhead [90], for the study of the desorption of gases from heated metallic filaments in a high vacuum.

TPD is one of the most widely analytical techniques used for characterizing the acid sites on oxide surfaces. It can also be used to measure the catalyst surface acidity (quantity and strength of the acid sites) and characterization of adsorptive properties

of materials [76]. Apart from that, TPD can also be applied to study; the kinetics and mechanisms of adsorption & desorption, the adsorbed molecules binding states, heterogeneity of surface energy, the temperature range of adsorbate release, the total desorbed amount, adsorption capacity, metal dispersion and surface area [87].

TPD method:

TPD by pyridine measures the amount and strength of the acid sites of the catalysts. A 0.22 g of the catalyst to be analyzed was first immersed in a closed vial containing pure pyridine (Merck, 99.9%) for 3 h. Then, the vial was open in a fume cupboard at room temperature conditions to allow excess pyridine to evaporate out. The sample was then loaded into a quartz micro tube reactor and supported over a quartz wool plug. A constant flow of nitrogen at  $20 \text{ cm}^3 \text{ min}^{-1}$  was set up to flow over the sample. During the first (pre-treatment) step, desorption of weakly adsorbed pyridine and stabilization was performed by heating the sample at  $150 \text{ }^\circ\text{C}$  for 1 h. The temperature of the oven was then raised to a final value of  $(1000 \text{ }^\circ\text{C})$  with a heating rate of  $10\text{K min}^{-1}$ . The effluent from the reactor outlet was channeled to the thermal conductivity detector (TCD) to be analyzed.

### 3.6.2.3 *Thermo gravimetric Analysis (TGA)*

TGA is another important analytical technique mentioned by Wang [76], which can be used as differential scanning calorimetry (DSC) or used during the heating processes, to monitor the energy released or adsorbed via chemical reactions. In addition to this, differential thermal analysis (DTA), another usage of TGA can be used to record the temperature difference between the specimen and one or more reference planes.

Thermo-gravimetric analysis (TGA) is a very convenient method for approximating the oxidation state of a component within a compound. It can be used to reduce or oxidize a sample in a control environment and measure its weight change by microbalance techniques. TGA is also used as a standard tool for studying the reaction of solids with gases. The measurement of weight loss (or gain) is normally carried out

in air or in an inert atmosphere, such as Argon, Nitrogen, Helium, and then recorded as a function of temperature [85]. For the present study, TGA was used to study the kinetics of de-coking on the commercial and lab spent catalysts. The commercial catalysts were collected from a local catalytic reforming unit which had been coked under the pressure  $6 \text{ kg cm}^{-2}$ , after six cycles in a reforming unit and being regenerated five times. The TGA analysis was carried out in nitrogen inert gas and air, and measures the sample weight loss.

The current TGA method used here considers only the weight loss by coke burning at high temperatures, ignoring the removal of any volatile material constituents. The coke amount can be obtained by measuring the weight loss during coke burning in air. Figure 3-5: gives a flow chart of a typical TGA unit.

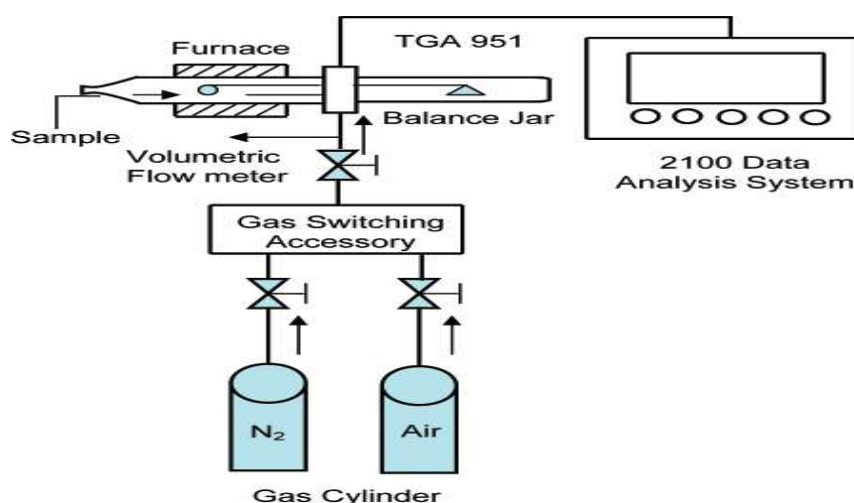


Figure 3-5: Flow chart of thermo-gravimetric analysis [91].

TGA method for coke characterization:

The spent commercial catalyst was finely ground to a mesh size of 0.4mm using a glass pestle and mortar. A sample weight of 95mg was placed in the pan of the Perkin Elmer Pyris 1 TGA unit. The coked sample was thermally pre-treated starting from 323 to 473 (50 to 200 °C) under pure N<sub>2</sub> gas with a flow rate of  $20 \text{ ml min}^{-1}$  to remove moisture and unbounded volatile material. After this, the pure N<sub>2</sub> gas was replaced by air and heated to a preset maximum temperature of 1073 K (800 °C) but maintaining the same flow rate. The weight loss with time, at a fixed heating and flow rate was recorded to evaluate the kinetics of de-coking.

The de-coking process in the present study can be divided into three stages. Stage one from 473 to 673 K (200-400 °C), stage two from 673 to 873 K (400-600 °C) and stage three from 873 to 1073 K (600-800 °C). The weight percentages of coke that have been removed from the coked catalyst for each stage were measured in accordance to method used by Wang et al. [11] illustrated by the following equation:

$$Coke (wt)\% = \frac{Coke_{Re}}{Total_{Coke}} * 100\% \quad (3-4)$$

#### 3.6.2.4 Temperature programmed oxidation (TPO)

The coked catalysts were analyzed for coking properties using the SNG instrument-TPDRO 1100 series. The TPO method is one of the few methods accepted for this type of analysis and is based on the complete combustion of coke deposited on the Pt/Al<sub>2</sub>O<sub>3</sub> catalyst.

Temperature programmed oxidation, used for various purposes, is described by Kanervo [87]. These purposes can be summarized as:

- Characterization of coke species in deactivated catalysts.
- Total coke content in deactivated catalysts.
- Mechanisms and kinetics of oxidation reactions.

The coke oxidation description, according to Hill [7], is that the coke reacts with the oxygen to form carbon dioxide and water as per the following equation:



Where, x is referred to as the H/C ratio.

Based on Hill's [7] assumption, coke on the metal is removed at a lower temperature, because it has a higher x value, while coke on the support, has a lower x value and is removed at a higher temperature. An example mentioned by Hill [7] is that, the oxidation temperature of coke deposited on the metal occurs between 430 to 620 K (157 to 347 °C).

Whereas the oxidation peak for the coke deposited on the alumina support occurs between 620 to 820 K (347 to 547 °C).

TPO method:

The CO<sub>2</sub> production was monitored by a thermal conductivity detector (TCD) in the TPO measurement. The pre-weight sample was charged to a glass quartz tube, which has a 1mm inner diameter to allow only a small fraction of gas to exit.

TPO studies were carried out using two different methods. In the first method, the coked catalyst was burnt in two different stages. In this method of TPO, the sample was heated with 20 cm<sup>3</sup> min<sup>-1</sup> in N<sub>2</sub> atmosphere followed by O<sub>2</sub> (5.0 v/v % in N<sub>2</sub>) with 3 different heating rates 10, 15 and 20 K min<sup>-1</sup>. For each of the 3 different heating rates, 6 different temperatures of 573, 673, 773, 873, 973 and 1073 K (300, 400, 500, 600, 700 and 800 °C) were analyzed. For each of the temperatures referred to above, 3 different dwell times of 30, 60 and 120 mins were measured at constant heating rate 10 K min<sup>-1</sup>.

The kinetics of de-coking was studied here by the second phase TPO experiment; a new method developed to study the activation energy of the combustion reaction. A 0.2 g of the industrial acquired coked reforming catalyst was charged to a quartz tube and pre-treated at 383 K (110 °C) in N<sub>2</sub> gas in order to remove unbounded impurities and moisture from the sample [28, 76]. The sample was then burned in 5.0 % O<sub>2</sub> in helium at a 20 cm<sup>3</sup> min<sup>-1</sup> flow-rate to a maximum temperature of 1123 K (850 °C) with a constant temperature ramp rate of 10 K min<sup>-1</sup>. Measurements of the sample weight loss were recorded at different observed temperatures.

### **3.6.3 *Fourier Transform infrared spectroscopy (FTIR)***

FTIR spectroscopy is an important and popular tool for structural elucidation and compound identification. It can be used for a wide range of sample types such as gases, liquids and solids to determine the chemical functional groups in the sample, such as OH, CO, organic and inorganic compounds.

For the present study, the FTIR technique was used in the investigation of the structure of carbon deposits on supported metal catalysts. It was also used to analyze

the structures of adsorbed molecules on a catalyst surface (the soluble components) or the soft coke, which can be also be determined using IR, UV-VIS and GC/MS [48, 80]. This soft coke is determined under controlled atmosphere conditions by the SHIMADZU FTIR 8400S instrument.

50 mg of coked catalyst sample was ground to powder form in an agate mortar and mixed well with KBr (potassium bromide) powder. The product was pressed into a self-supporting disc at (9000psi). The prepared sample disc was then placed in the centre of the reaction chamber, fixed in between a folded tungsten grid. The spectra were recorded by the SHIMADZU FTIR 8400S spectrometer. The above procedure was repeated for other samples after desorption of soft coke in nitrogen inert gas (after TGA, first stage).

## Chapter 4

### Results and Analysis

#### 4.1 Chapter overview

For the present study, *n*-hexane reforming was carried out in a high pressure micro-reactor using an industrial Pt/Al<sub>2</sub>O<sub>3</sub> catalyst. This study can basically be divided into 2 main sections namely, (a) the reforming process variable and modification of the catalyst support and (b) regeneration and kinetics of spent catalyst.

Under the reforming process variable, H<sub>2</sub> partial pressure and temperature were investigated against the influence of contact time. Here, overall conversions and product species are analyzed. For the *n*-hexane reforming reaction a simple kinetics was developed. As for the product species, an Array for Design of Experiment by Taguchi method was put in place. Modification of the catalyst support was tailored towards catalyst acidity. For this study, two further areas of interest were investigated i.e. the enhancement of support acidity and the selective poisoning of active sites. For the former, the reaction was carried out by introducing a pre-determined amount of carbon tetrachloride (CCl<sub>4</sub>) blended into the feedstock while for the later, di-methyl disulfide (DMDS) was used in the place of CCl<sub>4</sub>. For the reforming conditions mentioned above, the area of research was centered on the conversion and product distribution.

The 2<sup>nd</sup> part of this chapter, regeneration study of the spent industrial catalyst was done. In this part the detail analysis on factors required for the maximum recovery of catalytic activity was conducted.

## 4.2 Reforming process variables and modification of the catalyst support

### 4.2.1 Process variables and product classification for *n*-hexane reforming

The process variables chosen for this section are H<sub>2</sub> partial pressures ranging between 300 to 700 KPa (3-7 bars) and process temperatures varying between 623 to 723 K (350 to 450 °C). For this purpose, three H<sub>2</sub> partial pressures namely 300, 500 and 700 KPa (7, 5 and 3bars) and three process temperatures of 623, 673 and 723 K (350, 400 and 450°C) were chosen.

Products arising from reforming reactions can basically be divided into either reversible or irreversible reaction products for kinetic studies. The product distribution was then divided into 4 groups namely cracked products, coke precursors, isomers and aromatics. The cracked products are classified under irreversible, while the others are reversible reaction products. The cracked products are all those reforming products which are saturated products ranging from C1 to C4 *n*-alkanes, while the coke precursors include C2 to C6 olefins, others like the isomers refer to iso-C5 & C6; the aromatics are basically benzene. A list of the various products described above is listed in Table 4-1. It should be noted that *n*-C6 is the feedstock for the above reforming reaction.

Table 4-1: Grouping of Products from Reforming Reactions

Reforming Product Group			
Cracked	Coke precursors	Isomers	Aromatics
Methane	Ethylene	Iso-butane	Benzene
Ethane	Propylene	Iso-pentane	-
<i>n</i> -Propane+ <i>n</i> -Butane	Iso-propylene	Iso-hexane	-
-	others	Cyclo hexane	-

#### 4.2.2 Effect of contact time against pressure and temperature on *n*-hexane conversion

The reforming reaction was carried out as mentioned in chapter 3.3 over a 3½ hours time on stream. Sampling was done every ½ hour and analyzed with an on-line Gas chromatography. The conversion of pure *n*-hexane under the influence of contact time at different temperatures and pressures are shown by Figures 4-1 (A, B & C). Each sub graph, A, B and C in Figure 4-1 refers to the temperature fixed at 723, 673, and 623K respectively with varying H<sub>2</sub> partial pressure and contact time. The experiment was conducted using 3 different H<sub>2</sub> partial pressures of 300, 500 and 700KPa, while 7 different contact time was include which include 1.02, 1.12, 1.42, 1.78, 2.37, 3.56 and 7.11 minutes. For each of the experiment, the average results over 3 ½ hours time on stream was reported. It should be noted that analyzed time for each sample is every ½ hour using an on-line GC. The contact time was calculated based on a variation of flow of *n*-hexane (F) per gram of catalyst weight (W).

$$\text{Contact Time} = \frac{F(\text{g min}^{-1})}{W(\text{g})} \quad (4-1)$$

Based on the results obtained in Figure 4-1, a simplified version was derived on the average conversion under the influence of pressure and temperature and is shown in Table 4-2. The average conversion here refers to the conversion obtained from 2.4 to 7 minutes contact time. Having calculated the average conversion, it is then used to interpret the influence of temperature and pressure. The maximum average % conversion from Table 4-2 is 79.32% observed at 723 K and 300 KPa. From the same table, it can be seen that by maintaining the reforming reaction at 723 K and increasing the H<sub>2</sub> partial pressure from 300 KPa to 500 KPa results in a decrease on average conversion by 7.8%. A further increase by 200 KPa, results in a drop of 2.6% on the average *n*-hexane conversion. This indicates that lower H<sub>2</sub> partial pressure results in an increase in *n*-hexane conversion. The opposite is seen in the case of temperature. For this case we maintain the H<sub>2</sub> partial pressure at 300 KPa, and decrease the temperature by 50 K to 673 K, a marked decrease of 12.3% of *n*-hexane conversion is observed. Further decrease in temperature to 623 K decreases the *n*-hexane conversion by 8.3%.

Table 4-2: The average conversion at contact time 2.4 to 7 min, pressures 300, 500 and 700 KPa and temperatures 723,673 and 623 K.

Temperature (K)	Average conversions %		
	300 (KPa)	500 (KPa)	700 (KPa)
723	79.32	71.53	68.91
673	67.02	62.18	61.71
623	58.69	56.55	47.71

The above observation for changes in temperature and H<sub>2</sub> partial pressure is seen for all the other combinations. This indicates that changes in temperature are more significant than H<sub>2</sub> partial pressure.

From the above observations, the overall conversion increases by increasing the temperature and decreasing the H<sub>2</sub> partial pressure. This can be one of the main reasons why reforming reactions demand a high reaction temperature and low pressure. It was reported by Taskar [4] that a high process temperature and a low pressure favor the thermodynamic equilibrium as well as the reaction rate in two most important reforming reactions, i.e. dehydrogenation of naphthenes or cyclohexanes, and dehydrocyclization of paraffins. Moreover, higher increase in reaction temperature is not recommended because it can increase catalytic deactivation by increasing sintering. In some cases, the temperature might be raised in the case of declining catalyst activity or to compensate for lower quality feedstock.

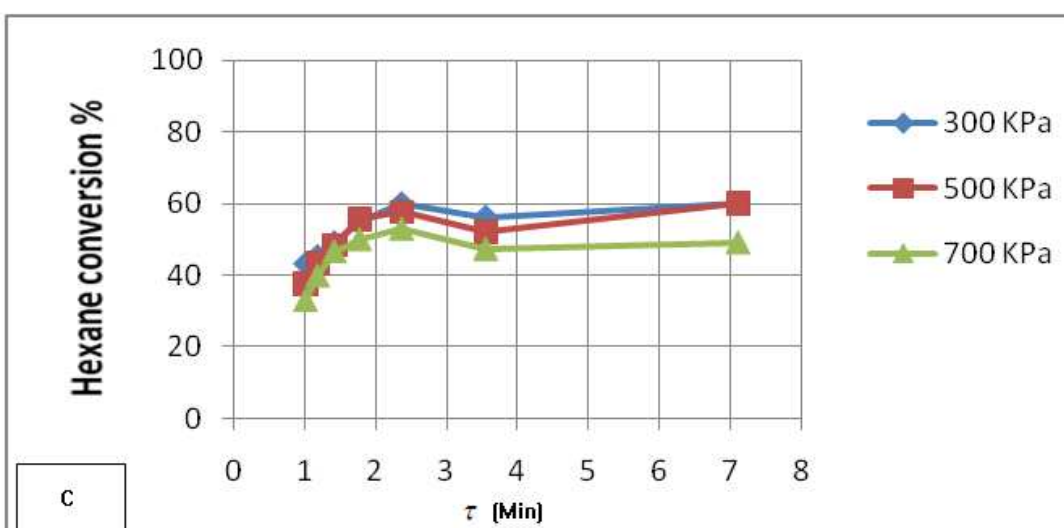
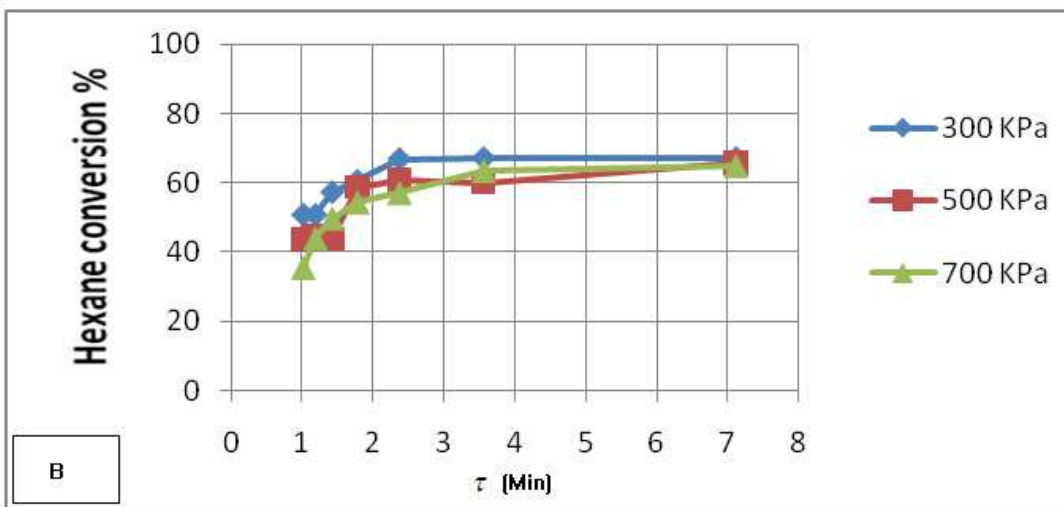
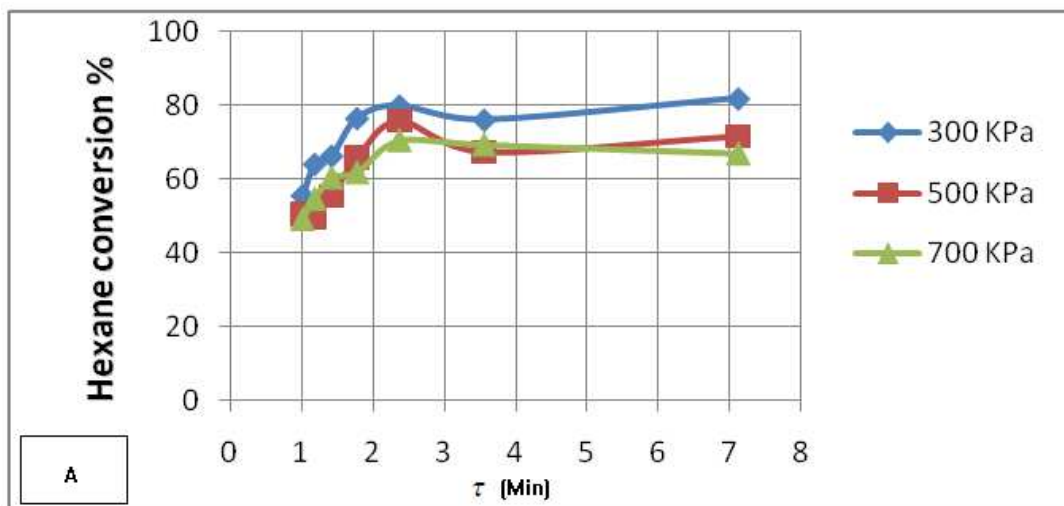


Figure 4-1: *n*-hexane % conversion over the Pt/Al<sub>2</sub>O<sub>3</sub> catalyst at 723 K [A], 673 K [B] and 623 K [C] using H<sub>2</sub> pressures of 300, 500 and 700 KPa.

### 4.2.3 *Effect of contact time against process variables on reformat species*

The influence of H<sub>2</sub> partial pressure and temperature on reformat species yields were done by varying the contact time against temperature and pressure. For this purpose, the process temperature was fixed at 723, 673 and 623 K while the H<sub>2</sub> partial pressure was maintained at 300, 500 and 700 KPa for each of the temperature set points. The results obtained from these experiments are shown in Figures 4-2 and 4-3. Each figure is divided into 3 similar smaller graphs and is marked as A, B and C. Figure 4-2 represents the reforming temperature condition set at 723 K while H<sub>2</sub> partial pressure is varied between 300, 500 and 700 KPa.

For each pressure mentioned above, the evolution of reformat species is represented by the smaller graphs A, B and C respectively. But in Figures 4-3 the pressure is set at 300 KPa while the temperature is varied between 623, 673 and 723 K respectively. Temperature of 723 K and H<sub>2</sub> partial pressure of 300 KPa was chosen as it gives the maximum conversion for the *n*-hexane reforming reaction studied. Based on this input an investigation into the effects of the reaction temperature and H<sub>2</sub> partial pressure on the reformat products was carried out.

The reformat species mentioned above is basically divided into four different reformat species labeled as: cracked, coke precursors, isomers and aromatic reformat species (please refer to Table 4-1).

#### 4.2.3.1 *The effects of contact time over H<sub>2</sub> partial pressure*

From Figure 4-2 (reaction temperature fixed at 723 K), it can be noticed that apart from aromatic, the H<sub>2</sub> partial pressure (between 300 to 700 KPa) does not have significant effect on the yield % of the other reformat products (isomers, coke-precursors and cracked). Observation from the same figure indicates that isomers are less affected by the H<sub>2</sub> partial pressure. Coke precursor selectivity on the other hand decreases slightly whereas for the cracked the reverse of the former is observed. In the case of aromatics, a lower H<sub>2</sub> partial pressure enhances overall yield.

From Figure 4-2, it can be noticed that contact time is more detrimental than H<sub>2</sub> partial pressure. From the same figure it can be noticed that the isomer reformates

yield has an initial increase from 1.0 to 2.4 mins, where it reaches the maximum yield of 29.2% at 300 KPa (Figure 4-2-A). After 2.4 minutes contact time the isomer reformat gradually decreases until 3.5 minutes. Thereafter until 7.1 minutes, no drastic change is observed. As for the cracked product a gradual increase in yield is observed with increase contact time which is more obvious at lower H<sub>2</sub> partial pressure. This finding is in agreement with Anup et al [93]. and Aberuagba [92, 93] who claim that at high contact time, some of the isomers are converted to cracked product group as a result increases the cracked reformat selectivity.

For the coke precursor a gradual increase was observed with increasing contact time, but the selectivity decreases with increasing H<sub>2</sub> partial pressure. This can be attributed to the fact that increase H<sub>2</sub> partial pressure subdues cracking activities as reported by Anup et al. [92] This is apparent since the coke precursors are unsaturated hydrocarbon. With an increase in H<sub>2</sub> partial pressure these get converted to saturated hydrocarbon products contributing to the crack reformat yield.

For aromatic selectivity significant drop was observed with increasing contact time at higher H<sub>2</sub> partial pressure. At lower H<sub>2</sub> partial pressure no significant change was observed. The same explanation as that used for coke precursor can be used for aromatics, where they tend to form cyclic hydrocarbon (saturated) on hydrogenation.

From Figure 4-2-A the selectivity to coke precursors at 300 KPa reached 22.1% at the highest contact time (7.1 mins) while it was 10% lower at 1.0 min contact time. The isomerization reaction in Figure 4-2-A followed a different path; it reached the maximum 26.8% at 2.4 minutes, and then decreased to 18.8% at 7.0 minutes contact time. As for the aromatic yield it had the highest yield of 18% at 7.0 minutes and lowest of 9.0% at 1.0 minute contact time. The cracked product also flow a similar trend to that of the aromatic having the lowest conversion of 12% at 1.0 minute and doubles at 7.0 minute contact time.

Similar trends and yields to that at 300 KPa (Figure 4-2-A) are observed for the isomer, cracked and coke precursor product group at 500 KPa H<sub>2</sub> partial pressure (Figure 4-2-B). This was not the case for aromatic, where with increase contact time and H<sub>2</sub> partial pressure, the yield decreased.

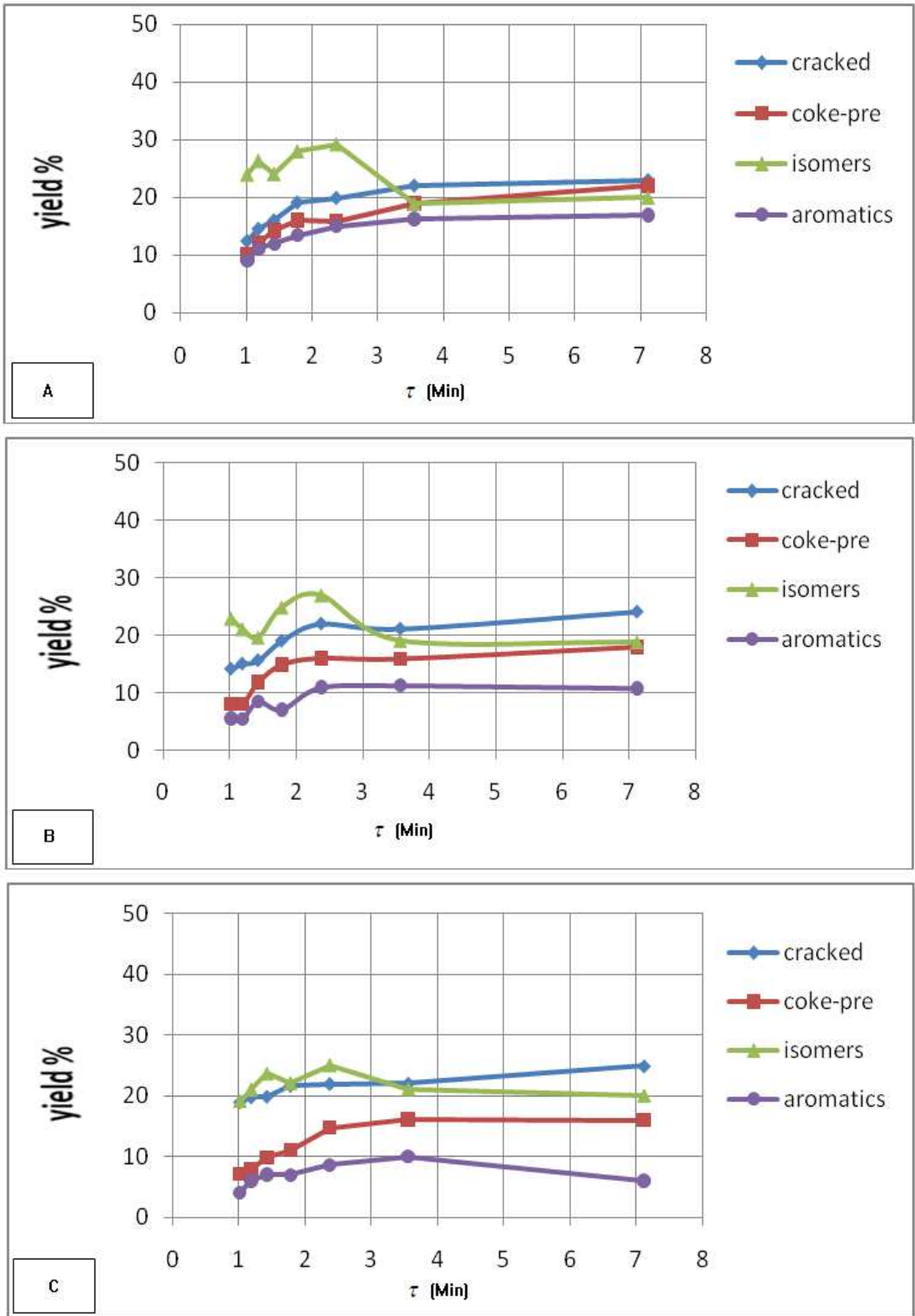


Figure 4-2: Yield % to reformat products as a function of contact time over the Pt/Al<sub>2</sub>O<sub>3</sub> catalyst, at 723 K and pressures at A-300, B-500 & C-700 KPa.

In Figure 4-2-C, it can obviously be seen that, conducting the reforming reaction at the highest H<sub>2</sub> partial pressure (700 KPa), increases sharply the cracked products with decrease in the coke precursors (decreases of catalyst deactivation rate). This is because H<sub>2</sub> inhibits the dehydrogenation reactions by lowering the concentration of the coke precursors [32]. However, the lowest pressure (300 KPa) favors the coke precursor over the cracked product. This essentially leads to higher deactivation rate of the catalyst. From the above observation it can be summarized as, applying a lower H<sub>2</sub> partial pressure and fixing contact time at 1.78 minutes has a positive effect on the reformat octane number.

#### 4.2.3.2 *The effects of the reaction temperature and contact time*

Having studied the effect of H<sub>2</sub> partial pressure on contact time, the second part of this study investigates the effects of the reaction temperature on contact time. In this case, we keep the H<sub>2</sub> partial pressure at 300 KPa (as recommended from the previous section) and vary the reaction temperature from 623 to 723 K against the same range of contact time as discussed above. The results from this study are shown in Figure 4-3. Similar to Figure 4-2, the results are shown in three segment labeled as A, B and C which represent the reaction temperature at 623, 673 and 723 K respectively.

From Figure 4-3 it can be seen that the reformat products yield in general increased with reaction temperature. The most important aspect of this study is to maximize the aromatics and isomers (desired) and minimize the cracked and coke precursors (undesired) product group. From Figure 4-3 it can be seen that lowering the reaction temperature decreased the cracked products as well as the formation of unsaturated hydrocarbons (coke precursors) which are the undesired reactions. These types of products are the main causes of catalyst deactivation. By accumulation of these products on the catalyst surface, it can block the catalyst pores. Furthermore, these compounds demand high reaction temperatures to be polymerized on the catalyst acid sites. Coke is more aromatic and stable at high reaction temperatures than at low reaction temperatures as reported by Wang and Manos [11].

On the other hand increasing reaction temperature also improves the yields of the desired products i.e. the isomers and aromatics. If the catalytic reaction is conducted

at a very high temperature, thermal degradation of the catalyst may occur in the form of active phase crystallite growth or sintering building up on the support or carrier pore structure which in the long run will result in structural collapse [34]. This may result in drastic measures to be taken for reforming catalytic process. In view of that, a temperature must be chosen to increase the desired over the undesired product group while maintaining the catalyst integrity. It was reported by Huayun [94] that, decreasing the reaction temperature, decreases the aromatics yield while increasing the reaction temperature caused an increment of coke precursors which lead to an increase in the deactivation rates. This coke precursors causes a rise in coke formation which is expected to increase with increasing the temperature [35, 36]. Liu [3], demonstrated that, increasing the reaction temperature thermodynamically shifts the equilibrium of the main reaction in the desired direction. Taskar [4], also indicated that by increasing reaction temperature acceleration of side reactions and coking rate increased.

From Figure 4-3 it can be seen that contact time has a greater influence than reaction temperature when desired product are required. From the same figure, it can be noticed that a contact time of 1.78-2.4 minutes is desirable to produce higher yields of isomer and aromatics yields at the expense of cracked and coke precursor product. Increasing the temperature by 50 K (623 to 673) results in an increase of 1.0 % isomer, 4.0% aromatics, 2% coke precursor and 0.5% cracked product yield. Further increase by 50 K (673 to 723 K) a drastic decrease of 6.0% cracked product and 2 to 3.0 % of all the other individual reformat product yield was observed. This is in agreement with the findings of Anup et al. [93] and Aberuagba [92, 93] they reported that, higher cracking activity is observed over Pt/Al<sub>2</sub>O<sub>3</sub> at a higher reaction temperature.

From the above observation it can be seen that the optimum contact time for *n*-hexane reforming is 1.78-2.4 minutes. By increasing contact time from 2.4 to 7.0 minutes, reformat products yield was observed to be more stabilize, causing an average increase of 4.5 to 5% for cracked and coke precursor product group respectively. While for the isomer product an average drop of 11% and a small increase of < 1.7% for aromatics were observed. The above observation is based on an average taken across the board over the 3 temperature readings. This indicates that

increasing contact time increases undesirable products over the desirable in *n*-hexane reforming.

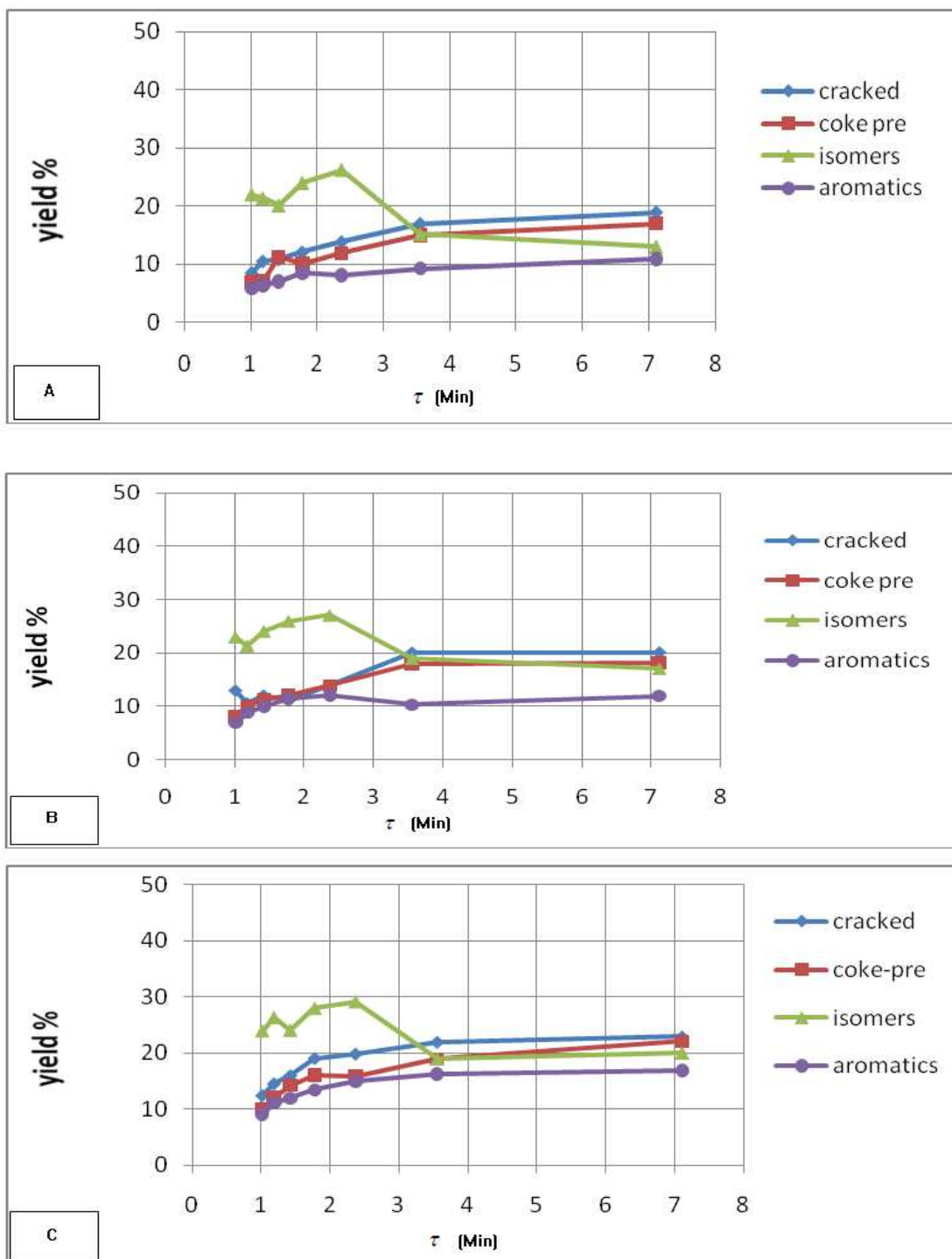


Figure 4-3: Effect of reaction temperature on H<sub>2</sub> partial pressure of 300 KPa, as function of contact time on *n*-hexane reforming over a Pt/Al<sub>2</sub>O<sub>3</sub> catalyst. [Reaction temperature A=623; B=673 and C = 723 K].

### 4.3 Design Expert software (version 6.0.6) using a Taguchi orthogonal array design

The classical method (full factorial design) used in statistical design of experiments requires a large number of experiments to be carried out to determine the most to the least importance of any one process variable analyzed. The number of experiment to be carried out (N) can be given by the equation  $N=L^m$ , where L is the number of levels for each factor and m is the number of factors or variables used. In this study the effect of three parameters ( $H_2$  partial pressure, reaction temperature and contact time) are to be analyzed. In view of that 27 ( $3^3$ ) different combinations of parameters are possible. It is therefore very difficult to identify and quantify the contribution of individual parameters as indicated by Adewuyi et al. [95]. Hence, there was an absolute need for a design of experiments strategy that can reduce the number of experiments as well as identify the contribution of each factor. To simplify and solve this problem a *Design -Expert* software (version 6.0.6) using a Taguchi orthogonal array design was used to identify the optimal reforming conditions which favors aromatics and isomers over cracked and coke precursor reformat products. For this purpose 3 factors and 3 levels were chosen and are shown in Table 4-3. The placement of factors number in Table 4-3 is based on; 1 for the highest *n*-hexane conversion and 3 for the lowest for each factor (temperature, pressure and contact time).

Table 4-3: Reforming conditions and levels used in this experiment

Factor	level		
	1	2	3
A:A Temperature (K)	723	673	623
B:B Pressure (KPa)	700	500	300
C:C Contact time (Min)	7.11	1.78	1.02

### 4.3.1 Optimization of percentage conversion of n-hexane reforming using Taguchi OAD method

For Taguchi orthogonal array design simulation, three factors were chosen which include reaction temperature, H<sub>2</sub> partial pressure and contact time. For each factor three levels a standard L9 orthogonal array employed by Cetinkaya et al. [96] was used. This is shown in Table 4-4. Each row of the matrix in Table 4-4 represents the average conversion at specified conditions. The statistical analysis of the results was carried out using analysis of variance (ANOVA), and the results are shown in Table 4-5. From the same table it is obvious that the model F- value for temperature which is 83.13% (average value) implies this model is significant and there is only 2.1 % chance that a “model F-value” this large could occur from noise effect. Apart from reaction temperature, contact time and H<sub>2</sub> partial pressure are also significant model terms since “Prob>F” is less than 0.05% for all 3 process variable.

Table 4-4: L9 Array for Design of Experiment by Taguchi Method

Run	Experimental Conditions			Hexane conversion%
1	2	3	1	67.085
2	1	1	1	66.934
3	2	2	3	43.520
4	3	2	1	59.985
5	3	3	2	54.631
6	3	1	3	32.917
7	1	2	2	65.787
8	1	3	3	55.517
9	2	1	2	54.230

The purpose of the analysis of variance (ANOVA) shown in Figure 4-4 is to investigate the factors which significantly affect the response factor. The significant factor from ANOVA analysis, grades the contribution on a percentage basis for the process variables used in this study which include temperature, H<sub>2</sub> partial pressure and contact time.

From ANOVA Table 4-5 and Figure 4-4 it can be seen that, the significant factors affecting the *n*-hexane conversion are contact time, which has a major contribution of 64.2%, followed by reaction temperature (26.58%) and a minor contribution 8.82% for H<sub>2</sub> partial pressure. In order to optimize *n*-hexane conversion, the effects of significant factors level are described by Figures 4-5.

Table 4-5: The ANOVA table of *n*- hexane conversion

Factors	DOF	Sum Sqrs	F Value	Prob>F	Contribution%
Temperature	2	278.228	66.556	0.0148	26.582
H <sub>2</sub> Pressure	2	92.279	22.074	0.0433	8.816
Contact time	2	671.978	160.747	0.0062	64.202
Error	2	4.180	-	-	0.399
Total	8	1046.666	-	-	100

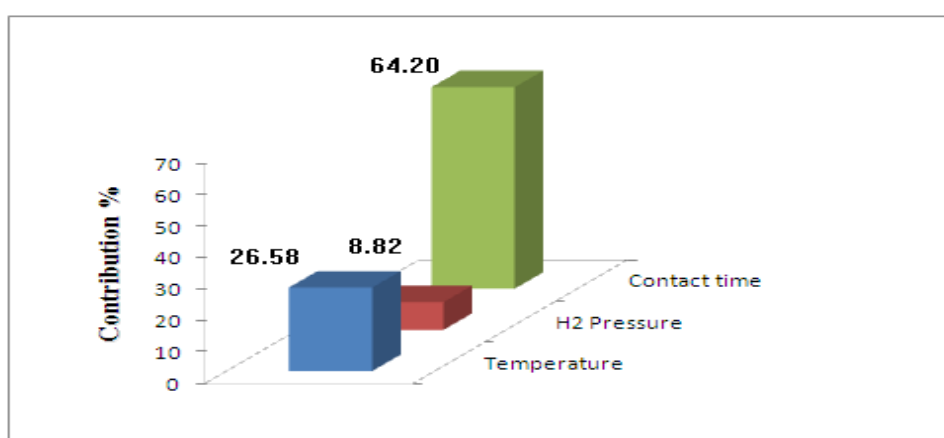


Figure 4-4: Percentage contribution of individual factors on variation in *n*-hexane conversion.

From Figure 4-5, it can be seen that, the highest conversion observed at level 1 for reaction temperature (A: A) which is at 723 K and reduces with decreasing temperature. The effects of contact time (C: C) for *n*-hexane conversion followed a similar path to that of the reaction temperature where conversion increases with increase in contact time, or in other words maximum *n*-hexane conversion is observed at level 1 which is at 7.1 minutes. As for hydrogen partial pressure (B: B), the conversion follows a reverse pattern to that of reaction temperature and contact time. Level 3 or 300 KPa is observed to have the maximum *n*-hexane conversion which decreases with increase in H<sub>2</sub> partial pressure. In conclusion the optimum operating conditions that enhance the *n*-hexane conversion are operating the process at reaction temperature 723 K at contact time 7.1 min with a H<sub>2</sub> partial pressure 300 KPa.

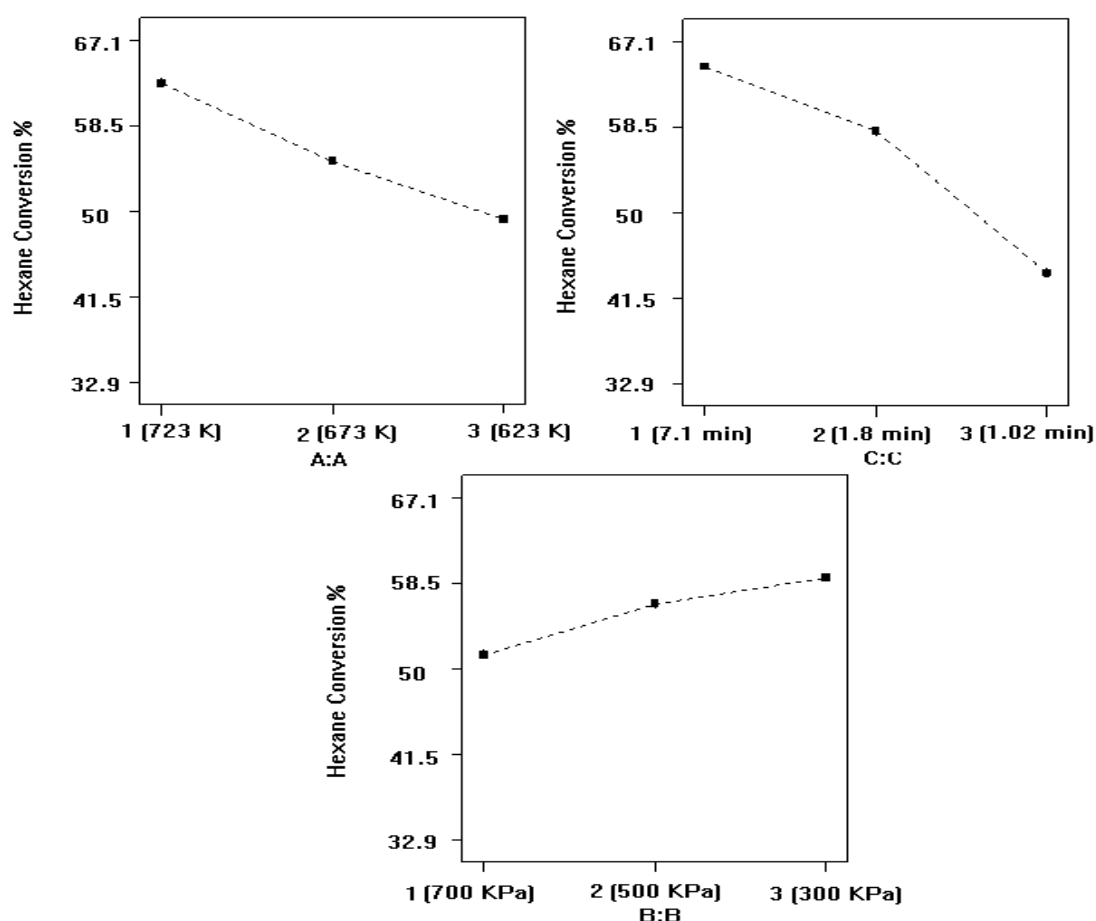


Figure 4-5: Effect of reaction temperature (A: A), contact time (C: C) and hydrogen pressure (B: B) on hexane conversion.

Having said so, the next step is to maximize the desirable (aromatics and isomers) and minimizing the undesirable (cracked and coke precursors) reformat product. It should be noted that desirable products improve octane number, while the undesirable decreases it.

#### 4.3.2 Optimization of aromatics reformat % yield using Taguchi OAD method

The next attempt in the Taguchi orthogonal array design is to find the optimum level for aromatic yield. For this purpose similar methods as described above was used and the results are shown in Figure 4-6. From Figure 4-6 be can be seen that hydrogen pressure (51.9 %) is the major contributor followed by contact time (32.7 %) for the production of aromatic. The reaction temperature (<1 %) has no significant effects on the aromatics production.

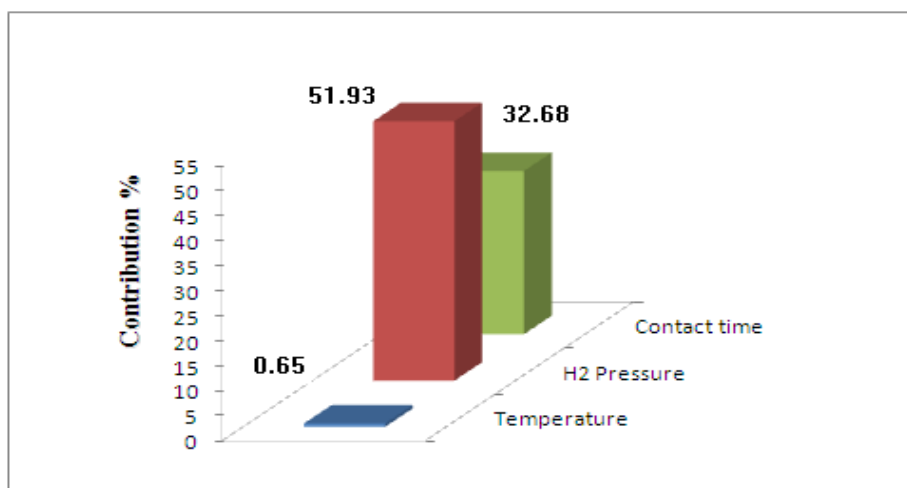


Figure 4-6: Percentage contribution of individual factors for aromatics yield.

The next step is to find the optimum level for each of the factors to maximize aromatic production. For this study the H<sub>2</sub> partial pressure and contact time are taken into consideration since reaction temperature proved to have insignificant role. The variation for each of these significant factors was plotted and is shown in Figures 4.7. From the Figure 4.7, it is shown that, the H<sub>2</sub> partial pressure (B:B) in level 3 (300 KPa) has the highest yield selectivity for aromatics. George et al. [8], reported that, lower hydrogen partial pressure favors dehydrogenation of naphthenes and dehydrocyclization of paraffin. But low H<sub>2</sub> pressure reduces the activity of the

catalyst. Therefore the choice of hydrogen pressure for a reformer is an important matter of balancing product yields against deactivation rates as recommended by [3, 24, 41]. As for contact time (C:C) level 1 (7.1 min) is most favorable for highest selectivity for aromatic production.

Although the reaction temperature (A:A) has insignificant effect in our present situation, but Huayun [94], indicated that higher reaction temperature induces higher production of aromatics which increases octane rating however Agbajelola [24], warn that this will reduce catalyst life. In view of that an optimum temperature condition should be taken into consideration for the final Taguchi analysis.

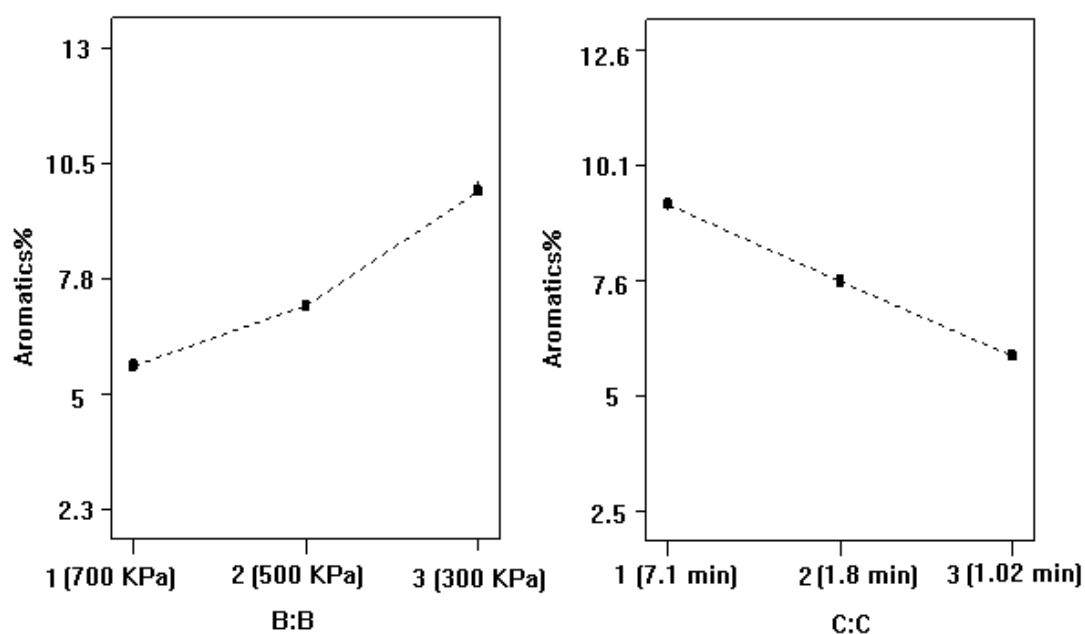


Figure 4-7: Effect of H<sub>2</sub> pressure (B: B) and contact time (C: C) level for aromatic yields.

#### 4.3.3 Optimization of isomers reformat % yield using Taguchi OAD method

The Taguchi OAD method for optimization of isomer reformat yield is calculated and presented in Figure 4-8. From the same figure it can be observed the contribution from all three process variable factor is more or less quite similar unlike the earlier studies. Contribution factors for contact time, reaction temperature and H<sub>2</sub> partial pressure are 35.7, 25.3 and 18.7 % respectively.

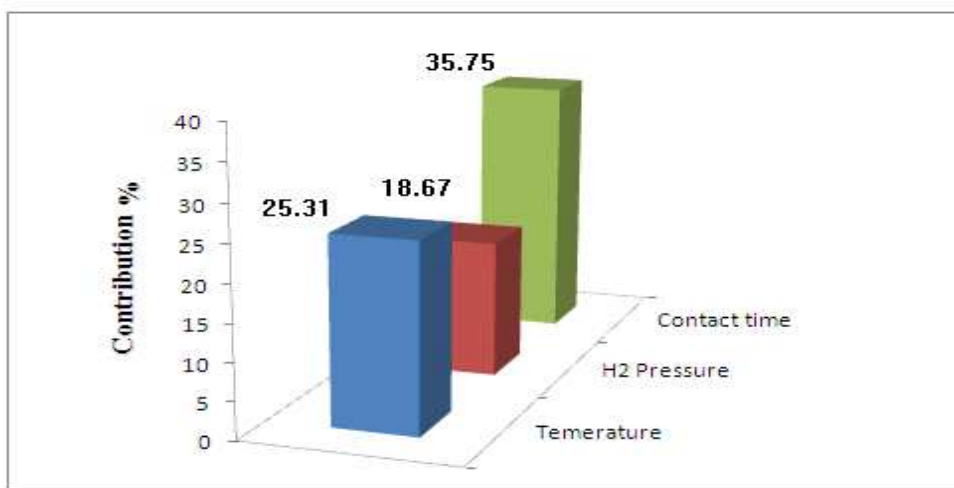


Figure 4-8: Percentage contribution of individual factors on isomers yield.

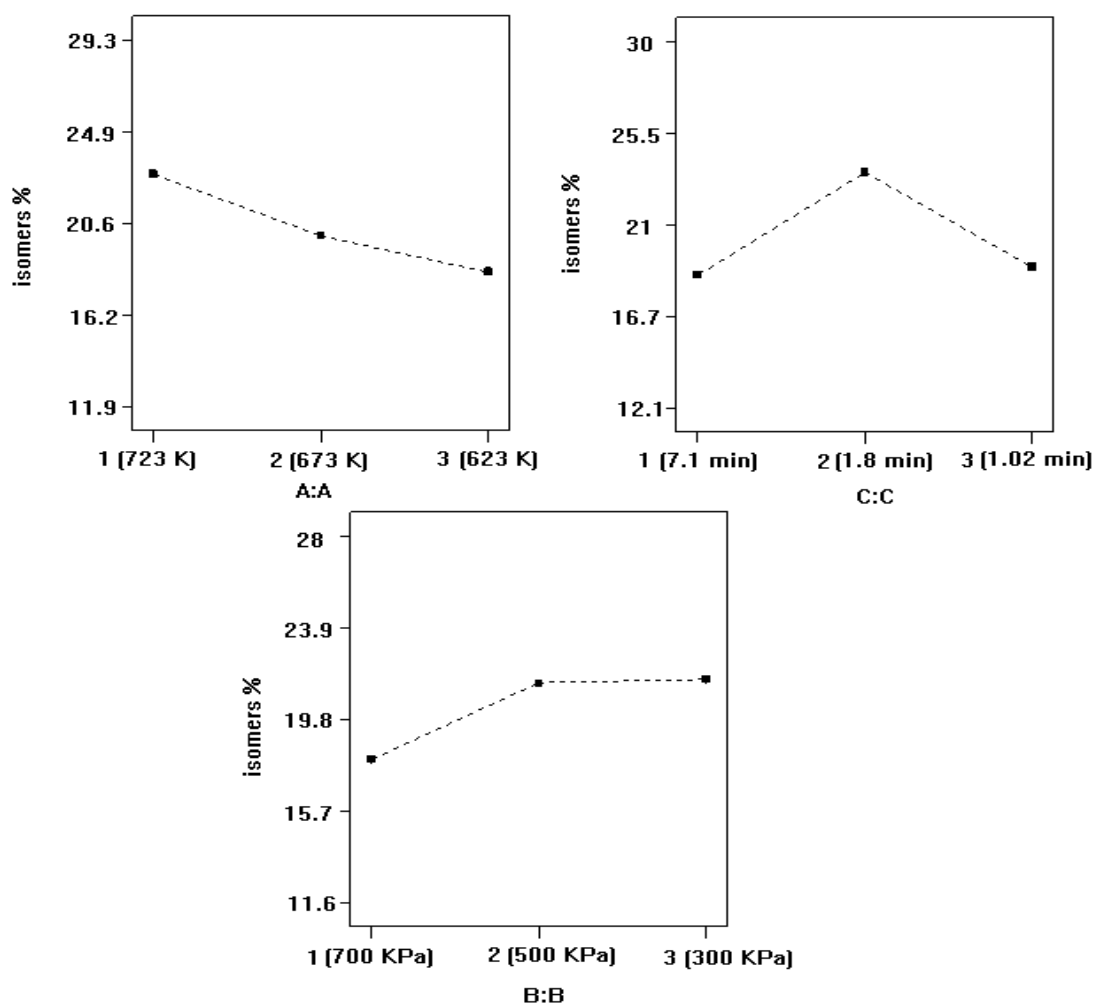


Figure 4-9: Effect of reaction temperature (A: A), contact time (C: C), and H<sub>2</sub> partial pressure (B:B) level on isomers yield.

Plots of the influence of variation of process variable for all three are highlighted in Figure 4-9. From the plot on reaction temperature (A:A), isomers yield is found to maximize at level 1 (723 K), in other words it increases with increasing reaction temperature. Contact time on the other hand maximizes at level 2 (1.78 min) for isomer reformat production. It was reported by Anup et al. [92] that increasing the residence time of the reactant on the catalyst leads to an enhanced yield of the skeletal isomers, but a much longer residence time results in cracking/polymerization of these products. The effect of H<sub>2</sub> pressure in isomers yield is less significant as compared with reaction temperature and contact time, but it favors lower H<sub>2</sub> partial pressure.

Base on the present study, the optimum process conditions for isomers production is operating at a reaction temperature of 723 K with 1.78 min contact time and using H<sub>2</sub> partial pressure of 300-500 KPa.

#### ***4.3.4 Minimizing of cracked reformat % yield using Taguchi OAD method***

In the earlier case maximizing of aromatic and isomer reformat was the main priority. For the present case minimizing of the cracked reformat is the main priority. In view of that Taguchi OAD was applied to the cracked product reformat main process variable contributor and it is presented in Figure 4-10. Based on this figure it can be seen that the contact time is the main contributor where its contribution stands at 73.9 %, followed by reaction temperature at 15.0 % and H<sub>2</sub> partial pressure at 8.4%.

In order to improve the octane number, the cracked reformates yield need to be reduced. Since contact time and reaction temperature are the main contributor for this process variable, it has to be minimized. In order to have a better understanding on the effect of contact time and temperature a plot on its effect of level of variation is conducted and is presented in Figure 4-11.

From Figure 4-11, it can be seen that cracked product reformates has the lowest yield at 1.02 min (Level 3 for contact time). Here it can be seen that with decreasing contact time, yield % of cracked reformat products decreases.

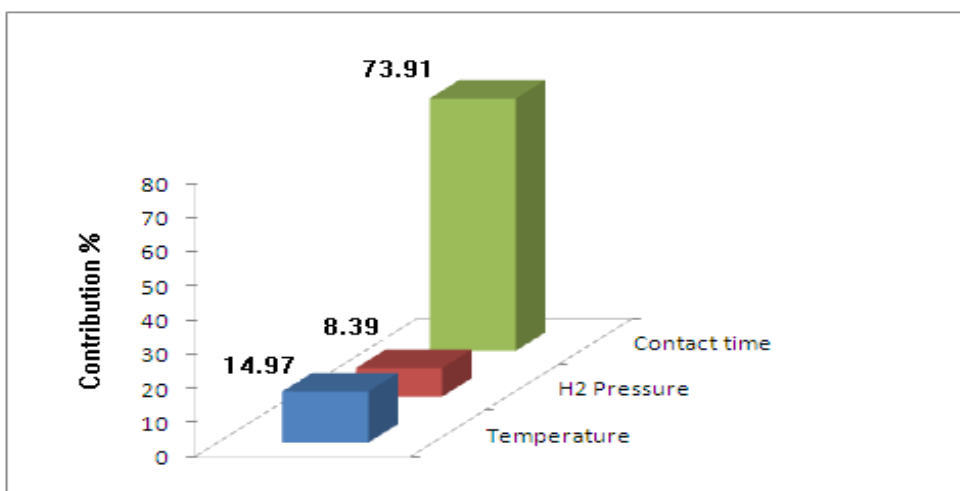


Figure 4-10: The percentage contribution of individual factors on ‘cracked’ yield.

This is in agreement with the findings of Aberuagba [93]. The same trend was observed for reaction temperature i.e a lower yield was obtained at lower temperature. H<sub>2</sub> partial pressure does not impose much significant effects of on cracked reformat product yield, but, it was observed that the higher H<sub>2</sub> partial pressure favors these types of undesired products. Based on this information the process should be operated on a lower contact time (1.02 mins) and reaction temperature (623 K) and probably lower H<sub>2</sub> partial pressure (300 KPa) to minimize cracked reformat product yield.

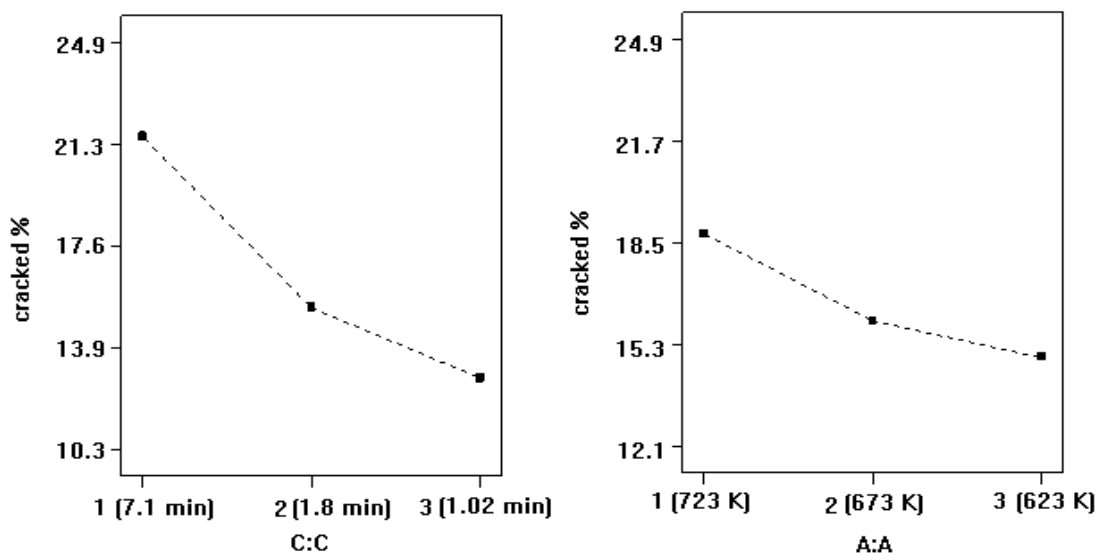


Figure 4-11: The effect of contact time (C:C) and reaction temperature (A:A) level on ‘cracked’ yield.

#### 4.3.5 Minimizing coke precursors reformat % yield using Taguchi OAD method

The same procedure as the other reformat products mentioned above was carried out for the coke precursors. The result is presented in Figures 4-12 and 4-13. Figure 4-12 shows that the major contributor is contact time (68.75 %) followed by reaction temperature (20.7 %) and the minor, H<sub>2</sub> partial pressure (7 %).

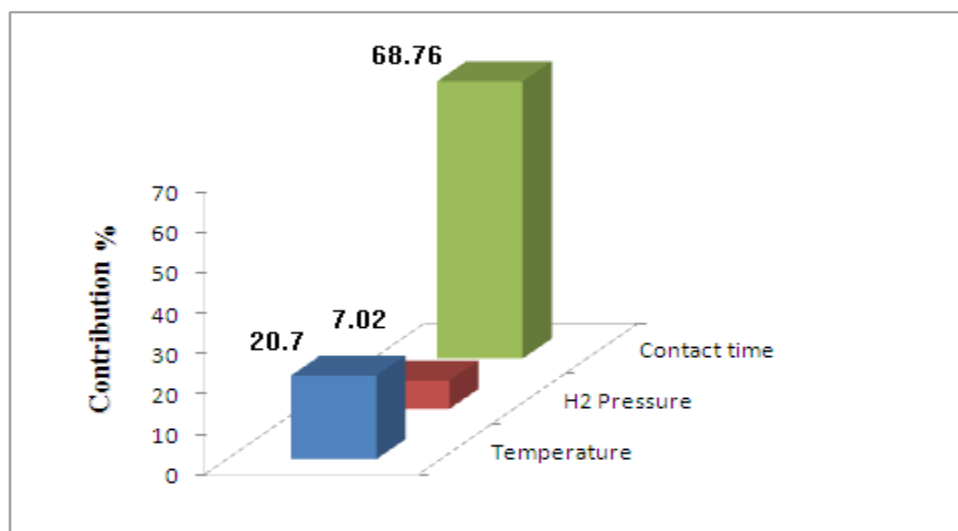


Figure 4-12: The percentage contribution of individual factors on variation in coke precursor's yield.

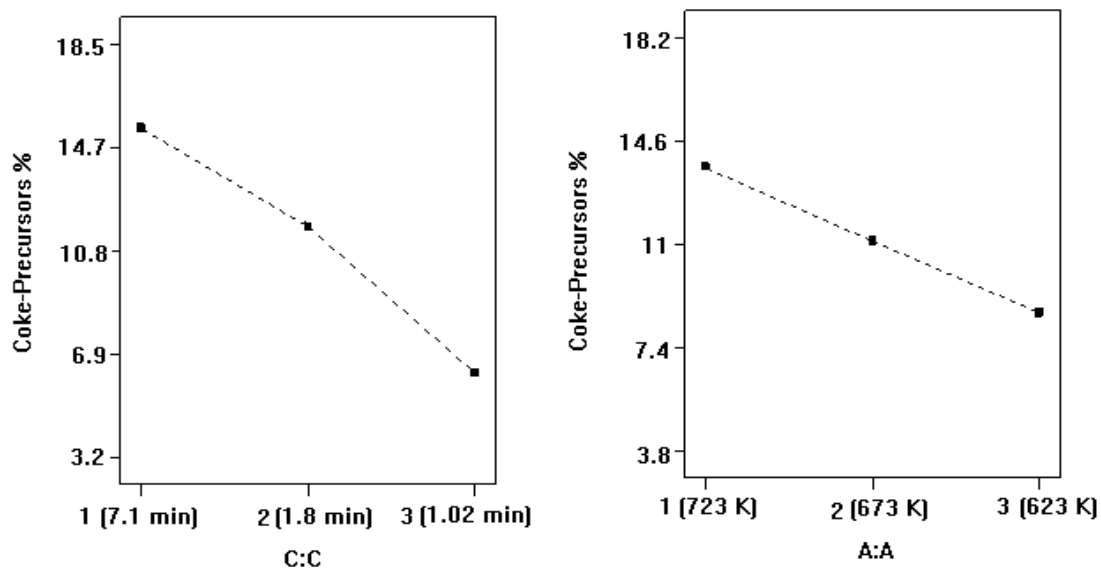


Figure 4-13: Effects of contact time (C: C) and reaction temperature (A: A) level on coke precursor's yield.

Since here too, H<sub>2</sub> partial pressure has little effect on the overall process, it will be of low priority, and the concentration will be taken for both the contact time and reaction temperature which is presented in Figure 4-13.

From Figure 4-13, it can be seen that the yield % decreases with increasing contact time. The same is also true for temperature. As mentioned by Aristidis et al. [36], the higher the reaction temperature, higher the desorption rate of coke precursor. George et al. [8], also reported that by increasing the temperature, yield of unsaturated products, which are coke precursors also increases.

Although the effect of H<sub>2</sub> pressure is not really a significant factor in this study but others like Liu et al. [32], reported that hydrogen inhibits the dehydrogenation reaction by lowering the concentration of the coke precursors; accordingly, it decreases the deactivation by coking. In order to minimize these coke precursors reformate, the process should be operated at lower contact time (1.02 mins) and reaction temperature (623 K).

From the above results it can be concluded that for *n*-hexane reforming, the main process condition to improve yield is reaction temperature, operated at 723 K. To improve product selectivity towards aromatics, H<sub>2</sub> partial pressure is most critical parameter and the optimum level is operating the reaction at 300 KPa. For the desired isomers reformate contact time is most critical and to obtain maximum yield the operation at 1.78-2.4 mins is recommended. For the undesirable product (cracked and coke precursor), the main process variable is contact time. To produce the least selectivity, 1.7 min contact time is recommended for both.

Based on the summary given above, the optimum condition for *n*-hexane reforming tailored to the desired product is to operate at reaction temperature of 723 K, 1.7 minutes contact time and 300 KPa H<sub>2</sub> partial pressure.

#### **4.4 Kinetics study of *n*-hexane reforming**

The study of *n*-hexane reforming kinetics here is done in order to have a clearer understanding on the reaction mechanism and investigate the activation energies for reversible and irreversible reactions. The classification for the reformate species is

based on the reaction mechanism, while that from the activation energy, a clearer picture on this reaction can be identified. For the *n*-hexane kinetics we can basically divide reformate reaction into 2 parts, namely reversible and irreversible.

The reforming reactions termed as reversible will include isomerization, and aromatization, while hydrocracking will belong to the irreversible reaction. The reversible reactions are the most rapid reactions in the reforming process, till it finally reaches the thermodynamics equilibrium.

#### 4.4.1 Reversible reactions

Cyclization and dehydrocyclization of *n*-hexane to aromatics and isomers can be considered as reversible reactions. For this kinetics model (reversible) first order will be assumed and will follow the model introduced by Levenspiel [97], where the *n*-hexane conversion termed as uncompleted will be applied here. The concentration of the reversible reaction can be graphically calculated based on equations 4-2 through 4-10.



Starting with the concentration ratio:

$$M = \frac{C_{Ro}}{C_{Ao}} \tag{4-3}$$

Rate of reaction is:

$$-\frac{dC_A}{dt} = k_1 C_A - k_2 C_R \tag{4-4}$$

$$\text{At equilibrium } \frac{dC_A}{dt} = 0 \tag{4-5}$$

The fractional conversion of A at equilibrium conditions is

$$K_C = \frac{k_1}{k_2} = \frac{C_{Re}}{C_{Ae}} = \frac{M + X_{Ae}}{1 - X_{Ae}} \tag{4-6}$$

$$\frac{dX_A}{dt} = \frac{k_1(M+1)}{M+X_{Ae}}(X_{Ae} - X_A) \quad (4-7)$$

The integration of (4-7) gives

$$-\ln\left(\frac{X_A}{X_{Ae}}\right) = -\ln\frac{C_A - C_{Ae}}{C_{A0} - C_{Ae}} = \frac{M+1}{M+X_{Ae}} k_1 t \quad (4-8)$$

A plot of:  $-\ln\left(1 - \frac{X_A}{X_{Ae}}\right)$  vs t

Produces a linear graph.

$$Slope = k_1 \frac{M+1}{M+X_{Ae}} \quad (4-9)$$

From the slope (equation 4-10), the activation energy can be calculated using Arrhenius equation given below

$$k = k_o e^{-E/RT} \quad (4-10)$$

Figure 4-14 represent a plot of  $-\ln(1-X_A/X_{Ae})$  against t (min) for the reversible reaction where  $X_{Ae}$  is equilibrium conversion of *n*-hexane. The reforming reaction conducted at 3 different temperatures (623, 673 and 723 K) at fixed H<sub>2</sub> partial pressure of 300 KPa. The forward ( $k_1$ ), back ( $k_2$ ) and equilibrium ( $K_c$ ) reaction rate constants have been accounted for, according to the equations mentioned above. The activation energy has been accounted according to EQ (4-10) (Arrhenius equation), from the results showed, the highest reaction rate constant was observed at the highest reaction temperature (Table 4-6). This is well documented by Taskar [4], who claimed that increasing the reaction rate at a high reaction temperature, will favor isomerization (cyclization) and aromatization (dehydrocyclization). The activation energy for reversible reactions only requires 16.39 kJ/mol. This was determined by plotting of  $\ln(k)$  vs  $1/T$  (Figure 4-15).

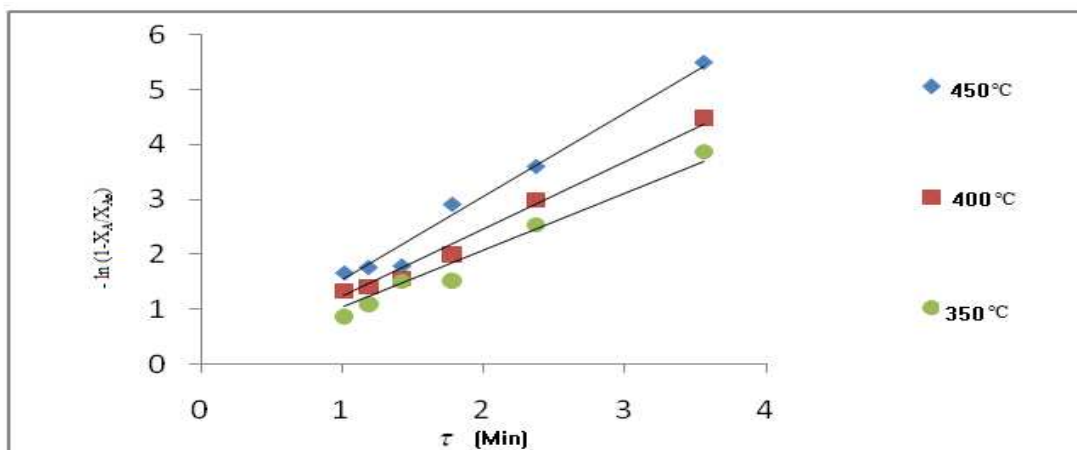


Figure 4-14: A plotting of  $-\ln(1-X_A/X_{Ae})$  versus  $t$  (min) for  $n$ -hexane kinetics at 300 KPa and varied temperatures over a  $Pt/Al_2O_3$  catalyst.

Table 4-6: Reaction rate constants:  $k_1$ ,  $k_2$  and  $K_c$  at varied temperatures for  $n$ -hexane reforming

Reaction temperature (K)	Forward reaction rate constant $k_1$ ( $\text{min}^{-1}$ )	Back reaction rate constant $k_2$ ( $\text{min}^{-1}$ )	Equilibrium rate constant ( $K_c$ )
723	0.868	0.421	2.060
673	0.613	0.332	1.844
623	0.554	0.417	1.327

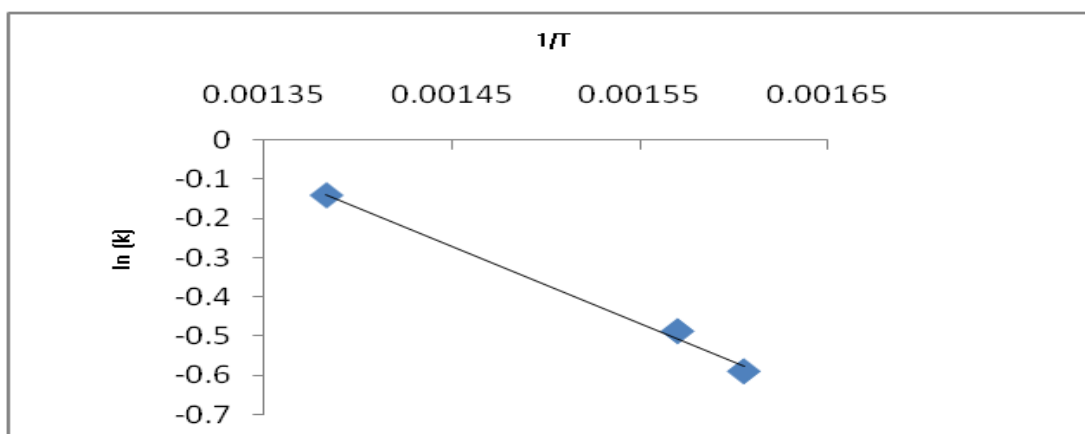


Figure 4-15: A plot of  $\ln(k)$  versus  $1/T$ .

#### 4.4.2 Irreversible reactions

In catalytic *n*-hexane reforming, the exothermic reactions such as, cracking of paraffin to small molecular weight products is considered as irreversible reaction. The irreversible reaction is simply a special case of a reversible reaction in which  $C_{Ae} = 0$  or  $X_{Ae} = 1$  or  $K_C = \infty$ . [97].

For a first order kinetics model for an irreversible unimolecular type:



The first order rate equation is

$$-r_A = \frac{dC_A}{dt} = kC_A \quad (4-12)$$

The separation and integration of equation (4-12) gives

$$-\ln\left(\frac{C_A}{C_{A0}}\right) = kt \quad (4-13)$$

The rate of reaction in terms of conversion is

$$\frac{dX_A}{dt} = k(1 - X_A) \quad (4-14)$$

The rearranging and integrating gives

$$-\ln(1 - X_A) = kt \quad (4-15)$$

A plot of  $-\ln(1 - X_A)$  vs.  $t$ , gives a straight line and the slope =  $k$  (rate constant).

Irreversible reactions are kinetically controlled. This includes reactions such as cracking of paraffins to their smallest molecule components (methane, ethane...etc). A plot of  $\ln(1 - X_A)$  vs  $t$  (min) gives the linear graph (Figure 4-16). The slope of this line is the rate constants according to the equations given above (EQ 4-15). In table 4-7, the highest rate constant was observed at the highest reaction temperature. This is why increasing the reaction temperature favors the formation of cracking (irreversible) products.

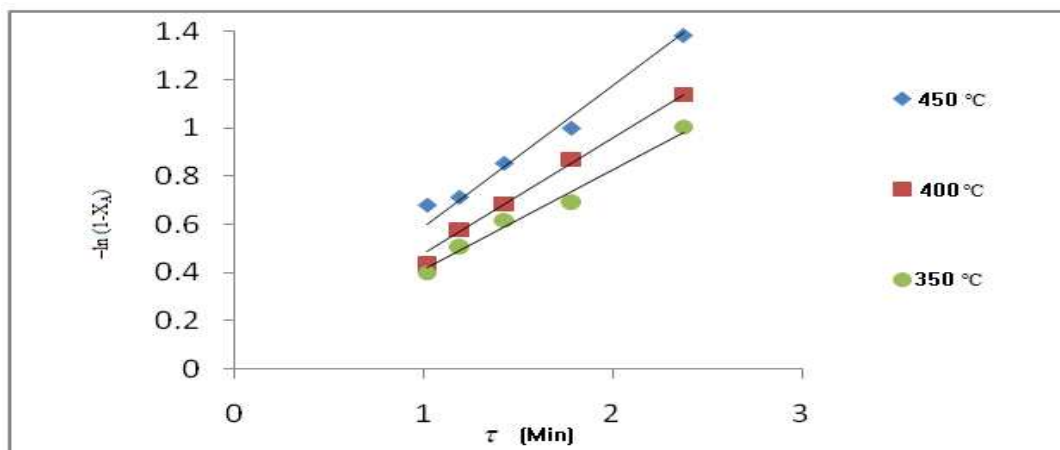


Figure 4-16: A plot of  $-\ln(1-X_A)$  versus  $t$  (min) for irreversible  $n$ -hexane kinetics at 700 KPa at varied temperatures over a  $\text{Pt}/\text{Al}_2\text{O}_3$  catalyst.

Table 4-7: Rate constants ( $k$ ) at 700 KPa at varied temperatures for  $n$ -hexane irreversible reforming reaction

Reaction temperature (K)	Rate constant $k$ ( $\text{min}^{-1}$ )
723	0.589
673	0.479
623	0.415

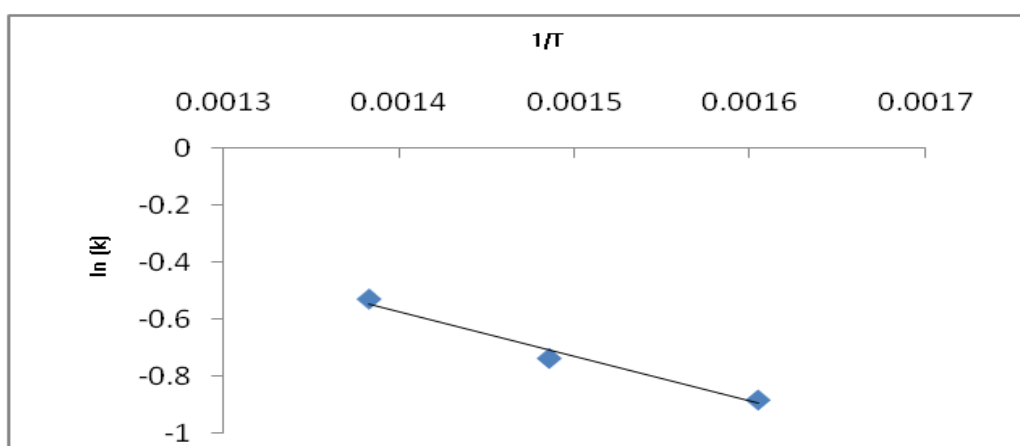


Figure 4-17: A plot of  $\ln(k)$  versus  $1/T$  (K) for  $n$ -hexane irreversible reforming reactions.

From Figure 4-17, the activation energy for this reaction was calculated to be 13.4 kJ mol<sup>-1</sup>. In the study of *n*-hexane aromatization over Pt/Al<sub>2</sub>O<sub>3</sub> by Aberuagba [24] the activation energy was reported to be 19.5 Kcal mol<sup>-1</sup>. In this study the lower activation energy recorded could be due to mass transfer or diffusion controlling this reaction.

#### **4.5 Effects of adding CCl<sub>4</sub> as an acid booster for *n*-hexane reforming reactions**

To recap, a Pt/Al<sub>2</sub>O<sub>3</sub> catalyst is bi-functional in nature; the role of Pt is to catalyze the dehydrogenation reaction, whereas the role of the support is to provide the acid sites which are responsible for the isomerization reactions. These acid sites are generated by addition of chlorine to the alumina support. Chlorided alumina acts as an acid and catalyzes carbon skeletal rearrangement through carbonium ion mechanisms. Proper acid activity is generally maintained by injecting trace amounts of a chloride compound with the feed based on the works by Nora et al. [30].

##### **4.5.1 Effect of adding CCl<sub>4</sub> on *n*-hexane conversion**

Introduction of carbon tetra chloride to pure *n*-hexane feed is to increase the acidity of the catalyst. The acidity of the catalyst should be tailored to favor higher isomerization reactions, as well as aromatics yields. In the present work, we investigate the effects of adding carbon tetrachloride (CCl<sub>4</sub>) to the *n*-hexane feed using various concentrations of CCl<sub>4</sub> (1, 3 and 5 vol/vol %). A control without CCl<sub>4</sub> is also incorporated into the study for comparison purpose. Results from experimental and Taguchi OAD analysis explained earlier showed that contact time is the most critical parameter, while reaction temperature and H<sub>2</sub> partial pressure were less significant. In view of that the reaction temperature and H<sub>2</sub> partial pressure was fixed at 723 K and 300 KPa respectively, while the contact time was varied for the present investigation into the effect of CCl<sub>4</sub> acidity on *n*-hexane reforming reaction. The experiment for this study was carried out according to that explained in chapter 3 section 3.3.

For this study, four runs consisting of three concentrations addition of  $\text{CCl}_4$  of 1, 3 & 5 vol/vol% in pure  $n$ -hexane and another without  $\text{CCl}_4$  (represented as ‘W’) were compared and are presented in Figure 4-18. From the same figure it can be seen that for all the four runs, the conversions increase till they reach the maximum and then stabilized with increasing contact time. It was observed that, there is a slight increase of the average overall conversion by addition of  $\text{CCl}_4$  to the  $n$ -hexane feed. The average conversion refers to the average  $n$ -hexane conversion taken from contact time between 1.78 to 7.11 minutes. The calculated result from Figure 4-18 for the average  $n$ -hexane % conversion for 0, 1, 3 and 5% are 78.6, 84.9, 92.8 and 95.5 respectively. This indicates that by the addition of the first 1%  $\text{CCl}_4$  gives an improvement of 6.3% above that of the control (pure  $n$ -hexane ‘W’). Further addition of  $\text{CCl}_4$  thereafter (1 to 5 %) gives an additional increase of 10.6 % conversion.

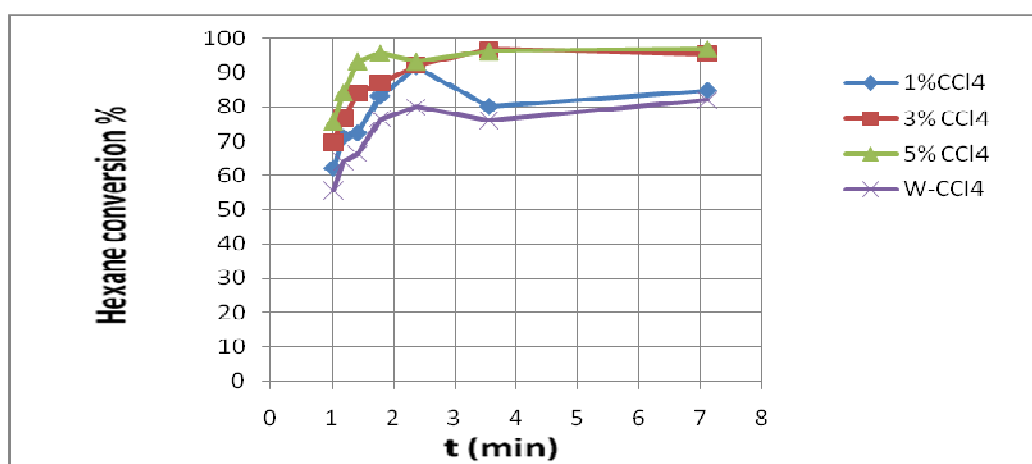


Figure 4-18:  $n$ -hexane conversion % over the  $\text{Pt}/\text{Al}_2\text{O}_3$  catalyst, at 723 K and  $\text{H}_2$  pressure at 300 KPa for 1 %, 3 %, 5 %  $\text{CCl}_4$  and pure hexane (W- $\text{CCl}_4$ ).

From the above observation it can be seen that the highest conversion of  $n$ -hexane was obtained from the addition of 5 %  $\text{CCl}_4$ , but 0 to 1% addition of  $\text{CCl}_4$  gives more value to the  $n$ -hexane conversion (6.3 %). This is because when going from 1 to 5% gives a moderate rise of 2.65 % per 1%  $\text{CCl}_4$  addition. Further as discussed earlier in this study, increasing the concentration of chloride causes a rise in the catalyst acidity. The higher acidity favors higher  $n$ -hexane conversion, but it should be noted that increase in acidity increases catalytic activity, resulting in more cracking reaction favoring gaseous products at the expense of liquid products. The later product is more meaningful for the reforming process.

#### 4.5.2 Effects of addition of CCl<sub>4</sub> on selectivity of reformat species

Since the main objective of *n*-hexane reforming process is to maximize isomers and aromatic product species, another set of experiment was carried out for this purpose. The reformat product species grouping are here similar to those explained in the previous sub-section. Further based on the *n*-hexane conversion results from the previous section, it can be noticed that the results obtained follows a similar trend with or without CCl<sub>4</sub> addition. Based on the Taguchi OAD analysis done in section 4.3, the process variable for this series of experiment was preset as; contact time, 1.78 minutes reaction temperature, 723 K and H<sub>2</sub> partial pressure, 300 KPa. This was done to ascertain the significant role in *n*-hexane reforming and at the same time improve catalytic stability so that the selectivity is directed to the desired reformat yield at the expense of the undesirable ones.

For this study the *n*-hexane reforming reaction, the process variable was fixed as explained above, and its affect of addition of CCl<sub>4</sub> from 0, 1, 3 and 5 vol/vol% in pure *n*-hexane was investigated. The result from these calculations is presented in Table 4-8. Under the total conversion column, the value in bracket indicate the selectivity normalized towards desired (isomer and aromatic) products.

Table 4-8: The effect of CCl<sub>4</sub> doping on yield selectivity of reformat species during *n*-hexane reforming over industrial Pt/Al<sub>2</sub>O<sub>3</sub> catalyst

CCl <sub>4</sub> Doping (%)	% Yield of Reformat species				
	Cracked	Coke precursor	Isomers	aromatics	Tot. Conv
0	19.87	15.88	29.18	15.01	79.9( 55.3)
1	22.87	19.88	30.92	18.01	91.7( 53.4)
3	25.19	15.66	30.19	21.01	92.1(55.6)
5	26.10	19.03	30.73	19.74	95.6(52.8)

From Table 4-8 it can be seen that the total *n*-hexane conversion over the Pt/Al<sub>2</sub>O<sub>3</sub> catalyst increased with increase in CCl<sub>4</sub> doping. This is expected because addition of CCl<sub>4</sub> increases the number of acid site on the catalyst as a result more products are formed.

It is interesting to know that with the addition of CCl<sub>4</sub>, the isomer reformates yield are practically unaffected. As for the aromatics reformat species they increase steadily by multiple of 3% from 0 to 3%, CCl<sub>4</sub> addition, but going from 3 to 5% a small drop of 1.3% (compared to that at 3%) was noticed.

The cracked reformat species increases steadily with increase in CCl<sub>4</sub> addition. This is also anticipated since increase in acid sites increases cracking activities as reported by Raj et al. [61]. Coke precursor follows a different route entirely. An oscillation type curve is observed. When going from 0 to 1% CCl<sub>4</sub> addition, an increase of about 4% yield is observed. Further addition to 3% the yield drops by 4.2% close to 0% addition. At 5% CCl<sub>4</sub> addition, coke precursor yield increases by about 3.6%. This indicates that CCl<sub>4</sub> addition induces dehydrocyclization reactions which are favorable to aromatic formation. Since dehydrocyclization dehydrogenation (formation of coke precursor) reactions produces excess hydrogen, a balance must be struck to stabilize the system. Some of these excess hydrogen is taken up by the cracked saturated reformat (reason for the increase the cracked reformat products). The rate of intake of H<sub>2</sub> by the cracked saturated reformat species is not fast enough to consume all the hydrogen produced resulting in an unbalance system generated by increasing CCl<sub>4</sub> addition. We believe this is one of the main reasons for the sudden drop of coke precursor at 3% addition of CCl<sub>4</sub>, while an increase yield of aromatic is observed at the same addition. At this stage dehydrocyclization competes with dehydrogenation, while the former is more predominant than the latter.

Further addition of CCl<sub>4</sub> to 5%, creates even more acid sites. This induces further competing reaction between the dehydrogenation and dehydrocyclization reactions, as a result a major increase in cracked reformat species over the aromatic reformat. This indicates that at 3% CCl<sub>4</sub> addition dehydrocyclization reaction will dominates while at 5% CCl<sub>4</sub> addition dehydrogenation (coke precursors) dominates. It is well documented by Anand et al. [21] that, the injection of CCl<sub>4</sub> at a high reaction temperature causes 2–3% of CCl<sub>4</sub> to be converted into coke and deposited on the

catalyst surface. As for the desired product (within bracket in 'Tot Conv' column), addition of  $\text{CCl}_4$  does not improve their yield significantly. The main function for  $\text{CCl}_4$  addition is to improve catalytic stability, or in other words it can be used to repair or replace damaged acid sites.

#### **4.6 Effects of dimethyl disulfide (DMDS) on *n*-hexane reforming**

Borgna et al. [9], in their study, showed that sulfur compounds poison the catalyst surface, resulting in deactivation of the catalyst. Others [19, 55] proved that sulfur is not totally unwanted, because a low concentration of sulfur in the feed or during the start-up of units can suppress excessive hydrogenolysis at the beginning of the run and improve the catalyst stability.

##### **4.6.1 *Effects of DMDS on the yield selectivity of reformat product species***

Dimethyl disulphide (DMDS) was used for selectively poisoning the catalyst active site to reduce the catalyst activity so that more preferred liquid product are produced rather than gaseous products. For the purpose of this study, the process variable selected based on the results obtained earlier using the Taguchi analysis for optimum *n*-hexane reforming process. These recommendations include maintaining the reaction temperature at 723 K,  $\text{H}_2$  partial pressure at 300 KPa and contact time of 1.78 minutes. The results from this analysis are presented in Table 4-9. Under the total conversion column, the value in bracket indicate the selectivity normalized towards desired (isomer and aromatic) products.

From the Table 4-9, it can be seen that addition of DMDS, in general both coke precursor and isomer selectivity increase, while that of cracked and aromatic reformates decreased. The total conversion initially decreased on addition of 10 ppm after which they start increasing on further addition until they reach the highest conversion of 82.3 % (2.4% above 0 addition) at 200 ppm of DMDS addition. This indicates that although the DMDS selectively poison the active acid sites, it selectively increased isomers and coke precursor reformates.

Table 4-9: The effect of DMDS doping on yield selectivity of reformat species during *n*-hexane reforming over industrial Pt/Al<sub>2</sub>O<sub>3</sub> catalyst

DMDS Doping (ppm)	% Yield of Reformat species				
	Cracked	Coke precursor	Isomers	Aromatics	Tot. Conv
0	19.87	15.88	29.18	15.01	79.9( 55.3)
10	11.96	19.02	29.15	11.06	71.2(56.2)
100	7.16	23.80	33.19	9.87	74.0 (58.2)
200	5.70	30.99	36.64	9.00	82.3(55.4)

In the case of coke precursor, increased yield was observed with increased addition of DMDS. In other words more unsaturated coke precursor is desorbed due to imbalance and limited free hydrogen. This effect is shown by the decrease of both the cracked and aromatic yield. This decrement of cracked products may be a result of poisoning of the catalyst acid sites rendering limited space on the catalyst to undergo cracking reaction. As for the aromatics, dehydrocyclization reactions are hindered as a result from competing reformat for active sites (Pt) as suggested by Garry et al. [19, 55].

On introducing 10 ppm DMDS, the total conversion decreases by about 8.7 %, but the selectivity towards desired product increased by about 1 % only. The cracked and aromatic yield decreases by about 8 and 4 % respectively. The coke precursor reformates on the other hand increases by 3 %. A similar trend was noticed with increased in DMDS doping, but the cracked and aromatic reformat products yield % decreased by reduced amount with increase of DMDS doping. The coke precursor on the other hand increases at a faster rate with similar increase of DMDS doping. George et al. [8] and Pieck et al. [8, 56], reported that small amount of S increased the amount of dehydrogenated compounds (coke precursors) by desorbing them from the catalyst. This partial sulfur poisoning of the Pt/Al<sub>2</sub>O<sub>3</sub> reduces the hydrogenation

/dehydrogenations activity and at the same time it decreases mono-functional metal-catalyzed reactions (hydrogenation /dehydrogenation activity).

As for the isomer reformates, they are unaffected at lower (10 ppm) doping of DMDS, but starts to increase above 100 ppm doping of DMDS. An interesting point to note is that the selectivity towards desired reformates has the optimum level at 100 ppm DMDS doping. Pieck et al. [56], suggested that there is a concomitant increase in the activity for acid-control for the isomerization reactions (skeletal rearrangement reactions) due to the partial sulfur poisoning of the Pt/Al<sub>2</sub>O<sub>3</sub>. Borgna et al. [9], also supports the above statement, that sulfur increases the activity for acid-controlled isomerization reactions.

From the above observation it can be concluded that 100 ppm of DMDS doping is the optimum level for *n*-hexane reforming reaction. The conversion although is much lower than at 200 and 0 ppm, gives the highest selectivity towards the desired reformat products.

#### **4.7 Kinetics and regeneration of industrial spent reforming catalyst**

It is a well documented fact that the major cause of catalyst deactivation in naphtha reforming is due to coking [11]. In order to embark on the regeneration studies, an understanding on the kinetics of carbon deposition at a macro level should be available. Deactivation of naphtha reforming start from the role of coking in catalyst degradation and extend further to the influence of conversion and in certain cases product selectivity. Rate of carbon deposition and its mechanism varies from one process to another a result it influences the nature and morphology of carbon deposits, their quantity and distribution between metal clusters and the support as reported by Pieck et al. [67]. Coke can either be present as chemisorbed (strong bonded as monolayer) or physisorbed (weakly bonded in multilayers). These absorbed molecules can totally cover the metal active site resulting in partial or total isolation of reactant from the active sites hastening the deactivation of the catalyst particles. Build-up of this deactivator in the pores of the catalyst will exert stress and finally fracture the support material.

In catalyst with wider pore structures, which are partially filled will limit access of the reactant to the active sites. If the average pore diameter shifts towards lower values after coking, location of coke either on the metal or the support and the nature of coke (hard or soft) become more critical for catalyst stability rather than coke content [31, 59, 66]. Increase in the average pore diameter may be an indication of structural damage.

For regeneration studies of spent catalyst which involve mechanisms of deactivation, regeneration conditions, textural properties and the nature of the metallic phase of the catalysts should be well understood. As a result each regeneration activity must be treated on case to case basis. Sample histories like purity, feedstock composition, industrial process conditions, etc. are important criteria to aid in the understanding and to devise a proper regeneration technique. Temperature regime can be the most critical parameter in the regeneration process because it directly influences the stability of the metallic phase and the support. Temperature above 773 K (500 °C) can also influence the de-structuring of the metallic phase by agglomeration, crystallization, volatilization or sinterization of the catalytic phases themselves or with the support forming inactive species [82].

TGA technique is utilized in this work to simulate and study commercial coked catalysts regeneration properties, coke formation mechanism and its affects to catalytic activity. TGA aided with thermo analytical techniques like TPO offers additional insights to the chemical reactivity of the coke and gas solid regeneration kinetics. All these techniques measure the weight loss by coke burning at high temperatures in different atmospheres.

Prior to selecting an industrial spent Pt/ Al<sub>2</sub>O<sub>3</sub> naphtha reforming catalyst, its history was collected. Based on the history of the spent catalyst it is understood that the catalyst was collected after the sixth cycle of operation in a commercial radial flow reactor unit at hydrocarbon pressure of 6 kg cm<sup>-2</sup>, temperatures from 763 to 793 K, WHSV= 2.0 h<sup>-1</sup>, and H<sub>2</sub>/HC molar ratio of 3.80. The detail information of the thermo-analytical techniques and calculation please refer to Chapter 3 section 3.6

#### 4.7.1 *Thermal gravimetric analysis (TGA)*

For the TGA studies two similar portion from the same batch of spent industrial catalyst were used. A similar technique as described below was followed, but the main difference lies on the heating rate used. Form Figure 4-19, the temperature range used was from 323 to 1073 K with a constant flow rate 20 ml min<sup>-1</sup> (using different gas medium for different temperature range) and heating rate of 10 K min<sup>-1</sup>. For the initial heating range from 323 to 473 K was done under N<sub>2</sub> medium (stage N<sub>2</sub>). This is basically done for the removal of water and volatile materials. The second heating range from 473 to 1073 K, the flow medium was switched to air with the same heating and flow rate. A duplicate test was also done for the same spent catalyst batch; the only difference was the heating rate was increased from 10 to 15 K min<sup>-1</sup>.

The weight loss resulting from the second heating range will be will be considered for the de-coking studies. This temperature range for each graph is then divided into 3 different stages denoted by stages 1, 2 and 3 in Figure 4-19 to differentiate the different coke species. The stage 1, from 473 to 673 K will be considered as ‘soft’ coke while 673 to 873 K (stage 2) as ‘hard’ coke and the last, stage 3 from 873 to 1073 K as non-volatile or ‘laid’ coke. Table 4-10 gives the numerical data accumulated from Figure 4-19. Matusek et al. [50], distinguished three types of carbonaceous deposits on Pt/Al<sub>2</sub>O<sub>3</sub>; one on metal particles, another on the metal–support perimeter and the third entirely on the support.

During the pretreatment stage (stage N<sub>2</sub>) it can be seen that a weight loss is steep and accounts about 2.97 and 4.12 mg or 36 and 44% (values in bracket in row 3 of Table (4-10) of the total loss from the catalyst for graph A and B respectively. This loss is considered as the loss from the moisture and volatile compounds (not associated with coke) present on the spent catalyst and will be omitted from all the coke calculations. This shows that higher heating rate increases volatile component removal.

The ‘soft’ coke (stage 1) reaction rate loss is observed gentler than the stage N<sub>2</sub>. This ‘soft’ coke from heating rates 10 K min<sup>-1</sup> and 15 K min<sup>-1</sup> accounts for 1.67 and 1.65 mg respectively of the absolute coke present in the spent catalyst and is presented in Table 4-10. This indicates that the heating rate does not influence

desorption of ‘soft’ coke species. Larsson et al. [15], reported that the soft coke (reactive coke) formed at the vicinity of the active sites of the metal.

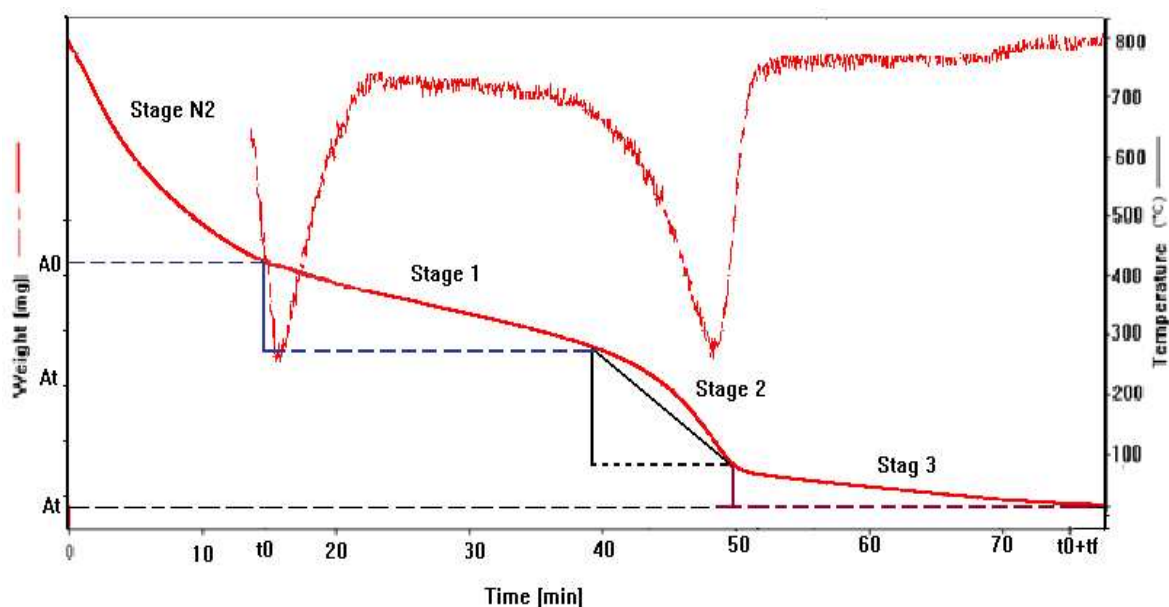


Figure 4-19: The original TGA curve; shows the catalyst weight [mg] versus the time [min] and temperature [°C] at heating rate  $10 \text{ K min}^{-1}$

Table 4-10: Coke and volatile species desorption from TGA at different heating rates.

Rate ( $\text{K min}^{-1}$ )	10		15	
Temp. Range (K)	Wt Loss (mg)	Coke species Norm (%)	Wt Loss (mg)	Coke species Norm (%)
323- 473 (v'tile)	2.97 (36%)		4.12 (44%)	
473-673 (soft)	1.67	31.7	1.65	31.3
673-873 (hard)	3.31	62.8	3.14	59.6
873- 1073 (laid)	0.29	5.5	0.48	9.1
Coke Cumm.	5.27 (64%)		5.27 (56%)	

As the temperature increases from 673 to 873 K (stage 2) a high and rapid weight loss of 'hard' coke amounting to 3.31 and 3.14 mg using a heating rate of 10 and 15 K min<sup>-1</sup> respectively was observed (Table 4-10). This indicates that heating have some influence on desorption of 'hard' coke. A higher heating rate retards desorption of 'hard' coke. Further it is possible that this type of coke is mostly present at the catalyst support and it has higher activation energy. JGlio et al. [82], confirmed that the slow heating rates are usually employed to better control the coke combustion.

From 873 to 1073 K [stage 3], the loss of non-volatile or 'laid' coke is drastically reduced. For heating rate of 10 K min<sup>-1</sup> the loss was 0.29 mg and for 15 K min<sup>-1</sup> is it 0.48mg. Since desorption rate is very low, this may indicate the air may have difficulty reacting or reaching the remnants of coke left over deep in the catalyst particles. It may also transformation of the coke into another species because of the high temperature equilibrium setting in. The non-volatile compounds may be too unstable to form or may decompose before it has an opportunity to be transported from the system [34].

From Table 4-10 it is interesting to note that although different heating rate was employed, the removal of volatile material differ by more than a mg, the rate of removal of coke varied, but the final cumulative coke yield remains almost the same. This shows that temperature is one of the main criteria for coke removal.

From the above observation it can be seen that the heating rate does not play a significant role when removing 'soft' or 'laid' coke. As for 'hard' coke, heating rate has a much more significant role. Lower heating rate (10 K min<sup>-1</sup>) is more efficient than a higher heating rate (15 K min<sup>-1</sup>). 'Hard' coke which is the main constituent of the coke material is more than double the quantity (62.8% of the total coke analyzed) of the sum of both the 'soft' and non-volatile coke material present on the spent catalyst. For regeneration studies a lower ramp rate is much more preferred since the major portion of the coke is the 'hard' type. This observation is in agreement with most industrial application. It should be noted that the slow heating rate are usually employed to better control the coke combustion [82]. This indicates that the 'hard' coke can be removed with proper de-coking methods. It is also interesting to see that the cumulative or sum of coke ('soft', 'hard' and 'laid' ) species removal are similar for both rates. This indicates that the structure of the coke material is unchanged when

applying different heating rate provided the temperature used is the same. The main difference is in the rate of species removal as described above.

For the present study it is assumed that the major portion of the coke is present on the catalyst surface. In view of that the desorption of coke from the catalyst surface can be assumed as 1<sup>st</sup> order based on the studies by Querini and Fung [17] and Yan Ren et. al [16, 91]. The coke is looked upon as tri-dimensional structure. Coke exhibits an increasing reaction order from almost zero to approaching 1 as the oxidation reaction set in. This is a typical reaction in a gas-solid reaction. Large surface coke particles decrease in size very slowly (reaction order close to zero) at the early part of the burning in order to generate similar size surface area coke particles (reaction order approaches 1). Using this assumption together with those of Ortega et al. [78] the kinetic model with respect to coke was created. To test the kinetic model the result from TGA with a heating rate of 10 K min<sup>-1</sup> was fitted to their model, and the following equation was used for the calculation of activation energy.

$$\frac{dC_c}{dt} = k_r C_c P_{O_2} \quad (4-16)$$

$$h = \frac{dT}{dt} \quad (4-17)$$

$$X = 1 - \frac{C_c}{C_{c^0}} \quad (4-18)$$

$$k = k_o \exp\left(-\frac{E_r}{RT}\right) \quad (4-19)$$

The integrated form is

$$\ln\left[-\ln\left(\frac{1-X}{T^2}\right)\right] = \ln\left[\frac{k_{oPO_2}}{h \frac{R}{E_r} \left(1 - \frac{2RT}{E_r}\right)}\right] - \frac{E_r}{RT} \quad (4-20)$$

Therefore, a plot of  $\ln [-\ln (1-X)]/T^2$  vs.  $1/T$ ; the slope gives the value of  $E_r$  and  $k_o$  from the intercept.

The results obtained from the above calculation are tabulated in Table 4-11 below. This current work further examines the exact mechanism of coke removal through

TGA experiments with two different heating rates for estimating the apparent activation energy of the process. The method of Ortega et al. [78], was used to estimate the activation energies. The highest activation energy was observed in stage 2 which is basically made up of ‘hard’ coke. It was demonstrated by Wang et al. [11] that relatively high apparent activation energy values should indicate decomposition via a chemical activated process, whereas low values should indicate diffusion limitation of the coke species. The coke with a high H/C ratio has high combustion reactivity and a low activation energy value. This indicates that the soft coke has a high H/C ratio while ‘hard’ coke has a lower H/C ratio [78].

Table 4-11: Activation energies and pre-exponential factors for the 3 coke species taken from TGA run at ramp rate of 10 K min<sup>-1</sup>.

Coke type	E <sub>r</sub> kJ/mol	k <sub>o</sub>	Temp range (K)
Soft	19.7873	1.8	473-673
Hard	86.3326	1.4X10 <sup>5</sup>	673-873
Laid	6.08098	0.06	873-1073

#### 4.7.2 *Fourier Transform infrared spectroscopy (FTIR)*

To complement the results from TGA, the FTIR surface analysis technique was used. The main objective of using FTIR is find the nature and location of especially the ‘soft’ coke species.

For this FTIR characterization two spectra of the same spent industrial catalyst were taken, one before the N<sub>2</sub> pre-treatment stage and the other after N<sub>2</sub> gas. Both this spectra are presented in Figure 4-20. Ruixia et al. [99] and Donald et al. [98, 99], from their studies suggested that the main absorption band at 3448.5 cm<sup>-1</sup> is due to the vibrations of hydroxyl groups on the catalyst surface and the shoulders at 1606.6 and 1637.5cm<sup>-1</sup> are possibly due to adsorption of olefin and aromatics on the catalyst

metal surface. This may indicate that the coke species found near the active metal is ‘soft’ coke and it is mainly made up of unsaturated hydrocarbon and heavy aromatics.

Li et al. [80], assigned the absorption bands between 3000 and 2800  $\text{cm}^{-1}$  to aromatic and aliphatic rings, which are probably produced by polycyclic aromatics like chrysene. Ruixia et al. [98], suggested that the other two absorption bands, at 2854.5  $\text{cm}^{-1}$  and 2925.8  $\text{cm}^{-1}$  were caused by symmetric and asymmetric flexion vibration of the C-H bonds associated with  $\text{CH}_3$ . The physisorbed  $\text{CO}_2$  shows in figure 4-20 by two successive bands at 2360.71 and 2341.42  $\text{cm}^{-1}$ , for both catalysts.

Evidence from work by Karge et al. [81], suggested that the absorption band at 1400.2  $\text{cm}^{-1}$  is due to ethylene type polymers adsorption. From these results and on comparison with Figure 4-20 strongly suggest that the commercial coked catalyst contains aromatics, alkyl groups, hydroxyl groups, aliphatic rings and olefins.

In case of spent Pt/ $\text{Al}_2\text{O}_3$  catalyst after nitrogen gas treated, it can be observed that the absorption band due to (C=C) and aromatics (coke precursors) between 3000  $\text{cm}^{-1}$  and 2800  $\text{cm}^{-1}$  are missing. This shows that elimination of these coke precursors is possible under  $\text{N}_2$  gas treatment. So nitrogen gas might be used here to disrobe the coke precursors (soft coke) from the spent catalyst. This is a well documented by Wang [76].

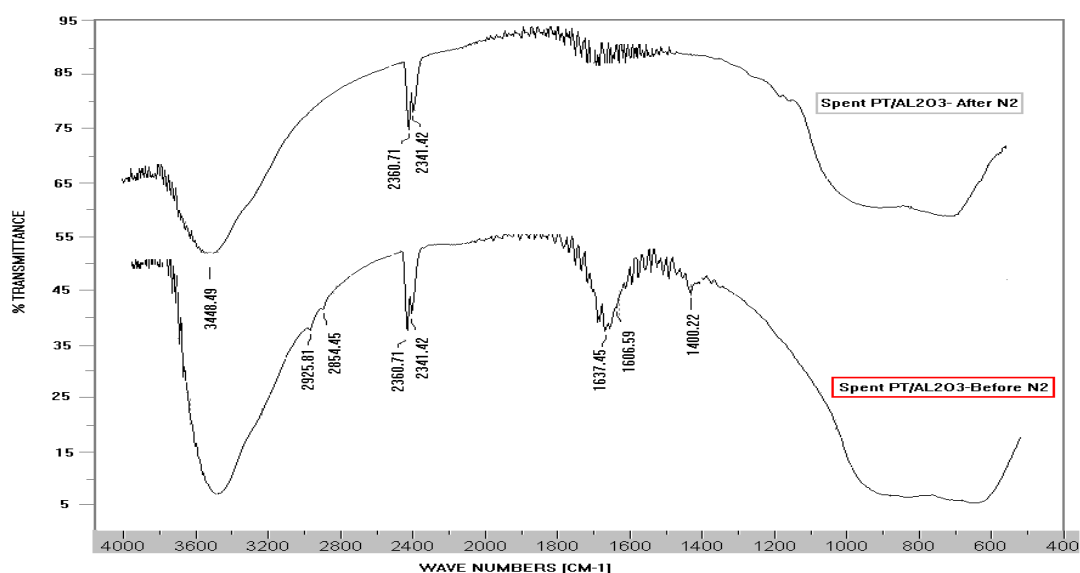


Figure 4-20: FTIR spectrum for spent Pt/ $\text{Al}_2\text{O}_3$  catalyst prior and after pre-treatment with  $\text{N}_2$  gas.

The de-Coking process is well described by TGA techniques. FTIR was used as evidence to show that soft coke can be removed after N<sub>2</sub> treatment. The ‘hard’ coke, the most abundance species, shows high activation energy of 86.3 kJ/mol. This ‘hard’ coke can be removed by proper re-generation process because it is chemically controlled phenomenon, the heavier non-volatile coke is diffusion controlled in nature and its existence is minimal.

#### **4.7.3 Temperature Programmed Oxidation (TPO)**

Having analyzed the nature of ‘soft’ coke and its regenerability, the next stage is to figure out how to tackle the removal of ‘hard’ coke. Based on the previous understanding, ‘hard’ coke is a chemically controlled phenomenon and usually found in the catalyst support sites. In order to understand the removal techniques, the chemistry of these coke species and its removal from the active sites must be understood. For this purpose we make use of the TPO, a surface technique which basically uses a simple temperature ramping program in an oxidizing atmosphere to dislodge and convert the coke species into its CO<sub>2</sub> form and volatize them from the surface of the catalyst. This technique is similar to TGA, but gives more information on the quantification of the CO<sub>2</sub> and temperature shift.

A similar technique used in TGA was extended to the TPO analysis. For this purpose the ‘soft’ and ‘hard’ coke were separately analyzed to find the influence of heating rate and oxidizing temperature on the coke species. For this purpose the industrial spent catalysts were treated under N<sub>2</sub> gas. In the 1<sup>st</sup> set of experiment, the 3 pretreated (void of volatile material) coked samples was heated till 873 K under 5% O<sub>2</sub> in N<sub>2</sub> medium at a flow rate of 20 ml min<sup>-1</sup>. For each sample the effect of using 3 different heating rates of 10, 15 and 20 K min<sup>-1</sup> was investigated. The result obtained from the 1<sup>st</sup> stage is given in Figure 4-21. The amount of CO<sub>2</sub> produced from the TPO analysis was directly related to the amount of coke species (‘hard’) present. Weight loss at different heating rates of 20, 15 and 10 K min<sup>-1</sup> is represented as ‘a’, ‘b’ and ‘c’ respectively and given in Figure 4-21.

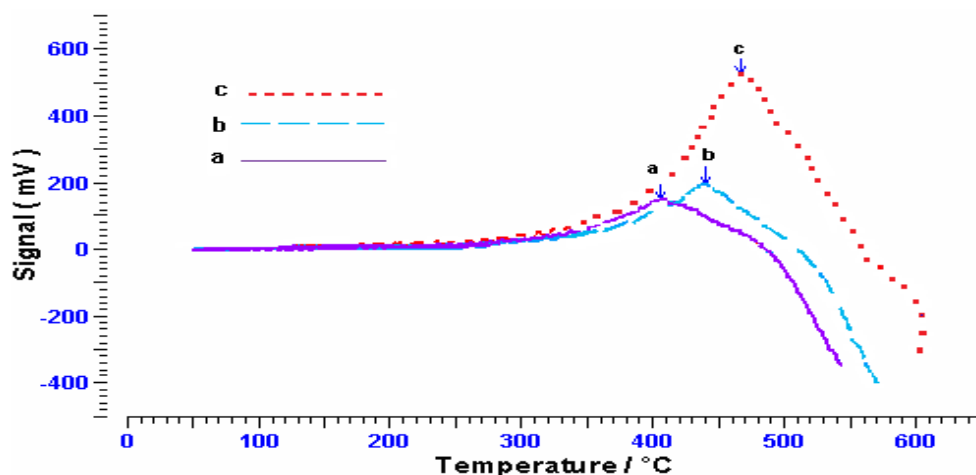


Figure 4-21: TPO results on commercial spent reforming catalyst at different heating rates, [a=heating rate 20 K min<sup>-1</sup>; b=15 K min<sup>-1</sup>; c=10 K min<sup>-1</sup>].

From Figure 4-21, it can be observed that increase in heating rate decreases CO<sub>2</sub> production. Querini & Fung [16], suggested that this phenomenon may be due to the fact that large coke ensembles are first broken down into smaller ensembles before being released as CO<sub>2</sub>. This assumption is based on first order reaction rate.

Increasing the heating rate leads to decrease in CO<sub>2</sub> production and shifting the oxidation peak to a low temperature. A slow heating rate is usually employed in industrial applications to have a better control of coke combustion [82]. When employing slow heating rate, temperature regime is important, because during the regeneration processes, coke removal and metallic phase stability must to be maintained. Final temperature is critical parameter because it directly influences the stability of the metallic phase and the support. Regeneration is an exothermic reaction. At high heating rate, if not fully controlled, will give rise to temperature runaway.

In the 2<sup>nd</sup> set of experiments, the 3 pretreated coked samples were heated under 5% O<sub>2</sub> in N<sub>2</sub> medium at a flow rate of 20ml min<sup>-1</sup> with heating rate of 15 K min<sup>-1</sup>. In this case three different final temperatures were used (873, 973 and 1073) K. The results obtained are shown in Figure 4-22. Labeled as ‘I’, ‘II’ and ‘III’ in the same graph represent the different final temperature used which is 873, 973 and 1073 K respectively. This was done so as to investigate the optimum temperature in which ‘hard’ coke can be removed.

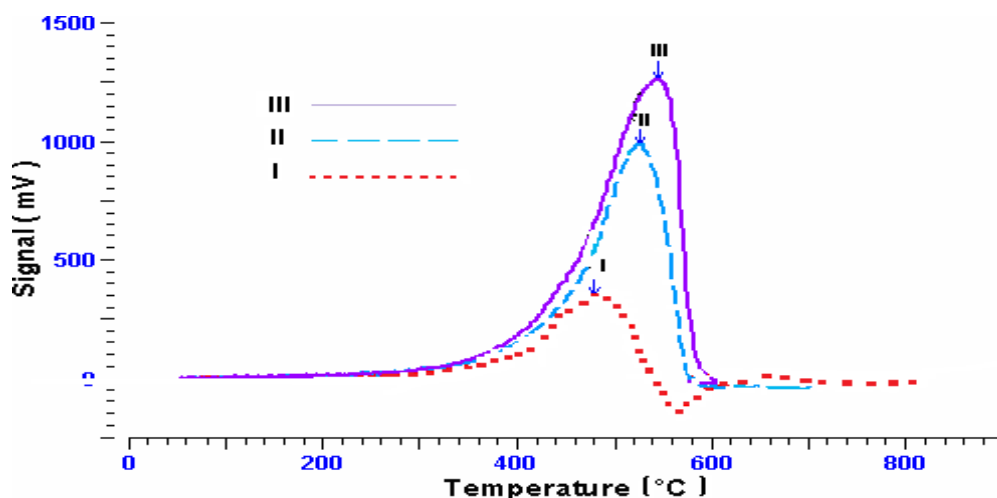


Figure 4-22: TPO results from a commercial spent reforming catalyst at different temperatures [I= 873 K II = 973 K III = 1073 K].

From the same Figure 4-22, it can be seen that the highest oxidation peak for ‘I’ (873 K) was observed at 753K (480 °C) whereas for 973 K and 1073 K the highest oxidation peaks have shifted to 793 K (520 °C) and 813K (540 °C), respectively. This indicates that the ‘hard’ coke is not completely removed if the regeneration is conducted at a temperature of 873 K (600 °C), although this is supposed to be the final cut point for the volatilization of the ‘hard’ coke. A significant amount of the ‘hard’ coke is still trapped on the surface of the catalyst even after the regeneration temperature had been increased to 973 K (700 °C). At the regeneration temperature of 1073 K, significant amount of ‘hard’ coke is removed, but there are still some left-over on the catalyst. Performing at a higher temperature is not advisable as the integrity of the active metal catalyst may be affected. As a result, it is advisable to perform regeneration activities at a temperature close to but not higher than 1073 K.

From Figure 4-21 and 4-22, it can be seen that just one peak was detected for each different heating rate and maximum temperature used. Based on these observations, it can be assumed that for industrial spent catalyst ‘soft’ coke may have volatilized in N<sub>2</sub> gas.

To prove this assumption another set of experiment was conducted. Here 5% O<sub>2</sub> in N<sub>2</sub> with a flow rate of 20 ml min<sup>-1</sup> was introduced and heated from room temperature to 1073 K at a heating rate of 10 K min<sup>-1</sup>. The results are shown in Figure 4-23.

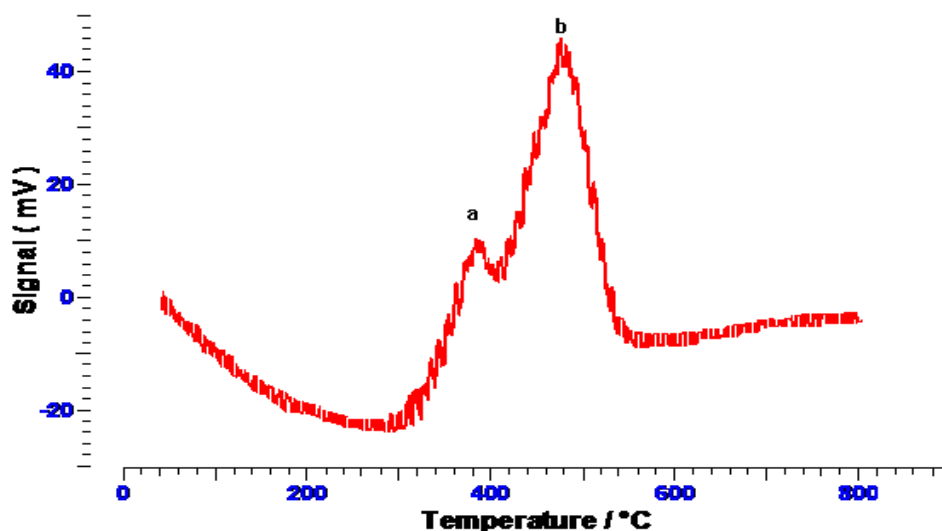


Figure 4-23: TPO result for industrial spent Pt/Al<sub>2</sub>O<sub>3</sub> reforming catalyst, at < 5% O<sub>2</sub> in N<sub>2</sub>, with a flow rate of 20 ml min<sup>-1</sup> and a heating rate of 10 K min<sup>-1</sup>.

From Figure 4-23 it can be seen that two oxidation peaks are present. The first peak (a) is the contribution from ‘soft’ coke which is closely attached on the vicinity of catalyst metal active site; whereas the bigger second peak (b) represents the ‘hard’ coke which is more tightly bound with the alumina support [31]. This further proves that N<sub>2</sub> gas regeneration is only capable of removing ‘soft’ coke only but not the ‘hard’ coke. This is in agreement with findings of Larsson et al. [15] they showed that, the ‘soft’ coke’ can be readily removed by N<sub>2</sub> gas. Further from our present study it can be concluded that combustion is necessary to remove the ‘hard’ coke.

The next step was to study how heating rate influence the removal of both ‘soft’ and ‘hard’ coke. For this purpose the TPO analysis was carried out at two different stages using 2 different mediums. In the first stage, N<sub>2</sub> was used (Figure 4-24), while in the second stage, 5.0 v/v % O<sub>2</sub> in N<sub>2</sub> was used. This is presented in Figure 4-25. For both stages, different heating rates (10, 15 and 20 K min<sup>-1</sup>) were used but, the dwell time of 120 minutes was fixed. Losses in soft, hard and total coke were recorded at various temperatures from 573 to 1073 K (300 to 800 °C) recorded after every 100 K. Both the soft and hard coke was calculated base on the equation given below [36, 77, 100].

$$\text{Soft coke} = \frac{\text{wt of catalyst before 1st stage} - \text{wt of catalyst after 1st stage}}{\text{wt of catalyst after 1st stage}} \times 100\% \quad (4-21)$$

$$\text{Hard coke} = \frac{\text{wt of catalyst after 1st stage} - \text{wt of catalyst after 2nd stage}}{\text{wt of catalyst after 2nd stage}} \times 100\% \quad (4-22)$$

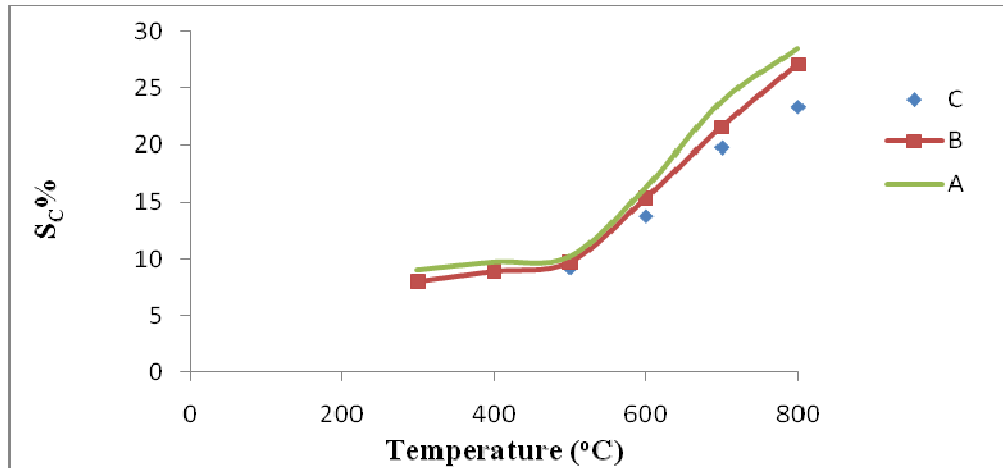


Figure 4-24: TPO results on weight % loss of soft coke ( $S_C$  %) during the 1<sup>st</sup> stage with different heating rates and temperature under a nitrogen atmosphere (A = 10 K min<sup>-1</sup>; B = 15 K min<sup>-1</sup>; C = 20 K min<sup>-1</sup>).

The results were explained using Figures 4-24 through 4.26. Figure 4-24 reflects the desorption rate of the ‘soft’ coke in N<sub>2</sub> gas atmosphere. In Figure 4-24 it can be seen that ‘soft’ coke weight percentages decrease with an increase in the heating rate. This may be due to the ‘soft’ coke becoming less stable at a low heating rate and becoming easily detachable from the surface due to rigorous phase transformation on the catalyst surface. In the case of a higher heating rate, the catalyst surface is less aggravated than at lower heating rate. The same result was observed in the TGA analysis, and it has been well documented that the low heating rate is always applied in the regeneration process to give better de-coking results than a higher heating rate [82]. As a result, the release of the ‘soft’ coke increases with lower heating rate and higher final temperature.

The same catalyst after the 1<sup>st</sup> stage is subjected to 5.0 v/v % O<sub>2</sub> in N<sub>2</sub> (removal of ‘hard’ coke) with the same combustion regime (2<sup>nd</sup> stage) to investigate its effect of multiply medium of heating on ‘hard’ coke removal. The result from this experiment

is presented in Figure 2-25. The weight percentage of coke removed from the catalyst was calculated as per the equation mentioned above.

It was noticed the results observed from Figure 4-25 showed an entirely reverse trend to that of Figure 4-24. Here the release of coke is retarded with an increase in temperature and heating rate. This observation can probably be explained by the fact that during the N<sub>2</sub> heat treatment (1<sup>st</sup> stage) most of the ‘soft’ coke and some ‘hard’ coke may have been volatilized or removed. Some of the ‘hard’ coke at higher temperatures may have undergone phase transformation to a more graphitic nature with the release of H<sub>2</sub> species. This graphitic coke tends to penetrate deeper and stick more strongly on the catalyst surface. This makes the coke sensitive (less reactive) and more difficult to remove.

Calvin & Bartholomew [34], explained this phenomenon by saying that at high temperatures the rate of formation of coke equals the rate of its de-composition, i.e. equilibrium occurs. However, during the transformation the volatility of coke decreases and makes transport from the system difficult. This phenomenon was also explained by Wang [76]. He indicated that the coke is more aromatic and stable at high reaction temperatures than at low reaction temperatures. As a result it is more difficult to remove due to its low volatility. Pedro et al. [79], found that the H/C ratio decreased with increase reaction temperature. This means the soluble light coke decreases and the insoluble heavy coke increases while increasing the temperature simultaneously.

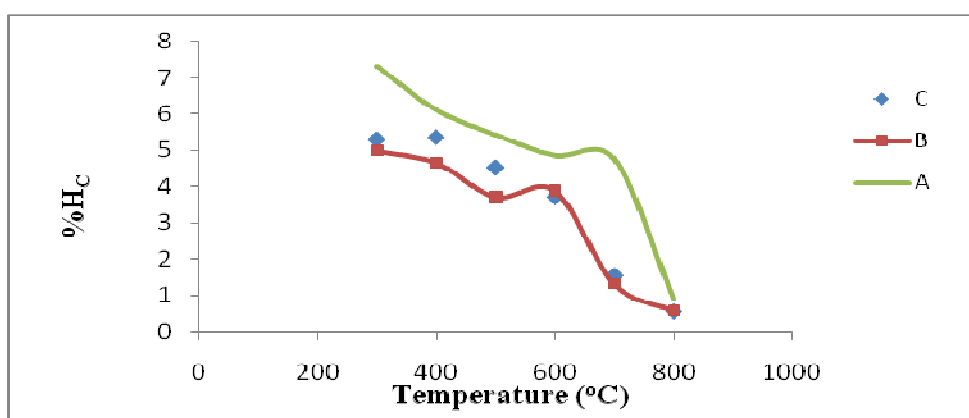


Figure 4-25: TPO results on weight % loss of Hard Coke (Hc %) at 2nd stage with different heating rates and temperatures under 5.0 v/v % O<sub>2</sub> in N<sub>2</sub>. (A = 10 K min<sup>-1</sup>; B = 15 K min<sup>-1</sup>; C = 20 K min<sup>-1</sup>).

A higher heating rate results in poor coke removal. At 1073 K, the coke removal capability becomes similar to that at a higher heating rate. The reason for this observation may be explained in that, at a higher heating rate the ‘hard’ coke is undergoing transformation to graphitic form. At a higher heating rate the transformation is faster which may result in different stages of transformation leading to more stable graphitic coke. This in turn results in a slower release of the coke species which is similar to that of higher temperature.

For the next set of observations, a serial treatment of N<sub>2</sub> and 5.0 v/v % O<sub>2</sub> in N<sub>2</sub> were analyzed. Here the result from 1<sup>st</sup> and 2<sup>nd</sup> stages were combined (sum of ‘soft’ and ‘hard’ coke) termed as total coke is presented in Figure 4-26. The same figure analyzes the effect of total coke removal with different heating rates and temperatures. This was done to interpret the effect of serial treatment on total coke removal when introduced to the regeneration process.

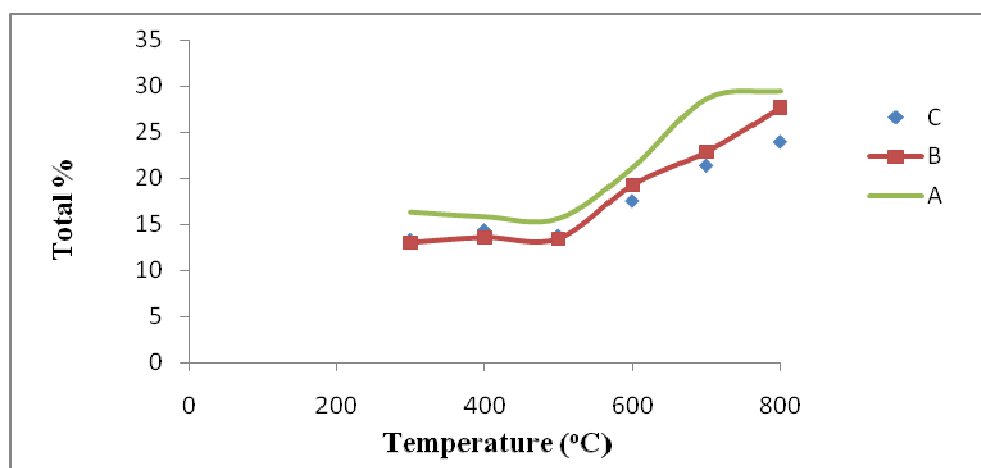


Figure 4-26: The sum of % weight loss of total coke from 1st and 2nd stage at different heating rates and temperatures (A = 10 K min<sup>-1</sup>; B = 15 K min<sup>-1</sup>; C = 20 K min<sup>-1</sup>).

The coke is usually made up of unsaturated hydrocarbons which may contain olefins and aromatics. The desorption rate of these compounds are directly related to the heating rate, temperature and dwell time. Besides these, the catalyst properties (metal crystallite size) and amount of the catalyst in the reactor all can play an important role in the amount of the material loss [34]. The contact time necessary to remove coke depends on the regeneration temperature. A short regeneration cycle (ca.

1 h at ca. 673 K) allows a partial recovery of the catalytic activity only [33, 82]. Essentially here, only coke associated with the metallic phase is removed.

The effect of coke ('soft' and 'hard') removal with respect to dwell time at different maximum temperature was analyzed. During these experiments the heating rate was maintained at  $10 \text{ K min}^{-1}$ . For this study, 3 different dwell times of 120, 60 and 30 minutes were evaluated against temperature range from 573 to 1073 K. Measurements were taken for every 100 K within the range. The result obtained from these experiments is presented in Figure 4-27.

Figures 4-27 are segregated into 3 mini graphs labeled as A, B & C representing the dwell time of 120, 60 and 30 minutes respectively at the maximum temperature analyzed. From 4.27 it can be seen that the 'soft' coke in general increases with increase in regeneration temperature and dwell time. The 'hard' coke on the other hand shows a reverse trend to that of the 'soft' coke. This indicate that as we increase the regeneration temperature and contact time more 'soft' and part of the 'hard' coke are removed or transformation to graphitic form occurred.

In the second phase of the TPO experiment; the previous (TGA) model was used in order to study the kinetics of coke deposition on the commercial Pt/Al<sub>2</sub>O<sub>3</sub> catalyst. Although TGA is considered more accurate in calculating the activation energy for different types of coke (hard, soft and laid) species, TPO was used to complement TGA results. TPO analysis can provide a good picture on the distribution of the reactive (soft) and un-reactive (hard) coke over catalyst functions, as suggested by Carlos et al. [71]. For this purpose the activation energy was calculated again using results from TPO analysis. The activation energy can gives an insight as to whether a reaction is controlled by mass diffusion, chemical, or catalyst activity limited. For a ball park figure, activation energy of 100 kJ/mol is catalytic activity limited or there is a presence of strongly bounded species as explained by Larsson et al. [15].

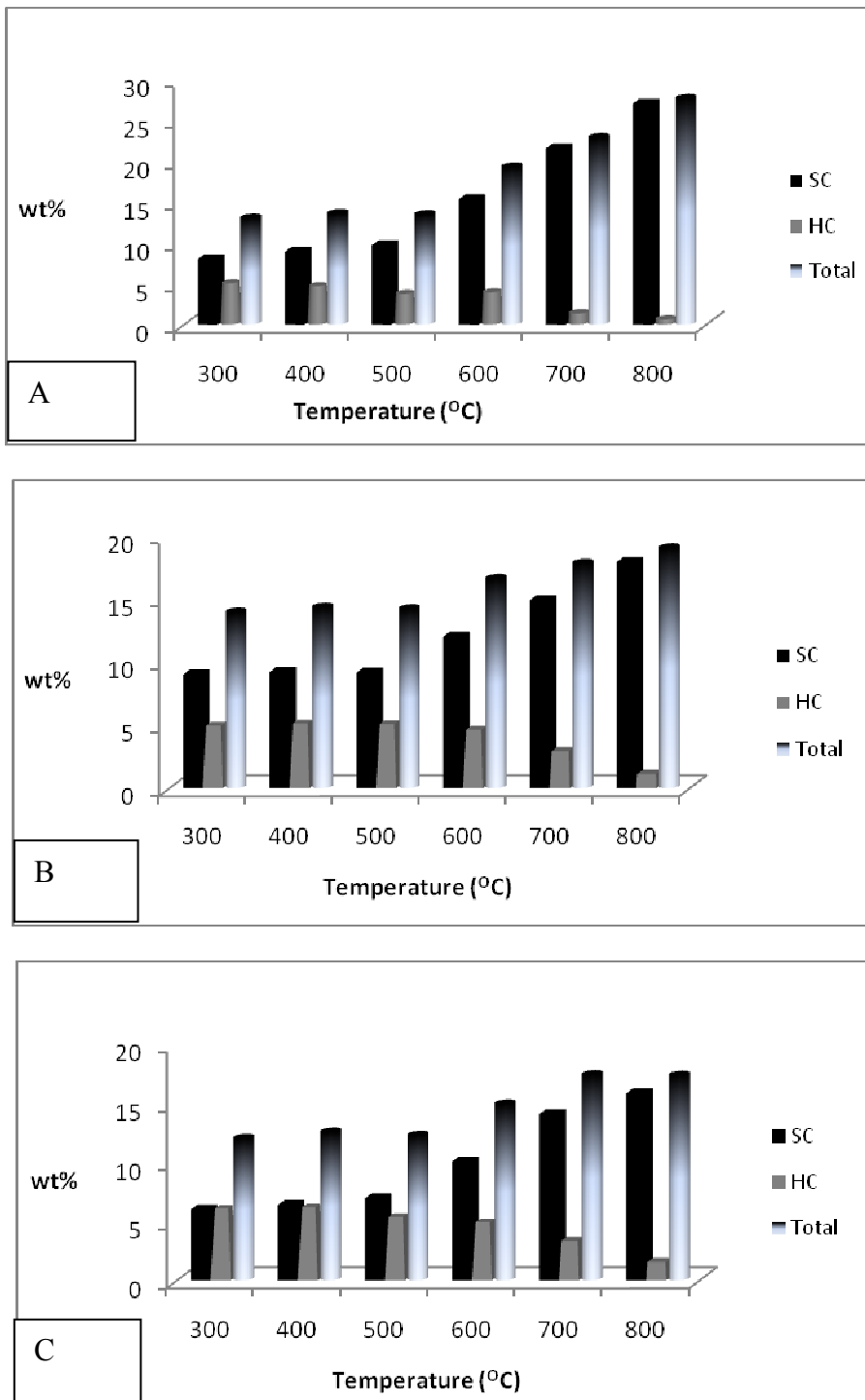


Figure 4-27: Effect of dwell time and varied regeneration temperature on industrial spent Pt/Al<sub>2</sub>O<sub>3</sub> spent catalyst [Dwell time for A= 120 min, B= 60 min & C= 30 min].  
(Sc=soft coke, Hc= hard coke and Total=hard coke + soft coke).

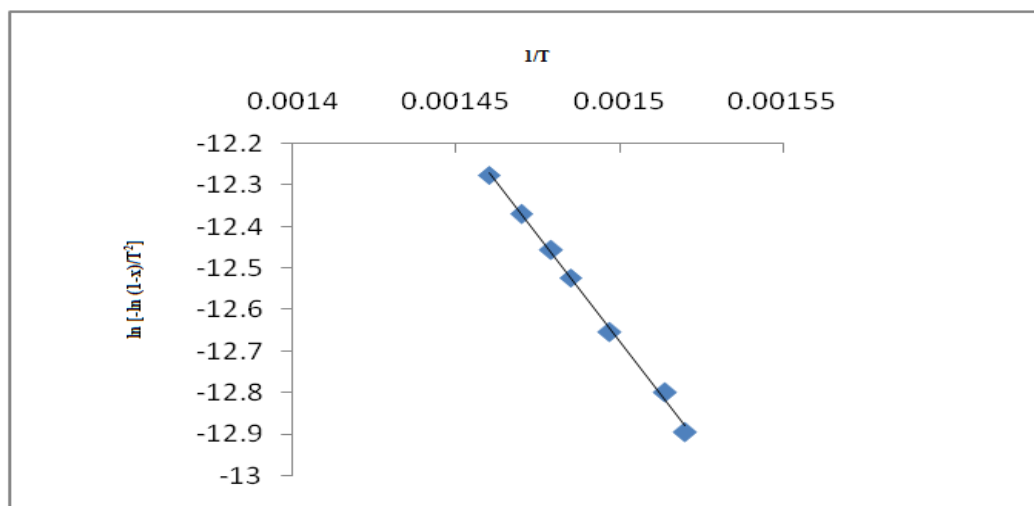


Figure 4-28: A plotting of  $1/T$  versus  $\ln [-\ln (1-x)/T^2]$  for the coked  $\text{Pt}/\text{Al}_2\text{O}_3$  catalyst.

From our results obtained from the TPO analysis, it was found that the activation energy  $E_r$  is 82.7 kJ/mol with a frequency factor of  $1.6 \times 10^6$ ; for the spent industrial catalyst. This result is similar to that obtained from TGA (86.3 kJ/mol) which is attributed to the 'hard' coke. This finding further supports that the major portion of the coke present in the spent catalyst is 'hard' coke and is most probably bonded to the support acid sites. The  $E_r$  obtained for the present study strongly suggests that the major coke deposition is chemically controlled limited and can be removed by proper regeneration procedures.

#### 4.7.4 Temperature Programmed Reduction (TPR)

To further understand the reducibility nature of the metal- support bonding and to complement the TGA and TPO analysis, a TPR analysis was carried out. Prior to embarking into the bonding of the coke material to the active site, it is important to determine the strength and nature of the bond between the active metal and support.

For this TPR studies, on a fresh industrial catalyst  $\text{Pt}/\text{Al}_2\text{O}_3$  was chosen to understand the bond strength and nature between the Pt metal and the  $\text{Al}_2\text{O}_3$  support. TPR analysis was carried out under a reducing gas stream of 5.1v/v %  $\text{H}_2$  in  $\text{N}_2$  gas with a flow rate of  $20 \text{ ml min}^{-1}$ . The catalyst sample was heated up to 1073 K with a temperature ramp rate of  $10 \text{ K min}^{-1}$ . Trace consumption of  $\text{H}_2$  in a monometallic  $\text{Pt}/\text{Al}_2\text{O}_3$ , was detected. For the purpose 2 different pretreated samples were analysed.

One sample was calcined and the other uncalcined catalysts. The calcination was done under air by heating the uncalcined catalyst from ambient to 673 K at a ramp rate of 10 K min<sup>-1</sup> in TGA INS. At 673 K a dwell time of 3 hours was observed. The results obtained from this analysis are shown in Figure 4-29. For further information on TPR analysis technique please refer to chapter 3 section 3.6 of this thesis.

From Figure 4-29, two peaks are observed. Peak I represent the consumption of H<sub>2</sub> for the fresh regenerated catalyst sample before calcination and Peak II after calcination. In the same figure, it was noticed that there is a pronounced reduction of Pt oxychlorinated (PtOCl<sub>2</sub>) species which weakly interact with alumina occurring at 523 K (250 °C) after for both cases (calcined and uncalcined catalysts). This reduction pattern has been frequently observed by several authors; [5, 18]. It can be seen that the calcined Pt/Al<sub>2</sub>O<sub>3</sub> catalyst adsorbed more H<sub>2</sub> than the uncalcined one.

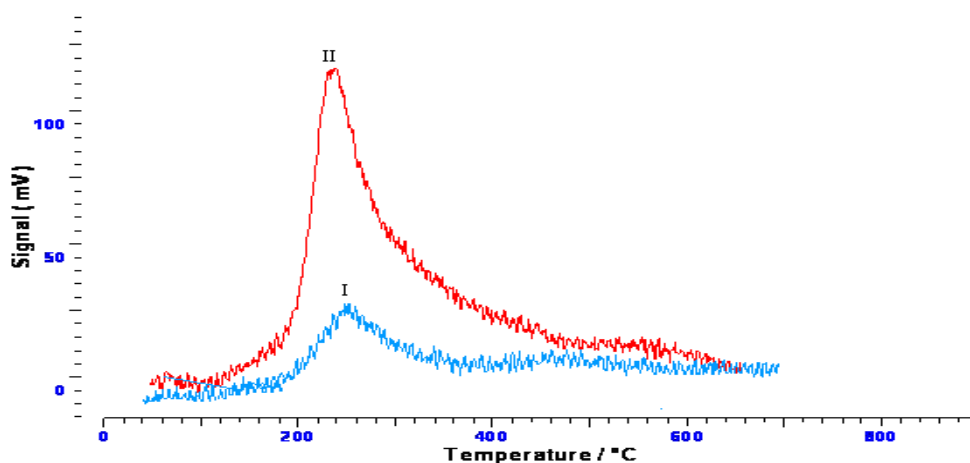


Figure 4-29: TPR traces for the consumption of H<sub>2</sub> in a monometallic Pt/Al<sub>2</sub>O<sub>3</sub> catalyst, Peak I and Peak II for catalysts before and after calcinations, respectively.

This indicates that the calcined catalyst is more difficult to reduce than the uncalcined catalyst. The reason for this is the presence of a Pt oxide species in the calcined catalyst are more strongly bounded to active sites than the uncalcined sample. This result is well documented by Pieck et al. [101] in their study of TPR, which was carried out for Pt/Al<sub>2</sub>O<sub>3</sub> and Re/Al<sub>2</sub>O<sub>3</sub> reforming catalysts. The authors mentioned that, the samples which were previously oxidized at 673 K (400 °C) showed lower oxidation temperatures and lower hydrogen uptake signals (increasing the oxidation temperature caused a rise in H<sub>2</sub> uptake).

On the other hand, higher oxidation temperatures would favor a greater segregation of the metal oxides. In the present study, the lower hydrogen uptake was observed (Figure 4-29) for the uncalcined catalyst sample, this is because of the oxidation state of the metal particles not existence in this case and the metal may be completely surrounded by large chloride molecules limiting access and shadowing the active metal site. Not like the calcined sample which shows the higher hydrogen consumption because of the presence of oxygen atoms as compared to the uncalcined one.

#### 4.7.5 *Temperature Programmed desorption (TPD)*

Pyridine is adsorbed on acid sites due to its basic character. Desorption of pyridine at low temperatures is related to the presence of weak acid sites while the desorption at high temperatures is because of the presence of strong acid sites. The total area under the TPD trace is representative of the total acidity of the catalyst [76]. In Figure 4-30, it can be seen that the fresh catalyst has a higher amount of strong acid 873 to 923 K (600 to 650 °C) than the weak acid sites 633 to 673 K (360 to 400 °C). These strong acids are most likely to be Lewis acids, while the weaker ones are the Bronstead acids.

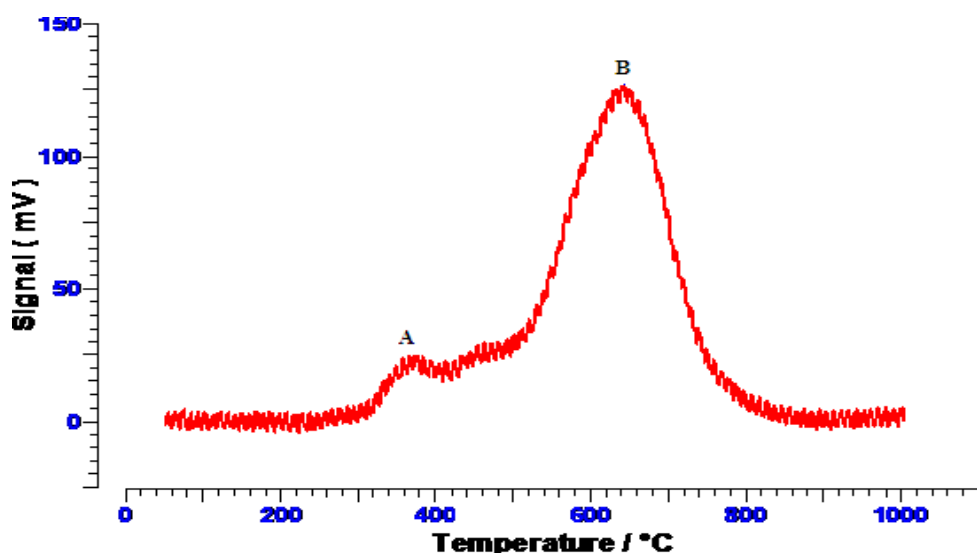
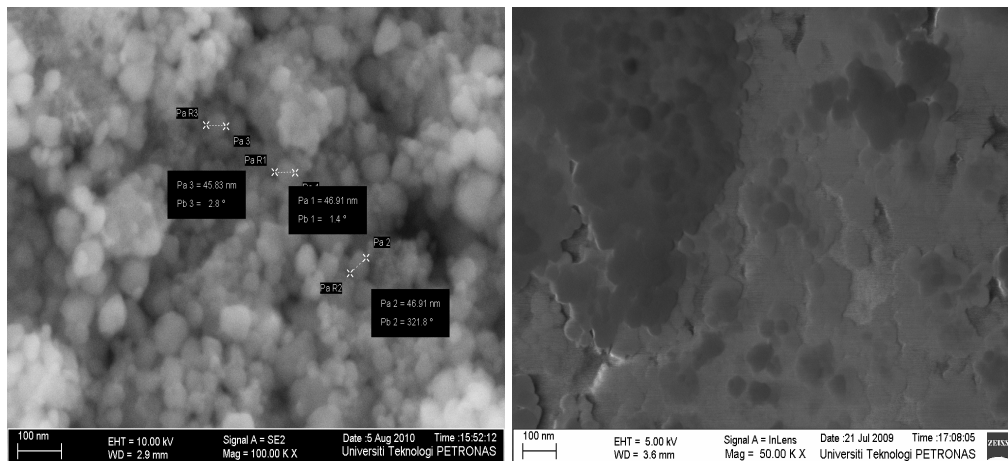


Figure 4-30: TPD trace for the fresh Pt/Al<sub>2</sub>O<sub>3</sub> catalyst.

#### 4.7.6 Field Emission Scanning Electron Microscopy (FESEM)

Having done the mechanical properties of the catalyst, the next step is to check the morphology of the catalyst surface. This was done to check for any transformation of the active catalyst particles on the catalyst support. For this purpose FESEM was used to characterize the catalyst particles distribution at high magnification for the fresh and spent industrial Pt/Al<sub>2</sub>O<sub>3</sub> catalysts. Figures 4-31 represent 4 images taken by the FESEM instrument using secondary electron and in-lens detectors for fresh and spent industrial catalyst, respectively.

##### A/ Fresh catalyst morphology



##### B/Spent catalyst morphology

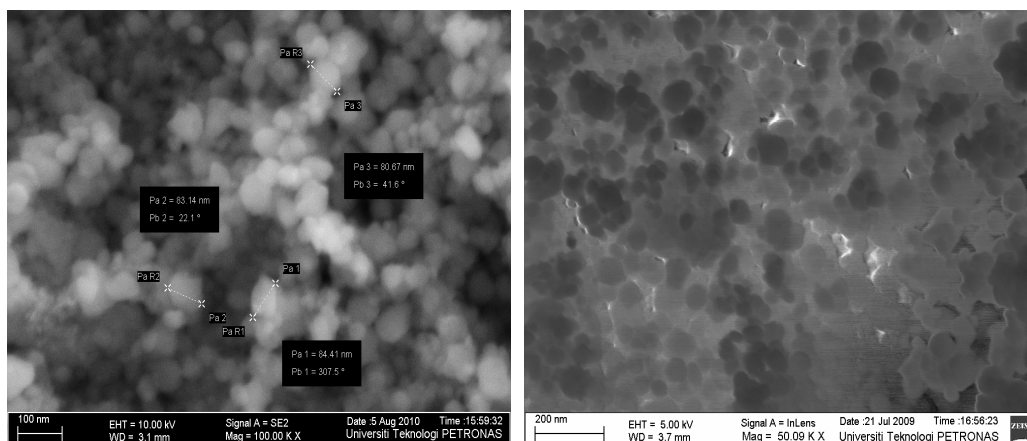


Figure 4-31: FESEM for fresh and spent catalyst by the in-lens (right image) and SE2 (left image).

The top pair represent the view of the fresh catalyst surface (left image) was used to determine the particles size of both fresh and spent catalysis using a secondary electron detector, whereas the vertical view (right images) of the catalysts as captured by an in-lens detector to determine the catalyst topography. The in-lens detector was used for applications which demand the highest magnification.

The particle sizes were quite different for both the fresh and spent catalysts. The spent catalyst has a bigger crystal size than the fresh one. The average particle size for a fresh catalyst is 46.3 nm and for that of a spent catalyst is 82.74 nm. The bigger particle size for the spent catalyst might be due to sintering induced by higher temperature oxidation during regeneration [49].

Catalyst deactivation may be the principal cause of the size difference and shift of surface morphology. During the reforming reaction the coke accumulates on the catalyst surface and the metal particles, either partial or total encapsulation. Coke or carbon, are easily deposited on the catalyst surface filling up the dug-out structure due to the presence of reactive sites created by the 'absence of nearest neighbor'. As a result, strong carbon filaments may dig itself into its pores and fracture the support material accordingly. This may result in agglomeration of the catalyst particles due to structure collapse [34].

## Chapter 5

### Conclusion and Recommendation

#### 5.1 Conclusion

The overall *n*-hexane reforming conversion was improved by increasing the temperature and contact time while decreasing the H<sub>2</sub> partial pressure. Higher reaction temperature is not recommended because it can increase catalytic deactivation by increasing the concentration of coke precursors and sintering process.

A high temperature (723 K) and the lowest H<sub>2</sub> pressure (300 KPa) it desorbs the desired reformates (isomers and aromatics) but when the H<sub>2</sub> partial pressure is increased to 700 KPa, the selectivity switch to the non-desired cracked reformato products affecting the catalyst activity towards desorption of unsaturated hydrocarbons (coke precursors).

Contact time of 1.8-2.4 minutes was found to be desirable towards production of higher yields of isomer and aromatics, but 2.4 minutes and above favors the cracked and coke precursor products (undesirable products). For this reason in Taguchi orthogonal array design, 1.78 has been taken as the optimum contact time. Furthermore, the carbon tetrachloride study confirmed this assumption.

Using Design of experiment 6.0.6 software (TOAD), the optimum operating conditions that enhance the *n*-hexane conversion to desired products was operating the process at reaction temperature 723 K at contact time 7.1 min with a H<sub>2</sub> partial pressure 300 KPa. From the TOAD analysis, H<sub>2</sub> partial pressure is most critical parameter when selectivity towards aromatics is desired. The optimum level for it is to operate the reaction at 300 KPa. For the desired isomers reformato contact time is most critical and to obtain maximum yield operation at 1.78 minutes is recommended.

The undesirable products of cracked and coke precursor the main process variable is contact time. To produce the least selectivity, 1.0 min contact time is recommended for both. Based on the above information the optimum condition for *n*-hexane reforming tailored to desired products is to operate at reaction temperature of 723 K, 1.78 minutes contact time and 300 KPa H<sub>2</sub> partial pressure.

Introducing carbon tetra chloride (CCl<sub>4</sub>) to *n*-hexane feed causes a rise in the catalyst acidity and this increase the hydrocarbon rearrangement reaction (isomerization). These types of reactions demand higher acidity. Unfortunately, the higher acidity favors the formation of cracked products too. The cracked product overwhelms the isomers at the present reforming condition as such it increases steadily with increase in CCl<sub>4</sub> addition while the isomers remain unaffected. Therefore the main reason for CCl<sub>4</sub> addition is to improve catalytic stability, or in other words it can be used to repair or replace damaged acid sites.

Suppressions of the cracking products have been well investigated by introducing DMDS to the reactant. DMDS decreases monofunctional metal-catalyzed reactions but concomitantly increases the activity for acid-controlled isomerization reactions (skeletal rearrangement reactions), which is the other important product. It has higher octane number than paraffins, but the addition of sulfur increases the deactivation rate by desorption of unsaturated hydrocarbon, such as coke precursors.

TGA found that, the hard coke de-coking rate was higher than the soft and laid coke. This is because increasing the regeneration temperature causes a rise in the reaction rate. Further increase in temperature converts the hard coke to laid coke where some of the 'hard' coke at higher temperatures may have undergone phase transformation to a more graphitic nature. This latter, tends to penetrate deeper and stick more strongly on the catalyst surface and is very difficult to react and remove.

TPO analysis showed that, at the higher heating rate (20 K min<sup>-1</sup>) is not recommended for regeneration process, while a lower heating rate (10 K min<sup>-1</sup>) is better for de-coking process.

The activation energy obtained for the present study, by using TGA and TPO techniques, strongly suggests that coke deposition can be removed by proper regeneration procedures.

FESEM results show that the commercial spent catalyst has a bigger particle size compared to that of the fresh counterpart. This is most probably caused by sintering of catalyst.

## 5.2 Work contributions

One of the most noteworthy contributions of this thesis is using various reforming conditions such as hydrogen partial pressure, temperature, contact time, feed chlorination and sulfidation. These give a clear picture to understand the effects of these parameters on product distributions as well as the catalyst activity.

Applying simple regeneration procedures for the spent catalyst by using TPO and TGA techniques, kinetics of the de-coking process, gives an insight view of regeneration behaviour and coke nature. Regeneration of catalysts using an inert gas such as N<sub>2</sub>, only can restores more than 50 % of the catalyst activity. This has been well proven here by the TPO technique.

## 5.3 Recommendations and Future work

- The present work concentrates only on reaction temperature, H<sub>2</sub> partial pressure and contact time for *n*-hexane reforming. It will be interesting to know how the higher homolog of paraffins will behave under similar conditions.
- The effects of reforming conditions, chlorination and sulfidation have been reported and investigated. For the future work other parameters such as, optimizing the catalyst size, changing the metal loading, catalyst to fuel ratio, using a multi metallic catalyst (modification of the catalyst with the other elements), and using mixtures of hydrocarbon feed should be investigated.
- Optimization of the level of catalyst acidity by oxy-chlorination during regeneration process has been widely practiced by refiners. Leaching of this chloride from catalyst should be well investigated for its prevention and retention especially with changing process variables. In this work, carbon tetra

chloride was used as a chloriding agent. Since it is a very poisonous material, and with concern for the environmental situation another chloriding agent should be explored.

- The de-coking process is directly related to heating rate; temperature and dwell time has been investigated and discussed. During regeneration attrition is one of the main factors which increase catalytic loss. Addition of promoter to increase catalyst integrity towards attrition at high temperature should be well investigated.
- Simulation and modeling of *n*-hexane reforming reaction and regeneration of spent catalyst is another area that can be explored.

## References

- [1] J. George, A. M. Antos, and J. Aitani, "Catalytic Naphtha Reforming" Second edition. New York .Basel: Marcel Dekker, Inc, 2004.
- [2] V. A. Mazzieri, J.M. Grau, C.R. Vera, Juan C. Y. Jose, M. Parera, C.L. Pieck "Role of Sn in Pt–Re–Sn/Al<sub>2</sub>O<sub>3</sub>–Cl Catalysts for Naphtha Reforming," *Catal.Tod*, vol. 107–108, pp. 643–650, 2005.
- [3] K. Liu, "Reaction and Coking Kinetics of N-heptane Catalytic Reforming" The Development of A new Vibrational Microbalance and Application for in Situ Determination of Catalytic Reforming Reaction and Coking Kinetics", " *in faculty of engineering*. Doctor philosophy New York: City University, 1995.
- [4] U. M Taskar, "Modeling and Optimization of A Catalytic Naphtha Reformer," *in Chemical Engineering*. Doctor of Philosophy: Texas Tech, 1996.
- [5] V.A. Mazzieri, J.M. Grau, J.C. Yori, C.R. Vera, C.L. Pieck, "Influence of Additives on the Pt Metal Activity of Naphtha Reforming Catalysts," *Appl. Catal A: General*, vol. 354, pp. 161–168, 2009.
- [6] J.M. Grau and J.M. Parera, "Naphtha Reforming Capacity of Catalysts with Different Metallic Functions," *Ind. Eng. Chem. Res.*, vol. 28, pp. 1596-1600, 1989.
- [7] J.M. Hill, "Effect of Tin on the Reactivity of Platinum Group Metals with Light Hydrocarbons," *in chemical engineering*. Doctor philosophy USA: Wisconsin-Madison, 1999.
- [8] J. George, A.M. Antos. J. Aitani, and M. Parera, "Catalytic Naphtha Reforming Science and Technology ", First edition ed, Marcel Dekker, New York Basel, 1995.
- [9] A. Borgna, T.F. Garetto, C.R. Apestegua, "Simultaneous deactivation by coke and sulfur of bimetallic Pt–Re(Ge, Sn)/Al<sub>2</sub>O<sub>3</sub> catalysts for n-hexane reforming," *Appl. Catal A: General*, vol. 197, pp. 11–21, 2000

- [10] R. G. Tailleur and Y. Davila, "Optimal Hydrogen Production Through Revamping a Naphtha-Reforming Unit: Catalyst Deactivation," *Energy & Fuels* vol. 22, pp. 2892–2901, 2008.
- [11] B. Wang, and G. Manos, "A novel Thermogravimetric Method for Coke Precursor Characterization," *J. Catal* vol. 250, pp. 121–127, 2007.
- [12] V.A. Mazzieri, C. L. Pieck, C. R. Vera, J. C. Yori, and J. M. Grau, "Analysis of Coke Deposition and Study of the Variables of Regeneration and Rejuvenation of Naphtha Reforming Trimetallic Catalysts," *Catal .Tod.*, Vol. 133–135, pp. 870–878, 2008.
- [13] Z. Tao, Z. Jingling and L. Liwu, "Relation between Surface Structure and Carbon Deposition on Pt/Al<sub>2</sub>O<sub>3</sub> and Pt-Sn/Al<sub>2</sub>O<sub>3</sub> Catalysts," *Elsevier Sc .Pub B.V.*,1991.
- [14] F. Yining, X. Zhusheng, Z. Jingling and L. Liwu, "studies on the degradation of bimetallic Pt-Sn/Al<sub>2</sub>O<sub>3</sub> catalysts in regeneration cycles," *Elsevier Sc .Pub B.V.*,1991.
- [15] S.C. Fung, C. A. Querini, and C.J. Mcoy "Coke and Product Profiles along Catalyst Bed in Reforming Reactions," *Elsevier Sc .Pub B.V.*, 1991.
- [16] L. M. Hulten, E.A. Blekkan, and B. Andersen, "The Effect of Reaction Conditions and Time on Stream on the Coke Formed during Propane Dehydrogenation," *J. Catal*, Vol. 164, pp. 44–53, 1996.
- [17] C.A. Querini and S.C. Fung, "Coke Characterization by Temperature Programmed Techniques," *Catal.Tod*, vol. 37, pp. 277–283, 1997.
- [18] J.N. Beltramini, T.J. Wessel, and R. Datta, "Deactivation of the Metal and Acid Functions of Pt/Al<sub>2</sub>O<sub>3</sub>-Cl Reforming Catalysts by Coke Formation," *Elsevier Sc .Pub B.V.*, 1991.
- [19] V.A. Mazzieri, C.L. Pieck, C.R. Vera, J.C. Yoria and J.M. Grau, "Effect of Ge Content on the Metal and Acid Properties of Pt-Re-Ge/Al<sub>2</sub>O<sub>3</sub>-Cl Catalysts for Naphtha Reforming," 2008.
- [20] P. A. Trimont, G. B. Marin, and G. F. Froment, "Reforming of C7 Hydrocarbons on a Sulfided Commercial Pt/Al<sub>2</sub>O<sub>3</sub> Catalyst," *Ind. Eng. Chem. Res.*, Vol. 27, pp. 51-57, 1988.

- [21] A. Iob, M. A. Ali, B. S. Tawabini, J. A. Anabtawi, S. A. Ali and A. Al-Farayedhi, "Prediction of Reformate Research Octane Number by FTIR Spectroscopy," *Fuel* vol. 74 1995.
- [22] A. V. Jain, N.C. Pradhan, A. K. Dalai, and N. Narendra, "Studies on Chlorided Pt/Al<sub>2</sub>O<sub>3</sub> Catalysts: Preparation, Characterization and N-butane Isomerization Activity," *Catal. Lett.*, vol. 86, pp. 221-227, 2003.
- [23] Y.T. Jin, and L. Liao, "Modeling and Optimization of A Semi-regenerative Catalytic Naphtha Reformer," *IEEE Conference on Control Applications*, pp. 28-31, 2005.
- [24] L. Daia, Y. Hashimoto, H. Tominaga and T. Tatsumi, "Reforming of Hexane with Pt/zeolite Catalysts," *Catal. Lett.*, vol. 45, pp. 107-112, 1997.
- [25] D.O. Agbajelola and F. Aberuagba, "N-Hexane Aromatization Over Pt/Al<sub>2</sub>O<sub>3</sub> under Helium and Hydrogen Diluents," *AU J.T. 10*, vol. 4, pp. 264-270 2007.
- [26] N. Itoh, S. Hara, K. Kakehida, Y. Kaneko, and A. Igarashi, "Effects of Hydrogen Removal on the Catalytic Reforming of *n*-Hexane in A Palladium Membrane Reactor," *Ind. Eng. Chem. Res.*, vol. 42, pp. 6576-6581, 2003.
- [27] T. N. Angelidis, D. Rosopoulou, and V. Tzitzios, "Selective Rhenium Recovery from Spent Reforming Catalysts," *Ind. Eng. Chem. Res.*, vol. 38, pp. 1830-1836, 1999.
- [28] L.S. Carvalho, C.L. Pieck, M.C. Rangel, N.S. Figoli, C.R. Vera, and J.M. Parera, "Trimetallic Naphtha Reforming Catalysts II. Properties of the Acid Function and Influence of the Order of Addition of the Metallic Precursors on Pt-Re-Sn/-Al<sub>2</sub>O<sub>3</sub>-Cl," *Appl. Catal A: General* vol. 269, pp. 105-116, 2004.
- [29] S. Chen, and G. Manos, "Study of Coke and Coke Precursors during Catalytic Cracking of N-hexane and 1-hexene Over Ultrastable Y zeolite," *Catal. Lett.*, vol. 96, pp. 3-4, 2004.
- [30] C. S. Hsu, "Practical Advances in Petroleum Processing." Vol1, P.R. Robinson, Ed. USA: *Springer Science Business Media, Inc.*, 2006.
- [31] S. F. Nora, M. R. Sad, J. N. Bekramlnl, E. L. Jablonskl, and J. M. Parera, "Influence of the Chlorine Content on the Behavior of Catalysts for n-Heptane Reforming," *Ind. Eng. Chem.*, vol. Vol. 19, pp. 545-551, 1980.
- [32] P. G. Menon, and Z. Paai, "Some Aspects of the Mechanisms of Catalytic Reforming Reactions," *Ind. Eng. Chem. Res.*, vol. 36, pp. 3282-3291, 1997.

- [33] K. Liu, S. C. Fung, T. C. Ho, and D. S. Rumschitzki, "Hydro gasification of Coke in Heptane Reforming over Pt-Re/Al<sub>2</sub>O<sub>3</sub>," *Ind. Eng. Chem. Res.*, vol. 42, pp. 1543-1550, 2003.
- [34] C.L. Pieck, P. Marecot, and J. Brbier, "Effect of Pt-Re Interaction on Sulfur Adsorption and Coke Deposition" *Appl. Catal A: General*, vol. 145, pp. 323–334, 1996.
- [35] C. H. Bartholomew, "Mechanisms of Catalyst Deactivation," *Appl. Catal A: General*, vol. 212, pp. 17–60, 2001
- [36] J.A. Moulijn, A.E. van Diepen, and F. Kapteijn, "Catalyst deactivation: is it predictable? What to do?" *Appl. Catal A: General*, vol. 212, pp. 3–16, 2001.
- [37] A. Aristidis, Brillis, and G. Manos, "Coke Formation during Catalytic Cracking of C8 Aliphatic Hydrocarbons over Ultrastable Y Zeolite," *Ind. Eng. Chem. Res.*, vol. 42, pp. 2292-2298, 2003.
- [38] P. Magnoux , A. Rabearitsara , and H. S. Cerqueira, "Influence of Reaction Temperature and Crystallite Size on HBEA Zeolite Deactivation by Coke," *Appl. Catal A: General*, vol. 304, pp. 142–151, 2006
- [39] T.F. Garetto, C.I. Vignatti, A. Borgna, and A. Monzon, "Deactivation and Regeneration of Pt/Al<sub>2</sub>O<sub>3</sub> Catalysts during the Hydrodechlorination of Carbon Tetrachloride," *Appl. Catal B: Environmental* vol. 87 pp. 211–219, 2009.
- [40] L.S. Carvalho, P.Reyes, G. Pecchi, N. Figoli, C. L. Pieck, and M. C. Rangel, "Effect of the Solvent used during Preparation on the Properties of Pt/Al<sub>2</sub>O<sub>3</sub> and Pt-Sn/Al<sub>2</sub>O<sub>3</sub> Catalysts," *Ind. Eng. Chem. Res.*, vol. 40, pp. 5557-5563, 2001.
- [41] H.P. Rebo, E.A. Blekkan, L. Bednarova and A. Holmen, "Deactivation of Pt-Sn Catalyst in Propane Dehydrogenation," *Elsevier Sc .Pub B.V* vol., 126, pp. 333-340, 1999.
- [42] C. Bartholomew, "Catalyst Deactivation and Regeneration." *ChemInform*, vol. 38, 2007.
- [43] T. Gjervan, R. Prestvik, B. Tøtdal, C.E. Lyman, and A. Holmen, "The Influence of the Chlorine Content on the Bimetallic Particle Formation in Pt–Re/Al<sub>2</sub>O<sub>3</sub> Studied by STEM/EDX, TPR, H<sub>2</sub> Chemisorption and Model Reaction Studies," *Catal. Tod* vol., 65, pp. 163–169, 2001.

- [44] M. Goven, "Preparation, Characterization and Reaction of Bimetallic Catalyst for Reforming," in *chemical engineering perak*: Universiti Technology PETRONAS, 2004.
- [45] I. Nam, J. W. Eldridge, and J. R. Kittrellt, "Coke Tolerance of Catalytic Reforming Catalysts," *Amer.Chem.Soc*, vol. 24, pp. 544-549, 1985.
- [46] J.A. Anderson, F.K Chong, and C.H. Rochester, "IR Study of CO Adsorption on Pt, Re and Pt–Re/Al<sub>2</sub>O<sub>3</sub> Catalysts before and after Coking," *J. Mol. Catal A: Chemical*, vol. 140, pp. 65–80, 1999.
- [47] Y.V. Guryev, I.I. Ivanova, V.V. Lunin, W. Grunert, and M.W Berg, "Characterization of Metal Segregation in Pt–Re/Al<sub>2</sub>O<sub>3</sub> Reforming Catalysts," *Appl. Catal A: General*, vol. 329, pp. 16–21, 2007.
- [48] T. Bin Lin, C.A Jan, and J.R Chanff, "Aromatics Reduction over Supported Platinum Catalysts. Improvement in Sulfur Resistance by Addition of Palladium to Supported Platinum Catalysts," *Znd. Eng. Chem. Res.*, vol. 34, pp. 4284-4289, 1995.
- [49] G. C. Bond, "The Role of Carbon Deposits in Metal-Catalysed Reactions of Hydrocarbons," *Appl. Catal A: General*, vol. 149, pp. 3-25, 1997.
- [50] G. J. Arteaga, J. A. Anderson, S. M. Becker, and C. H. Rochester, "Influence of Oxychlorination Treatment on the Surface and Bulk Properties of a Pt–Sn/Al<sub>2</sub>O<sub>3</sub> catalyst," *J. Mol. Catal A: Chemical* vol. 145, pp. 183–201, 1999.
- [51] K. Matusek, C. Kappenstein, M. Guerin and Z. Paal, "Reactions of *n*-hexane on Pt–Sn/Al<sub>2</sub>O<sub>3</sub> and Removal of Retained Hydrocarbons by Hydrogenation," *Catal. Lett*, vol. 64 pp. 33–36, 2000.
- [52] Z. Tao, Z. Jingling and L. Liwu, "Relation between Surface Structure and Carbon Deposition on Pt/Al<sub>2</sub>O<sub>3</sub> And Pt-Sn/Al<sub>2</sub>O<sub>3</sub> Catalysts," *Elsevier Sc. Pub B.V.*, 1991.
- [53] S. Ordóñez, F.V. Díez and H. Sastre, "Hydrodechlorination of Tetrachloroethylene over Vanadium-Modified Pt/Al<sub>2</sub>O<sub>3</sub> Catalysts," *Catal. Lett* vol. 72, pp. 3-4, 2001.
- [54] F. Epron , C. Carnevillier, P. Marecot, "Catalytic Properties in *n*-heptane Reforming of Pt–Sn and Pt–Ir–Sn/Al<sub>2</sub>O<sub>3</sub> Catalysts Prepared by Surface Redox Reaction," *Appl. Catal A: General*, vol. 295 pp. 157–169, 2005.

- [55] G.D. Zakumbaeva, T.V. Van, A.I. Lyashenko, and R.I. Egizbaeva, "Catalytic Reforming *n*-octane on Pt-Re/Al<sub>2</sub>O<sub>3</sub> Catalysts Promoted by Different Additives," *Catal.Tod* vol. 65 pp. 191–194, 2001.
- [56] G. M. Bickle, J. N. Beltramini, and D. Do, "Role of Sulfur in Catalytic Reforming of Hydrocarbons on Platinum-Rhenium/Alumina," *Ind. Eng. Chem. Res.*, vol. 29, pp. 1801-1807, 1990.
- [57] C.L. Pieck, P. Marecot, C.A. Querini, J.M. Parera, and J. Barbier, "Influence of Pt-Re Interaction on Activity and Selectivity of Reforming Catalysts," *Appl. Catal A: General*, vol. 133, pp. 281-292, 1995.
- [58] N. Viswanadham, R. Kamble, A. Sharma, M. Kumar, and A.K. Saxena, "Effect of Re on Product Yields and Deactivation Patterns of Naphtha Reforming Catalyst," *J. Mol. Catal A: Chemical* vol. 282, pp. 74–79, 2008.
- [59] C.A. Querini and S.C. Fung, "Coke and Product Profiles Formed along the Catalyst Bed during-Heptane Reforming II. Influence of S on Pt/Al<sub>2</sub>O<sub>3</sub> and Pt-Re/Al<sub>2</sub>O<sub>3</sub>," 1996.
- [60] M.R. Jovanovic, and P.S. Putanov, "Nature and Distribution of Coke Formed on Mono-Metallic Platinum and Bimetallic Platinum-Rhenium Catalysts," *Appl. Catal A: General*, vol. 159, pp. 1-7, 1997.
- [61] A. Dun, D. Quan, X. T. Cun, X.H. Bing, and L.S. Li, "The Mechanism of Sulfur-Poisoning of Pd (Pt)/Al<sub>2</sub>O<sub>3</sub> Catalysts and Their Regeneration," *Elsevier Sc. Pub B.V., Amsterdam.* 1991.
- [62] R. P. Singh, K. Alam, D. S. Redwan, and N. M. Abbas, "Determination of Chloride in Platinum-Rhenium Alumina-Based Reforming Catalyst by Ion Chromatography," *Amer.Chem.Soc.*, vol. 61, pp. 1924-1927, 1989
- [63] C.L. Pieck, P. Marecot, J.M. Parera, and J. Barbier, "Influence of Chlorine Content on Pt-Re Interaction and Coke Deposition," *Appl. Catal A: General*, vol. 126, pp. 153-163, 1995
- [64] A. Borgna, T.F. Garetto, C.R. Apesteguia, F.L. Normand, and Moraweck, "Sintering of Chlorinated Pt/Al<sub>2</sub>O<sub>3</sub> Catalysts: An in Situ Study by X-Ray Absorption Spectroscopy," *J. Catalysis*, vol. 186, pp. 433-441 1999.
- [65] S. C. Fung, "Redispersion of Iridium-Containing Catalysts: Chemistry and Kinetics," *Ind. Eng. Chem. Res.*, vol. 42, pp. 1551-1556, 2003.

- [66] S. A Ippolito, C. R. Vera, F. Epron, C. Especel, P. Marecot, C. L. Pieck, "Naphtha Reforming Pt-Re-Ge/Al<sub>2</sub>O<sub>3</sub> Catalysts Prepared by Catalytic Reduction Influence of the pH of the Ge addition step," *Catal.Tod*, vol. 133–135, pp. 13–19, 2008.
- [67] B. Wang and G. Manos, "Role of Strong Zeolitic Acid Sites on Hydrocarbon Reactions," *Ind. Eng. Chem. Res*, vol. 47, pp. 2948-2955, 2008.
- [68] C. L. Pieck, E. L. Jablonski, J. M. Parera, R. Frety, and F. Lefebvre, "Characterization of Residual Coke during Burning," *Znd. Eng. Chem. Res.*, vol. 31, pp. 1017-1021, 1992.
- [69] J. Hagen, "Industrial catalysis A partial approach" 2ed Germany: Wiley, 1999, pp. 186-187.
- [70] N. Macleod, J.R. Fryer, D. Stirling, and G. Webb, "Deactivation of Bi- and Multimetallic Reforming Catalysts: Influence of Alloy Formation on Catalyst Activity," *Catal.Tod* vol. 46 pp. 37-54, 1998.
- [71] B.Viswanathan, S. Sivasanker, and A.V.Ramaswamy, "Catalysis principles and application," 1 ed: Narosa, 2002.
- [72] L.Carlos , Pieck and J. M. Parera, "Comparison of Coke Burning on Catalysts Coked in a Commercial Plant and in the Laboratory," *Ind. Eng. Chem. Res*, vol. 28, pp. 1785-1788, 1989.
- [73] Z. Liu, G. Chen, J. Liang, Q. Wang and G. Cai, "Deactivation of Zeolite Catalysts in Methanol Conversion to Hydrocarbons," *Chinese academy of sciences . Elsevier Sc .Pub B.V., Amsterdam.*, 1991.
- [74] J. M. Parera, "Deactivation and Regeneration of Pt-Re/Al<sub>2</sub>O<sub>3</sub> Catalysts," *Elsevier Sc .Pub B.V., Amsterdam*, 1991.
- [75] T. Keskitalo, "Modeling of Chemical Reaction Kinetics with Data from Temperature-Programmed Experiments," in *Materials Science and Engineering*. degree of Doctor of Science in Technology: Helsinki University of Technology, 2007.
- [76] M.Guisnet, I. Neves, F.R. Ribeiro, C. Canaff, P. Magnoux and G. Perot, "Coking, Aging and Regeneration of Zeolites. Xii-Composition of Coke Formed on Ushy during Phenol Alkylation with Methanol-Mode of Formation," *Elsevier Sc .Pub B.V., Amsterdam*, 1991.

- [77] B. Wang, "Zeolite Deactivation during Hydrocarbon Reactions: Characterisation of Coke Precursors and Acidity, Product Distribution," in *Department of Chemical Engineering*. Doctor of Philosophy London: University College London, 2007.
- [78] Y. Song , H. Li , Z. Guo , X. Zhu , S. Liu , X. Niu , L. Xu, "Effect of Variations in Acid Properties of HZSM-5 on the Coking Behavior and Reaction Stability in Butene Aromatization," *Appl. Catal A: General*, vol. 292, pp. 162–170, 2005.
- [79] J.M. Ortega, A. G. Gayubo, A. T. Aguayo, P. L. Benito, and J. Bilbao, "Role of Coke Characteristics in the Regeneration of A catalyst for the MTG Process " *Ind. Eng. Chem. Res.* , vol. 36, pp. 60-66, 1997.
- [80] P.L. Benito, A. G. Gayubo, A.T. Aguayo, M. Olazar, and J. Bilbao, "Deposition and Characteristics of Coke over a H-ZSM5 Zeolite-Based Catalyst in the MTG Process," *Ind. Eng. Chem. Res.*, vol. 35, pp. 3991-3998, 1996.
- [81] C.L. Li , O. Novaroa, X. Bokhimi , E. Munoz , J.L. Boldu , J.A. Wang , T. Lopez , R. Gomez and N. Batina "Coke Formation on an industrial Reforming Pt–Sn/ Al<sub>2</sub>O<sub>3</sub> catalyst," *Catal. Lett*, vol. 65, pp. 209–216, 2000.
- [82] H.G. Karge, W. NieBen, and H. Bludau, "In-Situ FTIR Measurements of Diffusion in Coking Zeolite Catalysts," *Appl. Catal A: General*, vol. 146 pp. 339-349, 1996.
- [83] J. C. Afonso, A.G. Aranda, M. Schmal, and R. Frety "Regeneration of a Pt-Sn/Al<sub>2</sub>O<sub>3</sub>” Catalyst: Influence of Heating Rate, Temperature and Time of Regeneration," *Fuel Processing Tech.* vol. 50, pp. 35-48, 1997.
- [84] B. Schroder, C. Salzer, and F. Turek, "Selective Deactivation of A bifunctional Reforming Catalyst," *Ind. Eng. Chem. Res.* , vol. 30, pp. 326-330, 1991.
- [85] W.A.Dietz, "Response Factors for Gas Chromatographic Analyses," *Gas Chromatography*, vol. 5, 1967.
- [86] C. H. Bartholomew, R. J. Farrauto, "Fundamentals of Industrial Catalytic Processes," 2<sup>ed</sup> USA: John Wiley & Sons, 2006.

- [87] J. Liu, "High-Resolution and Low-Voltage FESEM Imaging and Microanalysis in Materials Characterization" *Elsevier Sc. Inc*, vol. 44, pp. 353-363, 2000.
- [88] J. Kanervo, "Kinetic Analysis of Temperature-Programmed Reactions," in *Chemical Technology for public examination and debate in Auditorium*, degree of Doctor of Science in Technology: Helsinki University of Technology 2003.
- [89] F. Delannay, "Characterization of Heterogeneous Catalysts." vol. 15, 1984.
- [90] Y. Amenomiya, R. J. Cvetanovic, "Application of Flash-Desorption Method to Catalyst Studies. III. Propylene Alumina System and Surface Heterogeneity," *J. Phys. Chem.* vol. 67, pp. 2705-2708, 1963.
- [91] P. A. Redhead, "Thermal Desorption of Gases Vacuum" vol. 12, pp. 203-201, 1962.
- [92] Y. Ren, N. Mahinpey, and N. Freitag, "Kinetic Model for the Combustion of Coke Derived at Different Coking Temperatures," *Energy & Fuels*, vol. 21, pp. 82-87, 2007.
- [93] A. K. Talukdar, K. G. Bhattacharyya, T. Baba, and Y. Ono, "1-Hexene Isomerization and *n*-hexane Cracking over HMCM-22," *Appl. Catal A: General*, vol. 213, pp. 239-245, 2001.
- [94] F. Aberuagba, "Aromatization of Heptene-2 on Pt/Al<sub>2</sub>O<sub>3</sub> Catalysts," *React Kinet Catal.Lett*, vol. 70, pp. 243-249, 2000.
- [95] H. Long, X. Wang, W. Sun, and X. Guo, "Conversion of *n*-octene over Nanoscale HZSM-5 Zeolite," *Catal Lett*, vol. 126, pp. 378-382, 2008.
- [96] N. N Mahamuni and Y. G. Adewuyi, "Application of Taguchi Method to Investigate the Effects of Process Parameters on the Transesterification of Soybean Oil Using High Frequency Ultrasound," *Energy Fuels*, vol. 24, pp. 2120-2126, 2010.
- [97] M. Kul, and U. Cetinkaya, "Application of the Taguchi Orthogonal Array Design to Cr (VI) Solvent Extraction," in *Minerals & Metallurgical Processing*, 2010.
- [98] O. Levenspiel, "Chemical Reaction Engineering," Third ed USA: john wiley&sons, 1999.

- [99] J. Ruixia ,X. Zaiku , Z. Chengfang, and C. Qingling, "Deactivation of the Pd-La /spinal Catalyst for the Preparation of 2,6-diisopropyl aniline," *Appl. Catal A: General*, vol. 250 pp. 209-220, 2003.
- [100] D.L. Pavia, G.M. Lampman, and G .S.kriz, "Introduction to Spectroscopy ", Third editions , 2001.
- [101] J. Wang, P.I. Chigada, S.P.Rigby, B. Al-Duria, and J. Wood, "Prolonging Catalyst Lifetime in Supercritical Isomerization of 1-hexene over a Platinum/Alumina Catalyst " *Chem. Eng. Sc*, vol. 64, pp. 3427 –3436, 2009.
- [102] M.B. González, C.L. Pieck, and J.M. Parera, "Total Metallic Dispersion of Sulfided Pt-Re/Al<sub>2</sub>O<sub>3</sub> Naphtha Reforming Catalysts" *Appl. Catal A: General*, vol. 205, pp. 305–312, 2001.

## APPENDIX A

### Experiment Results

**Table A-1: Reforming Conditions (723K -300KPa)**

Contact time (min)	cracking	Coke precursors	isomers	aromatics	Hexane conversion
1.016217	12.44449	10.03309	23.95176	9.08774	55.51708
1.185587	14.55092	12.09113	26.33531	11.09332	64.07068
1.422704	16.0024	14.23945	24.06782	11.97947	66.28914
1.77838	19.09567	16.03482	27.9772	13.4411	76.54879
2.371173	19.8728	15.88392	29.18124	15.01225	79.95021
3.55676	21.99218	18.93982	18.90467	16.27704	76.11371
7.113519	22.93075	22.06834	19.99403	16.90467	81.89779

**Table A-2: Reforming Conditions (723K -500KPa)**

Contact time (min)	cracking	Coke precursors	isomers	aromatics	Hexane conversion
1.016217	14.0954	8.087423	22.875492	5.5492	50.607515
1.185587	15.00743	7.989762	21.045882	5.44987	49.492944
1.422704	15.58118	11.822041	19.60089	8.45997	55.464081
1.77838	19.0022	14.88733	24.804472	8.09338	65.787382
2.371173	21.97732	15.997503	26.88402	9.9452	75.804043
3.55676	21.0991	15.8894	19.044678	11.241	67.274178
7.113519	24.0489	17.93784	18.77302	10.77837	71.53813

**Table A-3: Reforming Conditions (723K -700KPa)**

Contact time (min)	cracking	Coke precursors	isomers	aromatics	Hexane conversion
1.016217	18.99927	7.119109	19.07783	4.09328	49.28948
1.185587	19.80463	7.93451	20.99857	6.001123	54.73884
1.422704	19.90224	9.88941	23.66403	7.045982	60.50166
1.77838	21.70385	11.03821	23.09558	7.99218	61.82982
2.371173	22.00056	14.7442	24.06645	8.661983	70.47319
3.55676	22.06892	16.11423	21.09553	10.04299	69.32167
7.113519	24.90771	15.97783	20.00027	6.048655	66.93446

**Table A-4: Reforming Conditions (673K -300KPa)**

Contact time (min)	cracking	Coke precursors	isomers	aromatics	Hexane conversion
1.016217	12.94449	8.03309	22.95176	6.88774	50.81708
1.185587	10.55092	10.09113	21.33531	8.79342	50.77078
1.422704	12.0024	11.23945	24.06782	9.97947	57.28914
1.77838	11.09567	12.03482	25.98452	11.4411	60.55611
2.371173	13.8728	13.88392	27.09524	12.01225	66.86421
3.55676	19.99218	17.93982	18.90467	10.27704	67.11371
7.113519	20.03075	18.156023	16.99403	11.90467	67.08547

**Table A-5: Reforming Conditions (623K -300KPa)**

contact time (min)	cracking	Coke precursors	isomers	aromatics	Hexane conversion
1.016217	8.56921	6.93309	21.95176	5.849274	43.303334
1.185587	10.55092	7.09113	21.33531	6.409822	45.387182
1.422704	10.879224	11.23945	20.06662	6.997947	49.183241
1.77838	12.09567	10.103482	23.939702	8.4924118	54.6312658
2.371173	13.85728	11.88392	26.18128	8.0721225	59.9946025
3.55676	16.99218	14.93981	15.1190467	9.223904	56.2749407
7.113519	18.93075	16.97023	12.99403	10.90467	59.79968

**Table A-6: Reforming Conditions (1%CCL<sub>4</sub>, (723K -300KPa))**

Contact time (min)	cracking	Coke precursors	isomers	aromatics	Hexane conversion
1.016217	15.94449	10.03309	25.95176	10.066324	61.995664
1.185587	20.55092	11.09113	27.33531	12.09332	71.07068
1.422704	21.0024	10.23945	29.06782	11.97947	72.28914
1.77838	22.95671	19.83482	30.99772	18.01225	83.07232
2.371173	20.0728	19.03392	29.918124	15.94411	91.687094
3.55676	21.99218	20.93982	21.90467	15.23104	80.06771
7.113519	20.93075	23.88023	19.99403	19.90942	84.71443

**Table A-7: Reforming Conditions (3% CCL<sub>4</sub>, (723K -300KPa))**

Contact time (min)	cracking	Coke precursors	isomers	aromatics	Hexane conversion
1.016217	19.75837	11.87952	28.95171	9.08774	69.67734
1.185587	20.99053	14.76383	27.97431	13.09332	76.82199
1.422704	22.0024	15.76684	30.06782	15.97947	83.81653
1.77838	25.15567	15.63482	30.18752	21.04411	86.86212
2.371173	23.09728	17.0328	26.98742	19.71225	92.05023
3.55676	26.99218	18.44067	27.432876	23.927704	96.79343
7.113519	25.93075	25.59327	25.97621	17.90467	95.4049

**Table A-8: Reforming Conditions (5% CCL<sub>4</sub>, (723K -300KPa))**

Contact time (min)	cracking	Coke precursors	isomers	aromatics	Hexane conversion
1.016217	22.75837	11.09352	25.67331	16.08774	75.61294
1.185587	23.55092	14.088732	28.37321	18.09332	84.106182
1.422704	25.0024	18.23945	31.06782	18.97947	93.28914
1.77838	26.10567	19.03482	30.73239	19.74411	95.60699
2.371173	27.98728	16.99415	26.18521	22.01125	93.18389
3.55676	28.99218	18.99843	29.904672	18.28729	96.182572
7.113519	29.93075	23.093528	28.07731	15.93241	97.033998

# Appendix B

## Gas Chromatograph

Data File c:\HPCHEM\1\DATA\REEM\SIG20057.D

Sample Name: 450-6b-1/10

\_1\_newrga.mtd

Injection Date : 4/27/2010 8:30:12 PM

Sample Name : 450-6b-1/10

Location : Vial 2

Acq. Operator : manager

Inj : 1

Inj Volume : Manually

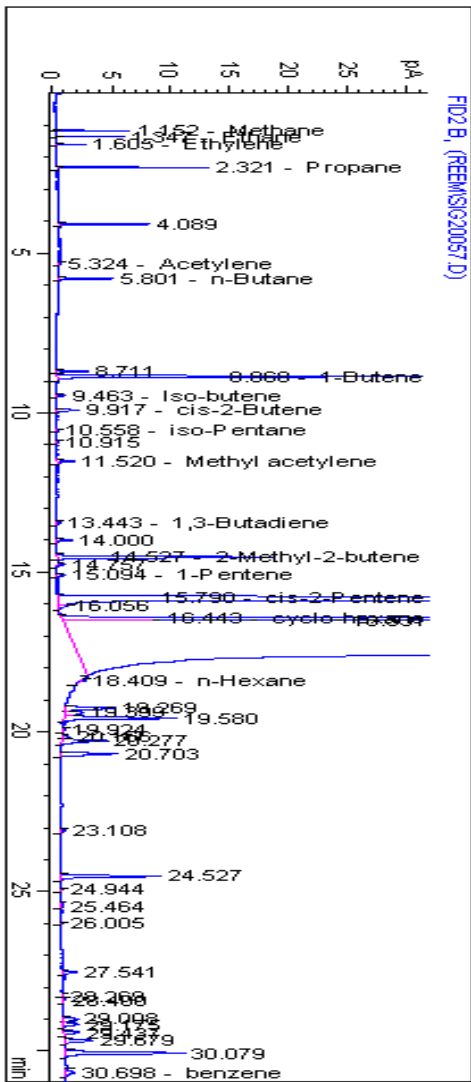
Acq. Method : C:\HPCHEM\1\METHODS\KGA.M

Last changed : 4/27/2010 8:18:11 PM by manager

(modified after loading)

Analysis Method : C:\HPCHEM\1\METHODS\REEMTD2.M

Last changed : 5/10/2010 11:21:38 PM by reem



## Appendix C

Table 3.5 Gas Chromatograph calibration of standard gases

No.	RT (min)	Signal	Gas Standard	Concentration (mol %)	Peak Area
1.	1.177	FID	Methane	5	4663
2.	1.405	FID	Ethane	3.99	7088.1
3.	1.735	FID	Ethylene	2.010	3629.9
4.	2.596	FID	Propane	2.010	5493.1
5.	4.678	FID	Proelene	0.989	81.426
6.	4.75	FID	Acetylene	0.988	2642.5
7.	6.155	FID	n-Butane	0.299	1101.1
8.	6.572	FID	1,2- Propadiene	0.964	1429.3
9.	6.696	FID	Trans-2-butene	0.300	1870.2
10	6.890	FID	Iso butane	0.300	2524.2
11	9.985	FID	1-butene	0.2990	1055.6
12	10.027	FID	Iso butane	0.3	1091.9
13	10.605	FID	Cis-2-butene	0.299	1012.7
14	11.083	FID	Iso pentane	0.100	1068.7
15	12.211	FID	Methyl acetylene	0.987	440.66
16	12.856	FID	n-pentane	0.100	435.56
17	13.405	FID	Trans-2-pentene	0.0990	2607.2
18	13.846	FID	1,3 butadiene	0.297	1059.3
19	15.394	FID	2 methyl-2butene	0.0485	420.170
20	15.986	FID	1-pentene	0.0997	644.98
21	16.591	FID	Cis-2-pentene	0.0945	404.82
22	19.000	FID	n-hexane	0.499	232.59
23	29.99	FID	Benzene (liquid)	0.219	245.11

## Appendix D

Thermo-gravimetric analysis (TGA) at  $15 \text{ K min}^{-1}$

